Report

ON THE THREAT

OF A MAGMA PLUME ERUPTION IN SIBERIA

AND STRATEGIES FOR ADDRESSING THE ISSUE

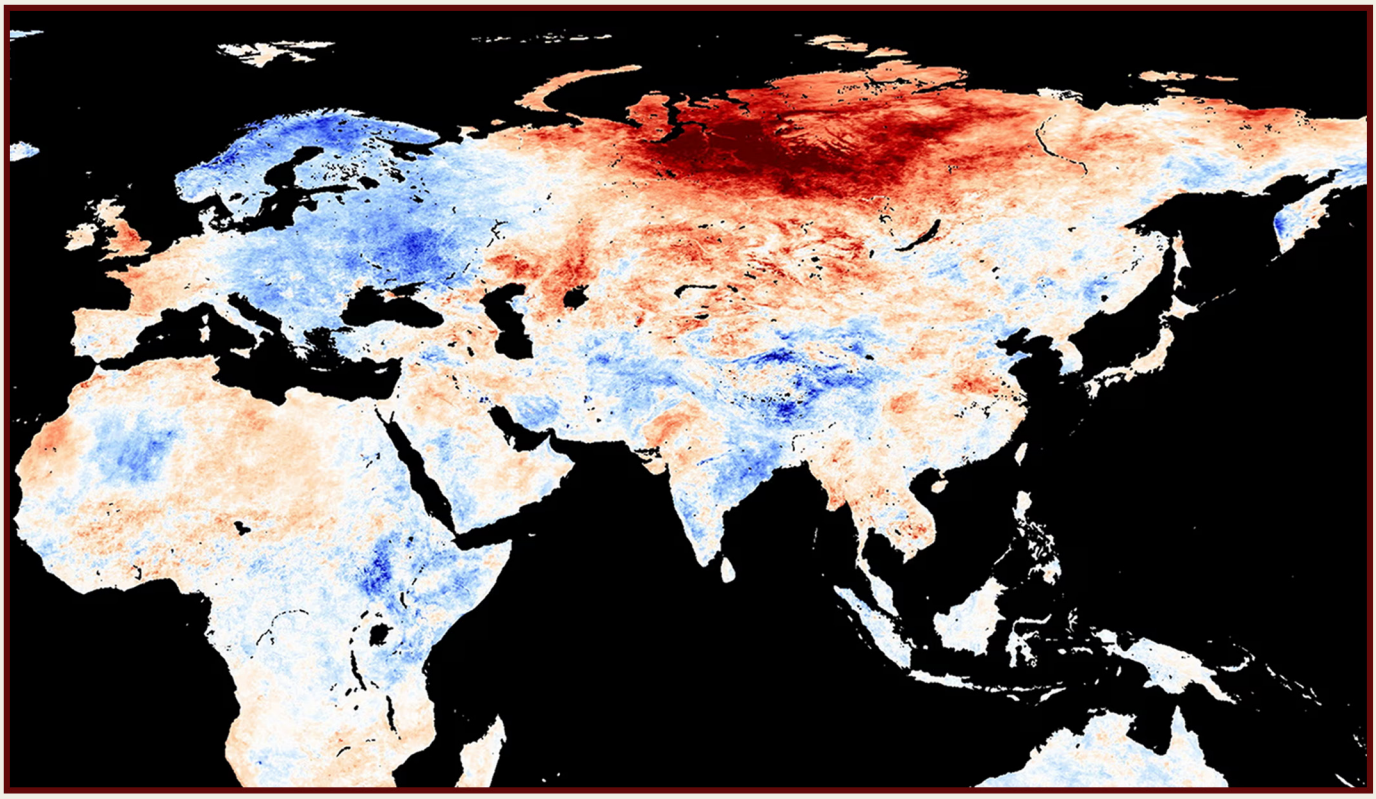

Report

ON THE THREAT

OF A MAGMA PLUME ERUPTION IN SIBERIA

AND STRATEGIES FOR ADDRESSING THE ISSUE

CONTENTS

Brief Description of the Geodynamic Model of Climate Change on Earth in the Current Period

Over the past 30 years, the Earth has experienced an unprecedented and synchronous increase in climate changes, anomalies, and extreme events across all layers of the planet and its geophysical parameters. The progression of these changes is accelerating exponentially. Comprehensive analysis of scientific data indicates that the primary drivers of the anomalies observed in all of Earth's spheres are astronomical cycles that impact the entire Solar System every 12,000 years.

This hypothesis of external astronomical influence is supported by the observation of similar climatic, geodynamic, and magnetic anomalies occurring simultaneously on other planets in the Solar System and their moons. For instance, increased wind speeds and the expansion of hurricane sizes have been recorded on Uranus, Jupiter, and Venus. Meanwhile, Mars has exhibited melting polar ice caps, alongside increasing volcanic activity on both Venus and Mars. Additionally, seismic activity on Mars has intensified, pointing to the emergence of anomalous geodynamic processes.

Critical changes within Earth's systems due to the 12,000-year astronomical cycle began in the current cycle in 1995. Notable geophysical anomalies recorded at that time included a sharp acceleration in Earth's rotation (Fig. 1), a shift in its axis[1] (Fig. 2), and the onset of a pronounced drift of the North Magnetic Pole[2] (Fig. 3). These phenomena suggest substantial changes occurring within Earth's core.

[1]Deng, S., Liu, S., Mo, X., Jiang, L., & Bauer Gottwein, P. (2021). Polar Drift in the 1990s Explained by Terrestrial Water Storage Changes. Geophysical Research Letters, 48(7). https://doi.org/10.1029/2020gl092114

[2]Dyachenko, A. I. (2003). Earth's magnetic poles. MCCME.

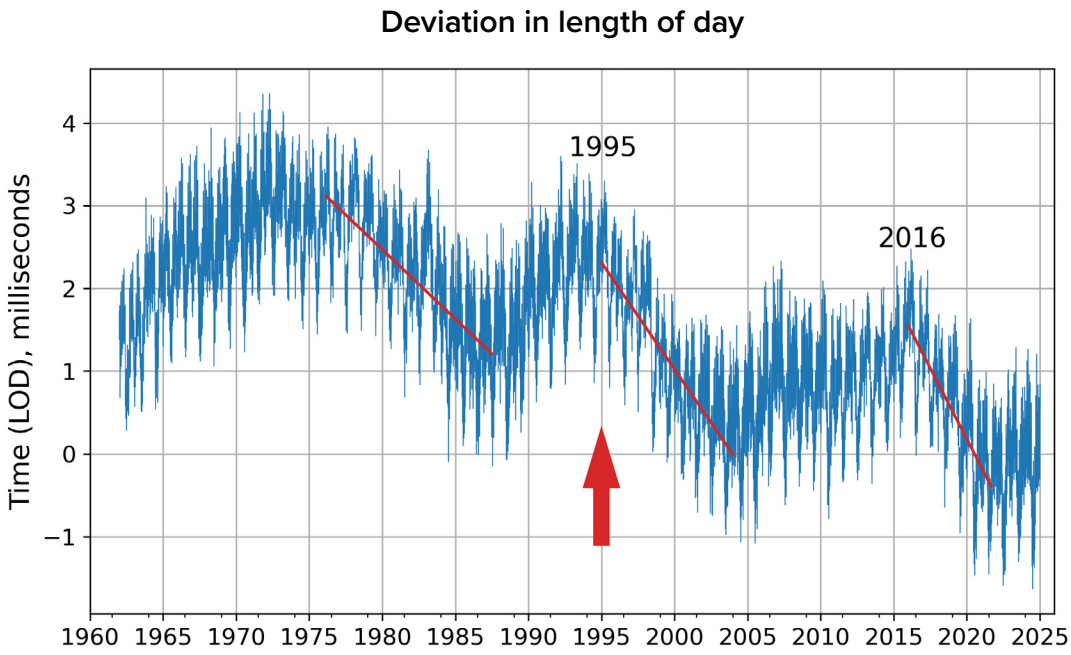

Fig. 1
Deviation of day length in milliseconds from 1962 to 2023
Source: IERS Earth Orientation Center of the Paris Observatory
Day length – Earth orientation parameters: https://datacenter.iers.org/singlePlot.php?plotname=EOP-C04_14_62-NOW_IAU1980-LOD&id=223

In the figure, red lines represent trend lines illustrating the rate at which the length of a day is decreasing. For example, the trend line on the left is relatively gentle, while the trend line on the right, which marks the acceleration since 2016, is almost vertical. This indicates that the length of a day is decreasing significantly faster, meaning the planet's rotation is accelerating.

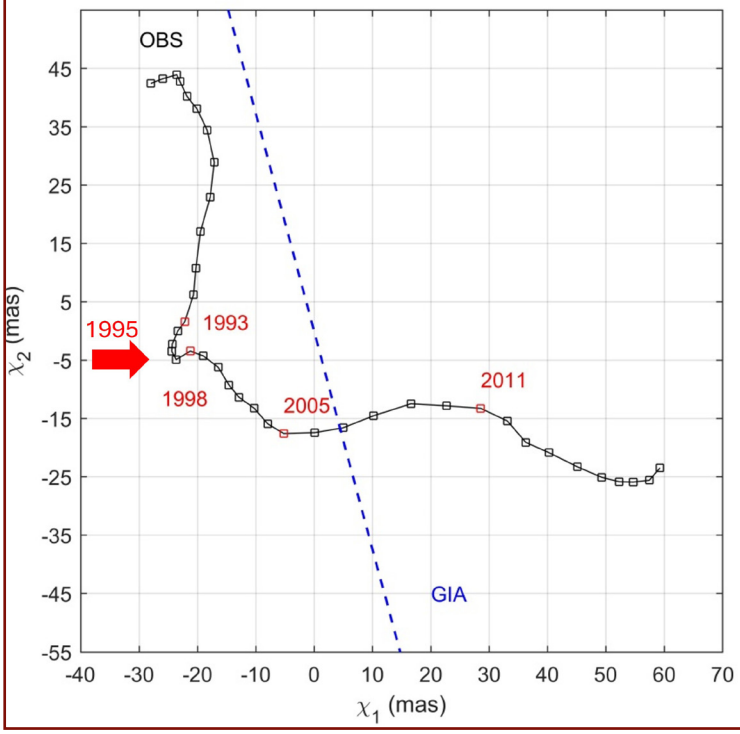

Fig. 2
Long-term trajectory of observed excitation after removal of annual and Chandler cycles using the moving average method.

Black line with squares: observed trajectory; blue dashed line: direction of polar drift caused by glacial isostatic adjustment (GIA).

The moving average subset size was set to 84 months, which is the least common multiple of 12 months (annual cycle) and 14 months (Chandler cycle), as per the study by Liu et al. (2017).

Source: Deng, S., Liu, S., Mo, X., Jiang, L., & Bauer Gottwein, P. (2021). Polar Drift in the 1990s Explained by Terrestrial Water Storage Changes. Geophysical Research Letters, 48(7). https://doi.org/10.1029/2020gl092114

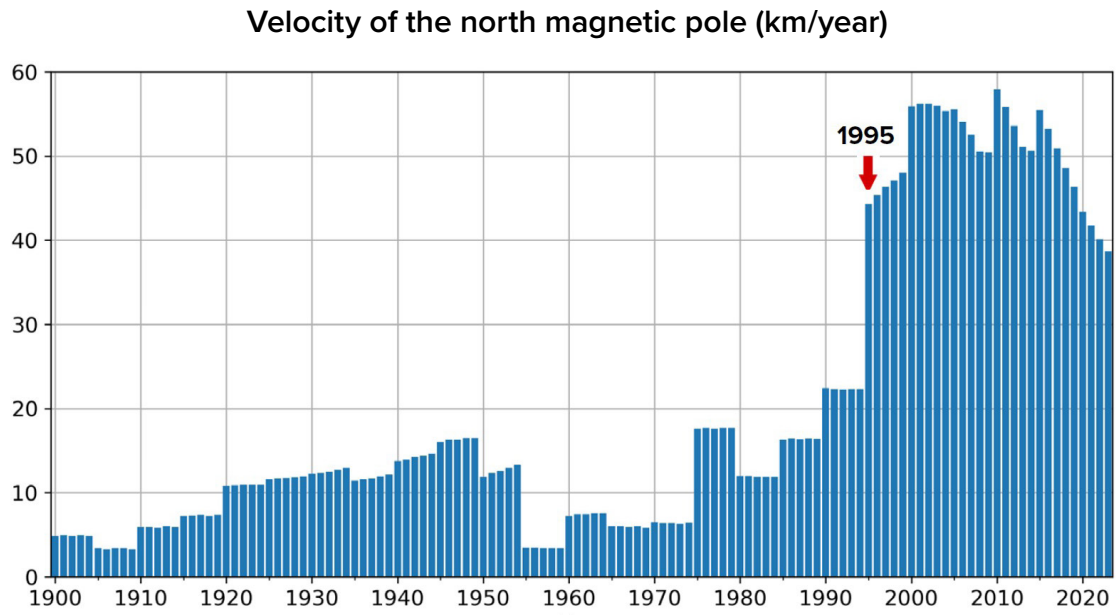

Fig. 3
Speed of the North Magnetic Pole Drift (km/year)
Source: NOAA data on the position of the North Magnetic Pole
https://www.ngdc.noaa.gov/geomag/data/poles/NP.xy

According to the hypothesis, at this point in time, the Solar System began entering a region where external cosmic forces started exerting significant influence on planetary cores. The changes observed in Earth's core in 1995 suggest an increase in the heating of the outer core, implying that additional energy began reaching Earth's core. Such profound changes in Earth's core require energy inputs quadrillions of times greater than all the energy ever produced by human civilization throughout its existence.

The influx of external energy into Earth's core triggered processes associated with mantle melting and magma ascent to the surface. This, in turn, initiated a chain reaction of seismic and volcanic activity, increased heat emanating from the Earth's interior, and a rise in climate-related disasters worldwide.

For instance, since 1995, a significant increase in seismic activity has been observed, characterized by higher frequency, magnitude, and energy of earthquakes. This trend affects both continental regions and the ocean floor (Fig. 4), including areas previously considered seismically inactive, indicating the global nature of these changes.

It is important to note that the rise in the number of earthquakes with a magnitude of 5.0 or higher is not attributable to advancements in seismic monitoring technology (Fig. 5) but reflects genuine changes in Earth's geodynamic system. Cumulative data from the International Seismological Centre confirm that the number of earthquakes has substantially increased over the past 25 years and continues to rise (Fig. 6).

Increase in Ocean Floor Earthquakes Along Mid-Ocean Ridges

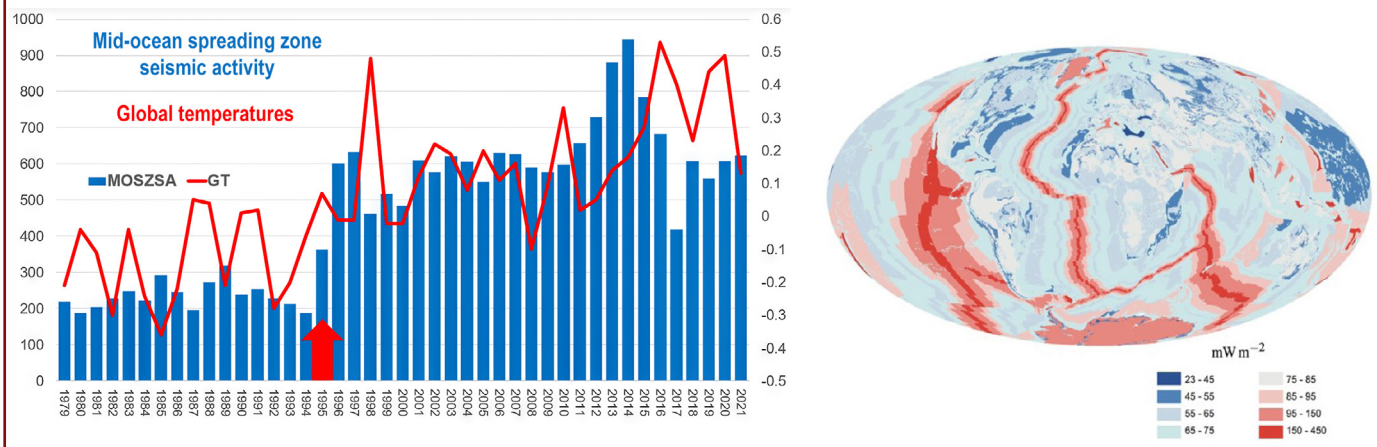

Fig. 4
Simultaneous Increase in Ocean Floor Earthquakes and Global Atmospheric Temperatures (Left) Geothermal Heating of Mid-Ocean Ridges (Right)
Source: Davies & Davies, 2010; Viterito, A. (2022). "1995: An Important Inflection Point in Recent Geophysical History." International Journal of Environmental Sciences & Natural Resources, 29(5). https://doi.org/10.19080/ijesnr.2022.29.556271

The diagram illustrates a sharp increase in the number of ocean floor earthquakes along mid-ocean ridges beginning in 1995, alongside a strong correlation between ocean floor seismicity and atmospheric temperatures. This indicates an additional deep heat source affecting both the oceans and the atmosphere.

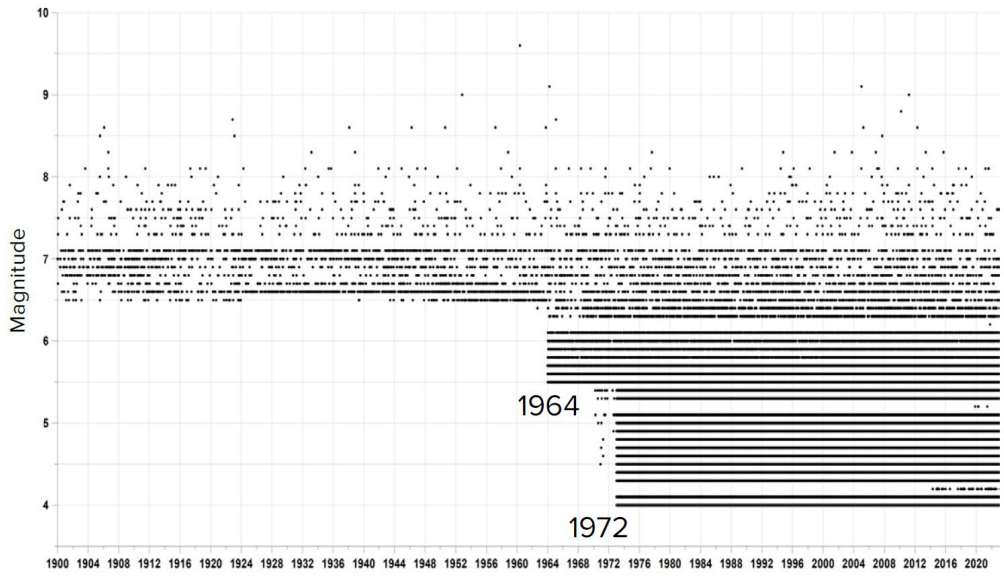

Fig. 5
Earthquake Magnitudes Recorded Over Time
Black dots represent earthquakes of varying magnitudes across different years. Before 1964, only earthquakes with magnitudes of 6.5 and above were recorded. Starting in 1964, with the introduction of more sensitive sensors, earthquakes of 5.5 and above were documented. Since 1972, earthquakes of 4.0 and higher have been consistently recorded, regardless of location.

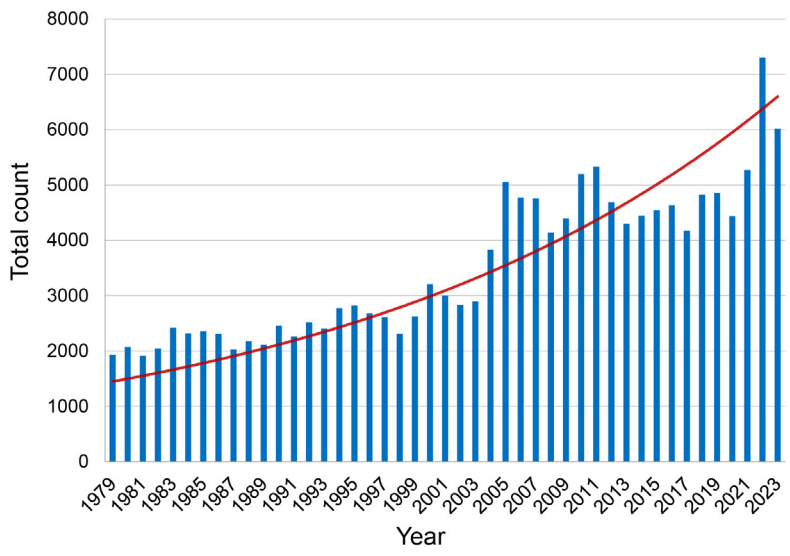

Fig. 6
M5+ Earthquakes from 1979 to 2023
Source: ISC database.

The dataset was compiled using the Maximum Magnitude Algorithm, selecting the highest magnitude value recorded in the ISC database for each event (see Appendix 1).

Source: ISC database.

Moreover, seismic activity near volcanoes is increasing, including at supervolcanoes such as Yellowstone (USA), Campi Flegrei (Italy), Taupo (New Zealand), and others that erupted during previous 12,000-year cycles. The total number of volcanic eruption days is also rising, accompanied by anomalous eruptions. In these events, the expelled lava is superheated and exhibits an atypical composition characteristic of magma from deeper mantle layers [3,4,5,6,7].

Particular attention is drawn to the increase in deep-focus earthquakes occurring at depths exceeding 300 kilometers (186 miles), and sometimes reaching up to 750 kilometers (466 miles) below Earth's surface. These events originate not in the Earth's crust but in the mantle, where the material typically deforms smoothly rather than fracturing. This makes the nature of such earthquakes highly unusual.

Given the extreme pressures and temperatures at these depths, these phenomena can be understood as powerful explosions comparable in energy to the simultaneous detonation of multiple atomic bombs within Earth's mantle. Additionally, deep-focus earthquakes often trigger significant seismic events in the Earth's crust, amplifying their destructive impact [8,9].

[3]Castro, J., & Dingwell, D. (2009). Rapid ascent of rhyolitic magma at Chaitén volcano, Chile. Nature, 461, 780-783. https://doi.org/10.1038/nature08458
[4]Smirnov, S. Z., et al. (2021). High explosivity of the June 21, 2019 eruption of Raikoke volcano (Central Kuril Islands): Mineralogical and petrological constraints on the pyroclastic materials. Journal of Volcanology and Geothermal Research, 418, 107346. https://doi.org/10.1016/j.jvolgeores.2021.107346
[5]Why the Tongan eruption will go down in the history of volcanology. (2022). Nature, 602, 376-378. https://doi.org/10.1038/d41586-022-00394-y
[6]Halldórsson, S. A., Marshall, E. W., Caracciolo, A., et al. (2022). Rapid shifting of a deep magmatic source at Fagradalsfjall volcano, Iceland. Nature, 609, 529-534. https://doi.org/10.1038/s41586-022-04981-x
[7]D'Auria, L., Koulakov, I., Prudencio, J., et al. (2022). Rapid magma ascent beneath La Palma revealed by seismic tomography. Scientific Reports, 12, 17654. https://doi.org/10.1038/s41598-022-21818-9
[8]Mikhailova, R. S. (2014). Strong earthquakes in the mantle and their influence in the near and far zone. Geophysical Survey RAS. http://www.emsd.ru/conf2013lib/pdf/seism/Mihaylova.pdf
[9]Mikhailova, R. S., Ulubieva, T. R., & Petrova, N. V. (2021). The Hindu Kush earthquake of October 26, 2015 with Mw=7.5, I0~7: Previous seismicity and aftershock sequence. Earthquakes in Northern Eurasia, 24(2015), 324-339. https://doi.org/10.35540/1818-6254.2021.24.31

Since 1995, there has been a rapid exponential increase in the number of such deep earthquakes (Figs. 7, 8), coinciding with other geodynamic anomalies that began during the same period. The rise in these intramantle explosions points to an increase in energy within Earth's depths and intensified mantle melting, which could result in large-scale volcanic eruptions.

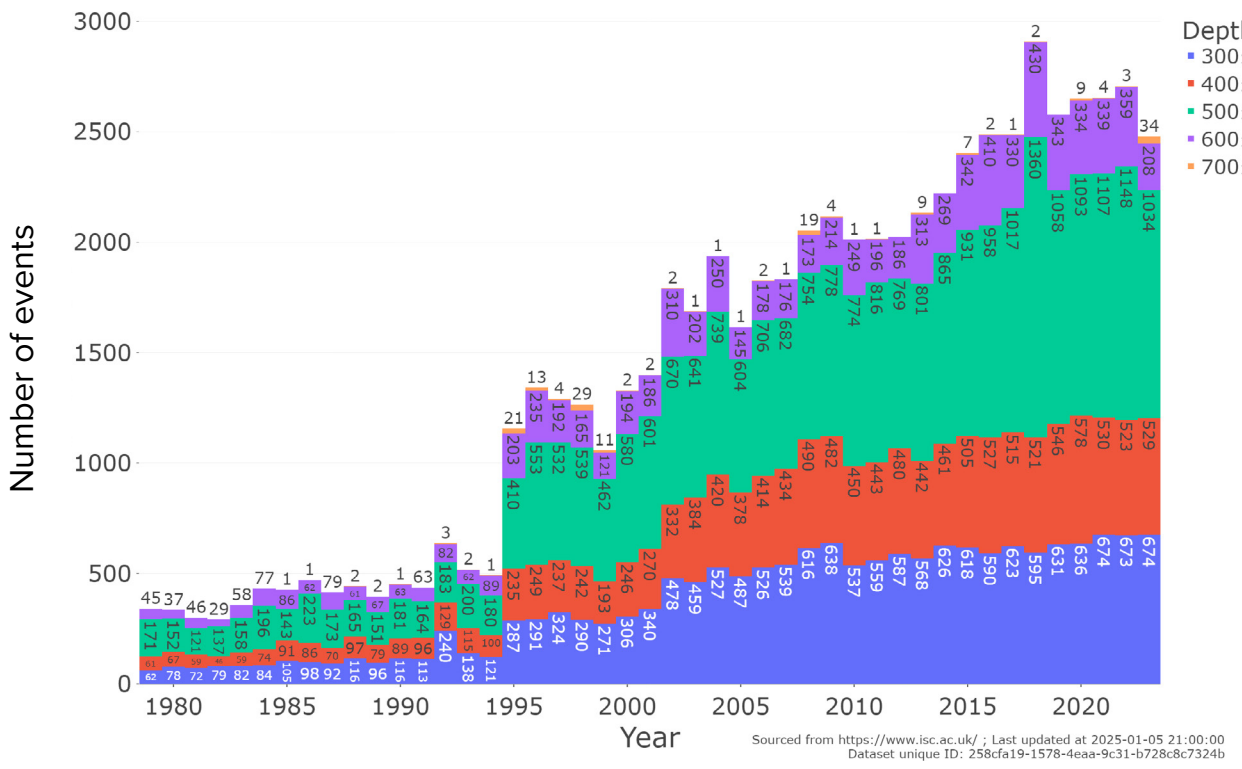

Fig. 7
Exponential growth in the number of deep-focus M3+ earthquakes worldwide since 1979. The graph is designed according to data sampling by the Special Median Magnitude Algorithm (see Appendix 1) contained in the ISC database for each of the events.

Source: ISC Database

The chart illustrates the geometric progression in the increase of earthquakes at depths exceeding 300 kilometers (186 miles) within Earth's upper mantle, a region traditionally considered plastic and incapable of fracturing. A significant surge is observed starting in 1995, coinciding with similar increases in many other geodynamic anomalies. Notably, the rise in deep-focus earthquakes is unrelated to an increase in the number of seismic monitoring sensors.

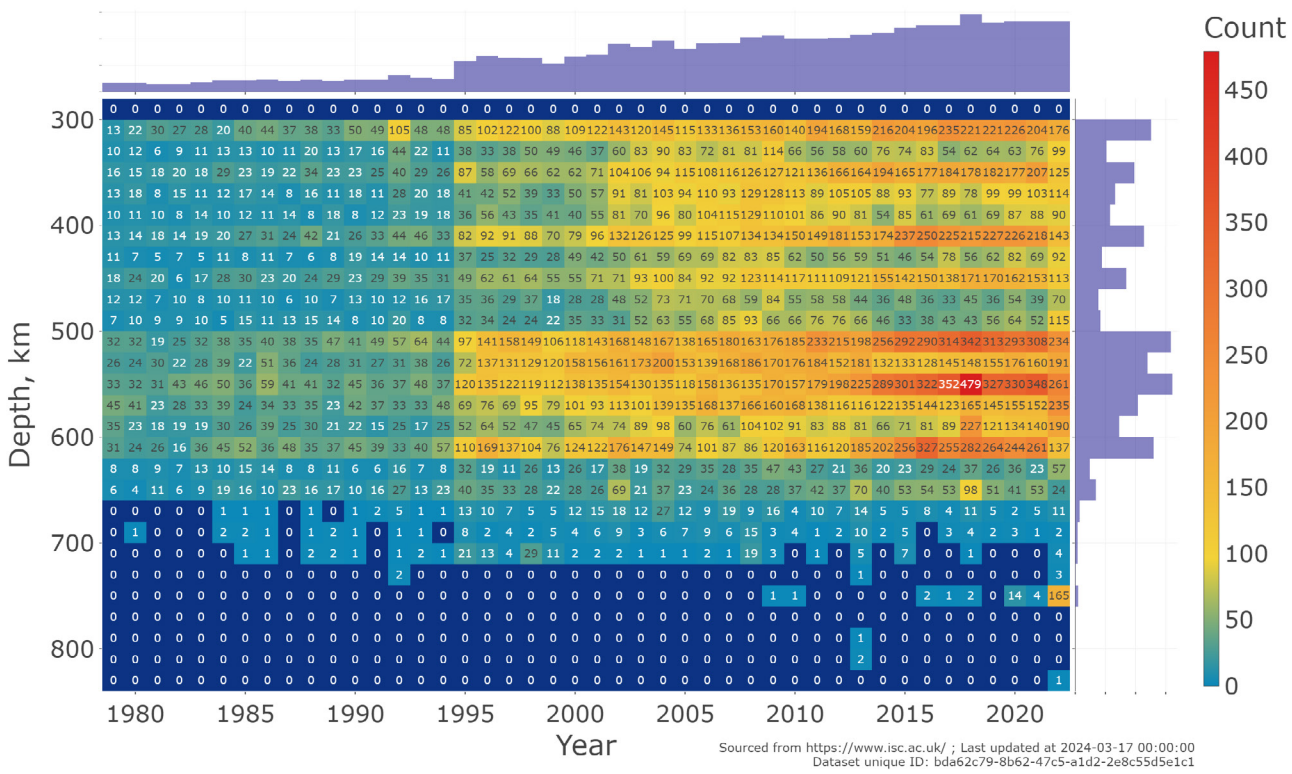

Fig. 8
Distribution of deep-focus M3+ earthquakes by year and depth
Source: ISC Database.

The increase in deep-focus earthquakes indicates melting of the mantle that is heated from the core. Due to centrifugal forces, molten magma within the mantle begins to rise sharply toward the Earth's surface. This movement erodes and heats the lithosphere from within at an accelerated rate.

The ascent of magma is directly responsible for increasing geothermal flux from the planet's interior and the activation of magma plumes beneath glaciers in West Antarctica and central Greenland. This process significantly accelerates the melting of glaciers and permafrost from the bottom up.

Today, the ocean is warming like never before, significantly intensifying extreme natural events such as floods, hurricanes, and tropical cyclones. The ocean plays a crucial role in regulating the planet's heat because it can absorb and redistribute excess heat, preventing catastrophic consequences. However, now that Earth's heating is intensifying due to geodynamic activity caused by astronomical cycles, the ocean has lost its function of removing heat from the depths. This has happened because of human-caused ocean pollution. Plastic waste breaks down into microplastics and nanoplastics, reducing the thermal conductivity of water (Fig. 9).

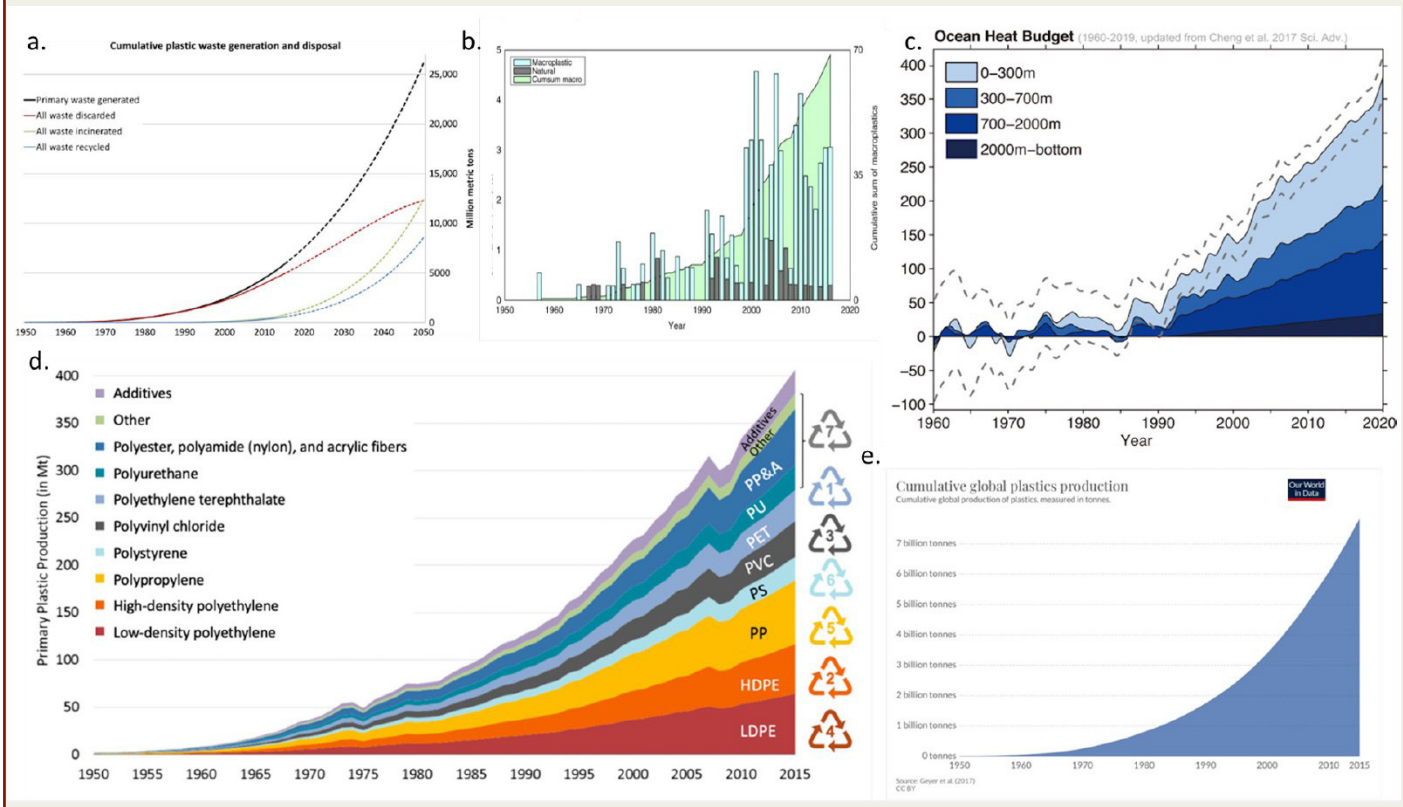

Fig. 9
Diagrams of changes in ocean temperature from 1960-2019 and their comparison with the diagrams of growth in the production of synthetic polymers, their use in various sectors of economy, and disposal of plastic waste in the ocean (from various sources)

a. Cumulative plastic waste generation and disposal
Source: Geyer, R., Jambeck, J. R., & Law, K. L. (2017). Production, use, and fate of all plastics ever made. Science Advances, 3(7).
https://doi.org/10.1126/sciadv.1700782

b. Cumulative sum of macroplastic in the ocean and annual counts
Source: Ostle, C., Thompson, R. C., Broughton, D., Gregory, L., Wootton, M., & Johns, D. G. (2019). The rise in ocean plastics evidenced from a 60-year time series. Nature Communications, 10(1622).
https://doi.org/10.1038/s41467-019-09506-1

c. Ocean heat budget from 1960 to 2019 (Purkey and Johnson, 2010; updated from Cheng et al., 2017)
Source: Cheng, L., Abraham, J., Zhu, J., Trenberth, K. E., Fasullo, J., Boyer, T., Locarnini, R., Zhang, B., Yu, F., Wan, L., Chen, X., Song, X., Liu, Y., & Mann, M. E. (2020). Record-Setting Ocean Warmth Continued in 2019. Advances in Atmospheric Sciences, 37, 137–142.
https://doi.org/10.1007/s00376-020-9283-7

d. Global primary plastic production by polymer type
Source: Geyer, R., Jambeck, J. R., & Law, K. L. (2017). Production, use, and fate of all plastics ever made. Science Advances, 3(7).
https://doi.org/10.1126/sciadv.1700782

e. Cumulative global production of plastics since 1950
Data source: Plastic Marine Pollution Global Dataset

The rise in water temperatures occurs not only at the surface but throughout the entire depth and on the ocean floor. Ocean heating is caused by rising magma, which especially heats the oceanic crust, which is thinner and more vulnerable than the continental crust.

Historical data from geological and ice cores indicate that Earth has faced similar catastrophic cycles every 12,000 years[10]. Every 24,000 years, these planetary catastrophes have been significantly more intense, as evidenced by studies of volcanic ash layers in ice cores[11] (Fig. 10) and other geochronological research. Earth is now entering such a cycle. However, the current cycle is exacerbated by anthropogenic factors, such as ocean pollution, which has further diminished the oceans' ability to regulate Earth's energy balance.

As oceans heat up, plastic waste breaks down into microplastics and nanoplastics, which further reduce the oceans' thermal conductivity. This loss of heat conductivity is critically important during periods of heightened geodynamic activity driven by astronomical cycles.

The accumulation of excess energy within Earth's interior has led to an increase in the number of deep-focus earthquakes and the rapid formation of new magma chambers, intensifying the planet's instability. This feedback loop accelerates Earth's heating and destabilization, pushing the planet closer to inevitable destruction.

Mathematical modeling indicates that the world's economic and social systems could collapse within the next 4–6 years due to the escalating damage from climate disasters. The exponential increase in catastrophic events threatens to render Earth uninhabitable within the next decade (Fig. 11).

Unlike previous cycles, the current state of the planet is exacerbated by pollution caused by human activity, leaving little hope for the survival of ecosystems or Earth itself. **It is important to understand that addressing ocean-related issues may slow the progression of cataclysms but will not stop them entirely.**

[10]Arushanov, M. L. (2023). Climate dynamics: Space factors. LAMBERT Academic Publishing.

[11]Sawyer, D. E., Urgeles, R., & Lo Iacono, C. (2023). 50,000 yr of recurrent volcaniclastic megabed deposition in the Marsili Basin, Tyrrhenian Sea. Geology, 51(11), 1001-1006. https://doi.org/10.1130/G51198.1

Catastrophic Volcanic Eruptions Happening With a 12,000-Year Cycle

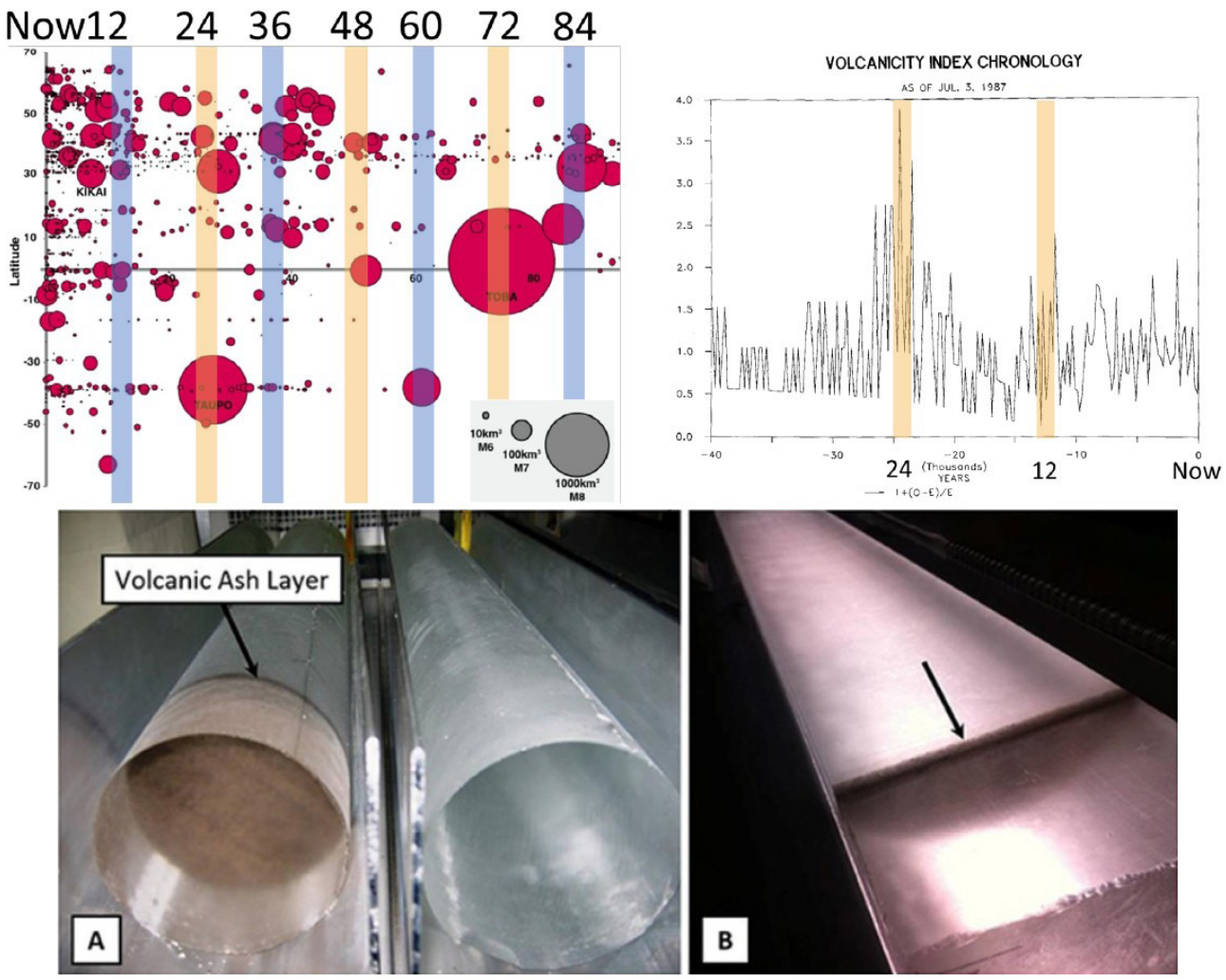

Fig. 10

Research data on volcanic ash layers from eruptions over the past 100,000 years in ice cores from Antarctica and the Arctic, compiled from various authors' works

Source: Brown, S. K., Crosweller, H. S., Sparks, R. S. J., Cottrell, E., Deligne, N. I., Guerrero, N. O., Hobbs, L., Kiyosugi, K., Loughlin, S. C., Siebert, L., & Takarada, S. (2014). Characterisation of the Quaternary eruption record: analysis of the Large Magnitude Explosive Volcanic Eruptions (LaMEVE) database. Journal of Applied Volcanology, 3(5). https://doi.org/10.1186/2191-5040-3-5

Bryson, R. A. (1989). Late quaternary volcanic modulation of Milankovitch climate forcing. Theoretical and Applied Climatology, 39, 115–125. https://doi.org/10.1007/bf00868307

Graphs illustrate catastrophic volcanic activity occurring every 12,000 years, with even more intense events every 24,000 years (accounting for dating uncertainties). These catastrophic episodes have led to sharp temperature fluctuations, natural disasters, volcanic winters, and mass extinctions of species. Many supervolcanoes that erupted during past cycles have begun exhibiting anomalous activity in recent years, particularly since 1995.

Progression of Escalating Disasters, Illustrated by Earthquakes

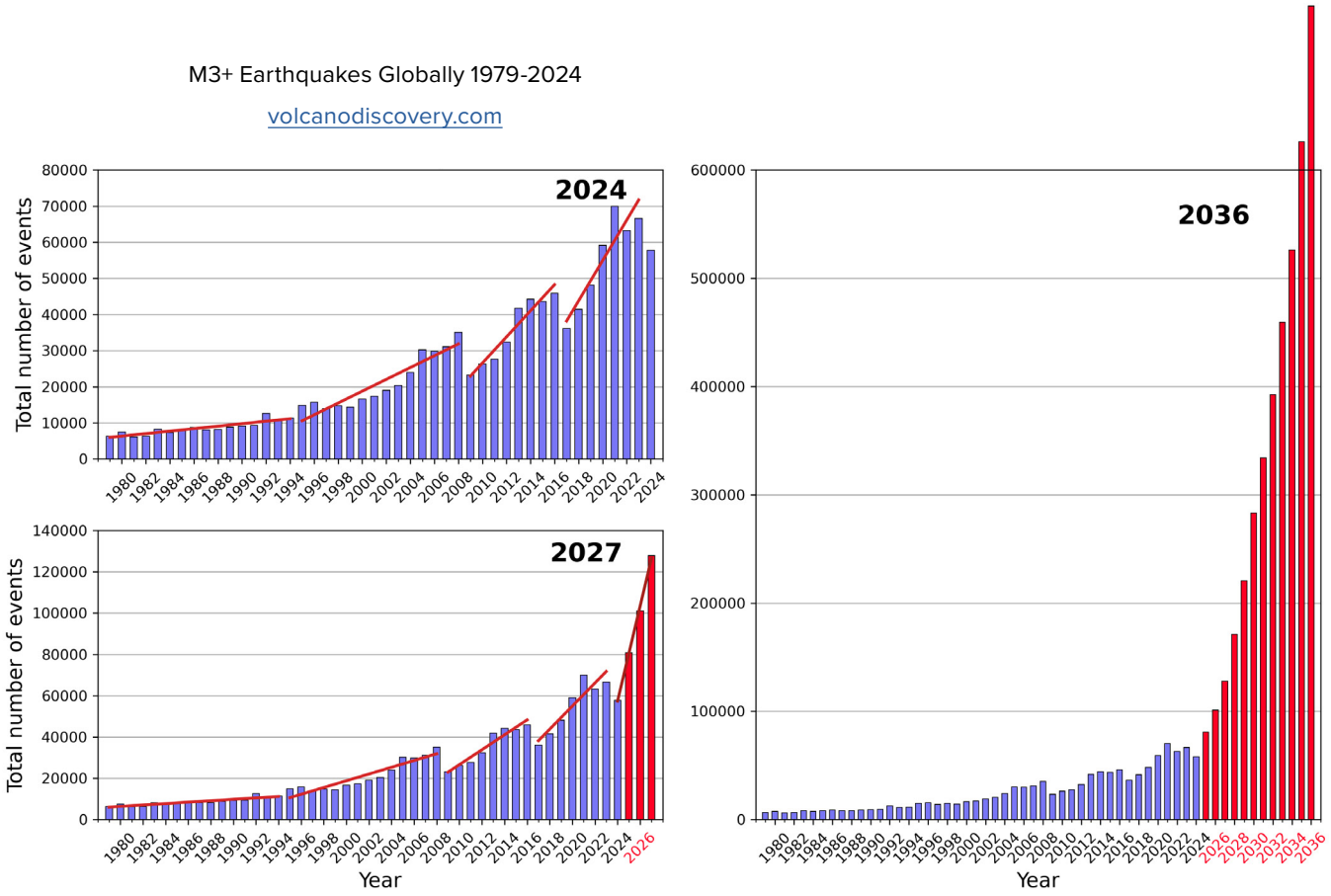

Fig. 11
Model of the exponential growth in the number of natural cataclysms on the example of earthquakes up to 2036

Graphs show the geometric progression in the frequency and magnitude of earthquakes worldwide based on current trends. At each successive stage, the number of earthquakes triples. By 2028, it is projected that Earth will experience 1,000 earthquakes per day with magnitudes above 3.0, compared to the current average of 125 such earthquakes daily.

It is highly probable that within six years, Earth will experience daily earthquakes as destructive as the one in Turkey and Syria on February 6, 2023.

This report addresses an additional threat posed by changes in Earth's core resulting from an influx of external energy. In 1997–1998, scientists, using satellite data from the Earth's Center of Mass Studies, observed an unprecedented phenomenon—a sudden shift of the planet's inner core. As a result, the core migrated northward along a trajectory from West Antarctica to Eastern Siberia and the Taimyr Peninsula in the Russian Federation. This core shift caused an uncontrolled ascent of magma in that direction, leading to the rapid rise of a massive magma plume beneath Siberia.

At present, the Siberian plume has already reached the base of the Earth's crust in the northern region of the East Siberian Craton and has begun lifting the plate. This indicates that molten magma has started burning its way to the surface.

An uncontrolled breakthrough of the Siberian plume can result in global extinction, leaving humanity no chance of survival. According to calculations, such an eruption would be 1,000 times more powerful than the most significant eruption of the Yellowstone supervolcano. Similar eruptions of a magma plume in Siberia occurred 250 million years ago, causing the Great Permian Extinction.

This report outlines three potential scenarios for the development of this situation and proposes steps to address the rising Siberian plume and mitigate the risks of its uncontrolled breakthrough.

Core Shift Toward Siberia in 1998

In 1997-1998, by studying the Earth's center of mass via satellite, scientists recorded an unparalleled phenomenon — a displacement of the Earth's inner core [12,13]. As a result, the planet's core shifted northward, along the line from West Antarctica to the Taimyr Peninsula in the north of Eastern Siberia (Fig. 12).

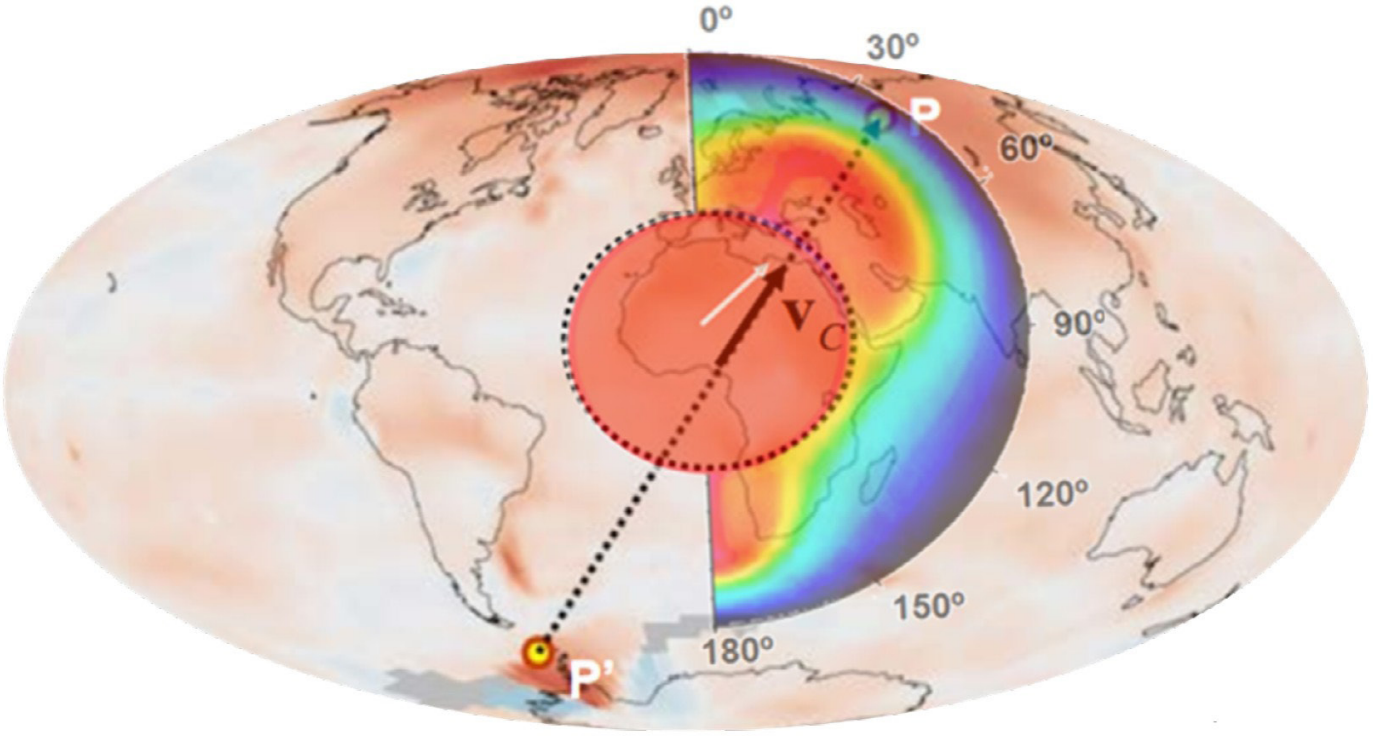

Fig. 12
Displacement of the core in 1997-1998 and thermal waves in magma caused by the core shift. (Barkin, Yu. V.)
The map depicts the displacement vector of the inner core from West Antarctica to Western Siberia, towards the Taimyr Peninsula. The scheme is overlaid on a map of atmospheric thermal anomalies.

Source: Geophysical implications of relative displacements and oscillations of the Earth's core and mantle. Presentation by Yu.V.
Barkin, Moscow, IFZ, OMTS. September 16, 2014.

[12] Barkin, Yu. V. (2011). Synchronous jumps in activity of natural planetary processes in 1997-1998 and their unified mechanism. In Geology of Seas and Oceans: Proceedings of the XIX International Scientific Conference on Marine Geology (Vol. 5, pp. 28-32). GEOS.
[13] Smolkov, G. Ya. (2018). Exposure of the solar system and the earth to external influences. Physics & Astronomy International Journal, 2(4), 310-321. https://doi.org/10.15406/paij.2018.02.00104

At the same time, four different research teams independently recorded abnormal changes in various geophysical parameters of the Earth, evidencing this event. According to the satellite data, a team of authors from Moscow State University and the Institute of Physics of the Earth of the Russian Academy of Sciences registered a displacement in the Earth's center of mass in 1998[14] (Fig. 13). Earth Rotation Service (IERS) recorded a sharp acceleration of the planet's rotation.

At the same time, at the Medicina station in Italy, scientists recorded a sudden shift in gravity[15]. Simultaneously, a sharp change in the Earth's shape[16] was observed, registered using a laser rangefinder system from US satellites.

According to the Doctor of Physical and Mathematical Sciences, Professor Yuri Barkin, Doctor of Technical Sciences, Professor Gennadi Smolkov[17], Doctor of Geographical Sciences, Professor Mikhail Arushanov[18], Academician of the Russian Academy of Sciences and Honored Professor of Lomonosov Moscow State University, Doctor of Geological and Mineralogical Sciences Victor Khain[19], and many other researchers, the displacement of the core resulted in changes in all the Earth's shells.

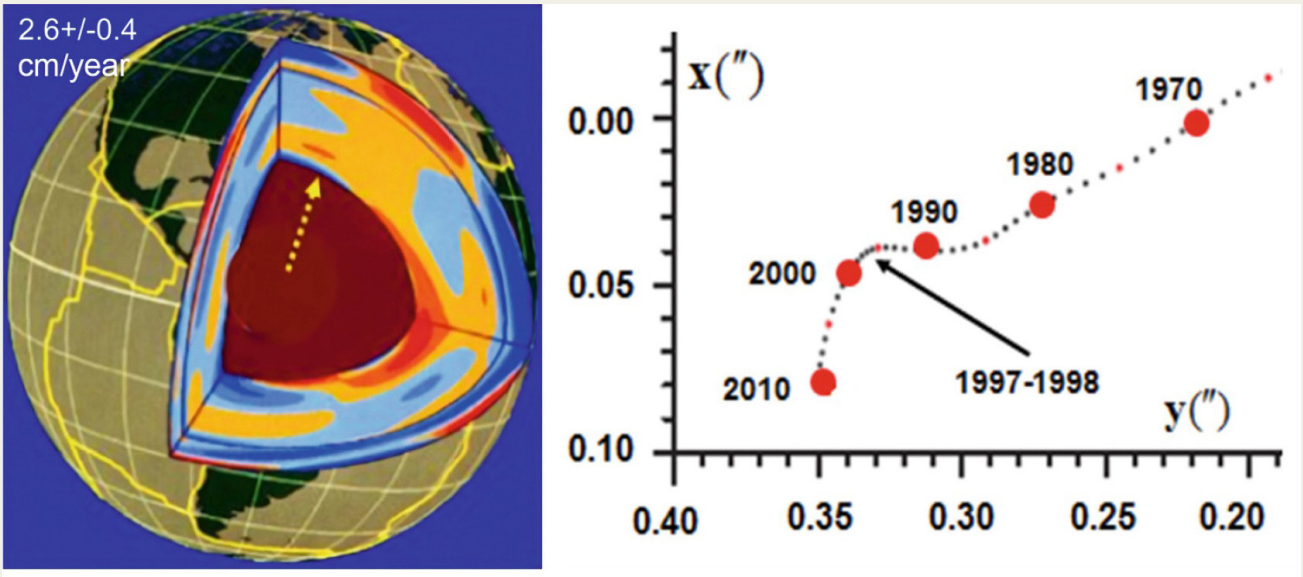

Fig 13

Internal structure of the Earth; the direction of the secular drift of the Earth's center of mass and the trajectory of its pole across the Earth's surface in 1990-2010 with an almost 90 degrees turn in 1997-1998 towards the Taimyr Peninsula

Source: Smolkov, G.Ya. (2020). Heliogeophysical Research. Issue 25, 14–29. Retrieved from http://vestnik.geospace.ru/index.php?id=569

Graph source: Barkin, Y.V., & Klige, R.K. (2012)

[14] Zotov, L. V., Barkin, Yu. V., & Lyubushin, A. A. (2009). Geocenter motion and its geodynamics. In Proceedings of the Conference "Space Geodynamics and Modeling of Global Geodynamic Processes" (pp. 98-101). Siberian Branch of RAS.

[15] Romagnoli, C., Zerbini, S., Lago, L., Richter, B., Simon, D., Domenichini, F., Elmi, C., & Ghirotti, M. (2003). Influence of soil consolidation and thermal expansion effects on height and gravity variations. Journal of Geodynamics, 35(4-5), 521-539. https://doi.org/10.1016/S0264-3707(03)00012-7

[16] Cox, C., & Chao, B. F. (2002). Detection of a large-scale mass redistribution in the terrestrial system since 1998. Science, 297(5582), 831–833. https://doi.org/10.1126/science.1072188

[17] Barkin, Yu. V., & Smolkov, G. Ya. (2013). Abrupt changes in trends of geodynamic and geophysical phenomena in 1997-1998. In Proceedings of the All-Russian Conference on Solar-Terrestrial Physics (pp. 16-21). Irkutsk.

[18] Arushanov, M. L. (2023). Causes of Earth's climate change as a result of cosmic impact, dispelling the myth of anthropogenic global warming. Deutsche Internationale Zeitschrift Für Zeitgenössische Wissenschaft, 53, 4-14. https://doi.org/10.5281/zenodo.7795979

[19] International Committee GCGE GEOCHANGE. (2010). Global environmental changes: Threat to civilization development (Vol. 1). London: GCGE. ISSN 2218-5798

It is important to note that this direction aligns with the abrupt drift of the North Magnetic Pole that started in 1995. Since the beginning of the last century, the pole was moving at an average speed of 10 km/year (6.2 miles/year), but then it suddenly increased its speed to a maximum of 57 km/year (35.4 miles/year) and changed its trajectory, heading toward Siberia and the Taimyr Peninsula[20] (Fig. 3, 14).

This indicates that the conditions for the core shift toward the Taimyr Peninsula began forming as early as 1995, driven by the liquefaction of Earth's outer liquid core. In 2013, researchers from the University of Leeds established that these changes in the magnetic field were caused by the accelerated flow of liquid iron in Earth's outer core[21] (Fig. 15), which likely commenced in 1995.

According to published data, there is a correlation between the frequency of magnetic field inversions and the intensity of mantle magmatism.[22,23,24] At the same time, it is known that magnetic field inversions are probably related to processes occurring in the outer core near the core-mantle boundary.[25] The correlation between changes in the intensity of mantle magmatism and the frequency of inversions of the Earth's magnetic field indicates that disturbances in the Earth's magnetic field occur in the outer core due to changes in the intensity of heat transfer at the bases of plumes located on the core-mantle boundary. The total heat output of the plumes is growing due to both the emergence of new plumes and an increase in the heat output of already active plumes. It may be assumed that geodynamic disturbances in the outer core and mantle occur during periods of a plume emergence and outpouring to the surface.[26]

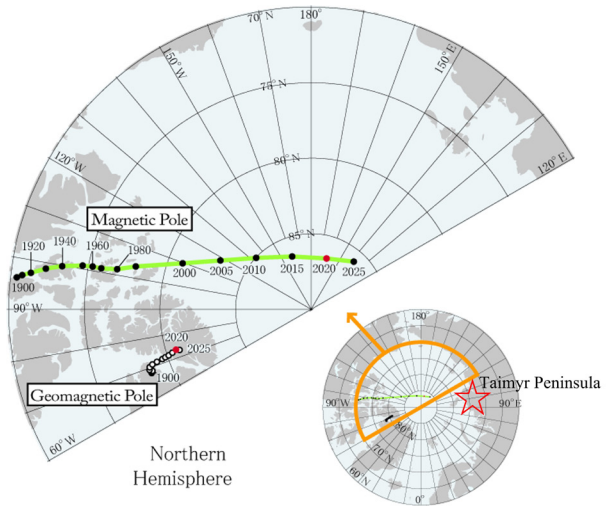

Fig. 14
Locations of geomagnetic poles and magnetic poles based on IGRF-13 from 1900 to 2015 by 5 years and at 2020 (red) and 2025 (prediction)

Source: World Data Center for Geomagnetism, Kyoto

[20]Dyachenko, A. I. (2003). Earth's magnetic poles. MCCME.
[21]Livermore, P. W., Hollerbach, R., & Finlay, C. C. (2017). An accelerating high-latitude jet in Earth's core. Nature Geoscience, 10, 62–68. https://doi.org/10.1038/ngeo2859
[22]Alain Mazaud, Carlo Laj, The 15 m.y. geomagnetic reversal periodicity: a quantitative test, Earth and Planetary Science Letters, Volume 107, Issues 3–4, 1991, Pages 689-696, ISSN 012-821X, https://doi.org/10.1016/0012-821X(91)90111-T
[23]Roger L. Larson, Peter Olson, Mantle plumes control magnetic reversal frequency, Earth and Planetary Science Letters, Volume 107, Issues 3–4, 1991, Pages 437-447, ISSN 0012-821X, https://doi.org/10.1016/0012-821X(91)90091-U
[24]Zonenshain, L.P., Kuzmin, M.I. *Deep Geodynamics of the Earth* // *Geology and Geophysics*, 1993, Vol. 34 (4), pp. 3–13.
[25]Dobretsov, N.L., Kirdyashkin, A.G., Kirdyashkin, A.A. *Deep Geodynamics*. Novosibirsk, Publishing House of the Siberian Branch of the Russian Academy of Sciences, GEO Branch, 2001, 408 p.
[26]Kirdyashkin, A.A., Kirdyashkin, A.G. Interaction of a Thermochemical Plume with Mantle Free-Convective Flows and Its Influence on Mantle Melting and Recrystallization // Geology and Geophysics, 2013, Vol. 54, No. 5, pp. 707–721.

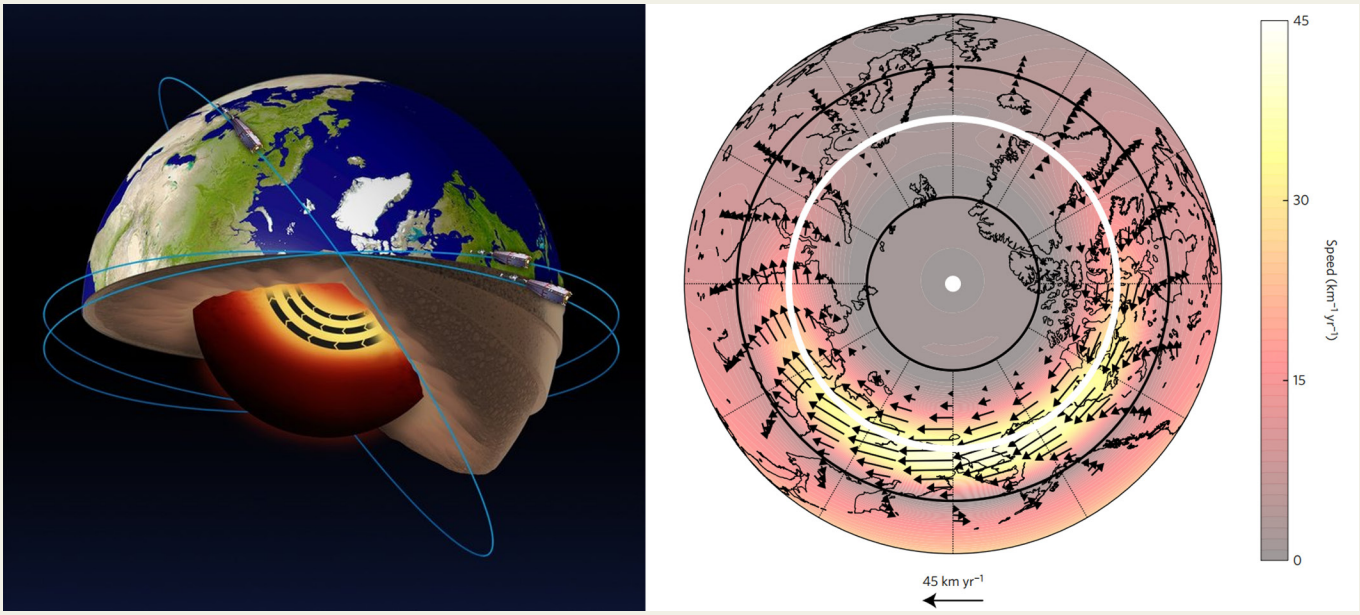

Fig. 15
Analysis of ESA Swarm satellite data has revealed the presence of a jet stream in the liquid iron part of the Earth's core at a depth of 3000 km below the surface, and also that this jet stream is accelerating
Source: ESA
Livermore, P. W., Hollerbach, R., & Finlay, C. C. (2017). An accelerating high-latitude jet in Earth's core. Nature Geoscience, 10, 62–68. https://doi.org/10.1038/ngeo2859

Therefore, the current drift of the North Magnetic Pole towards the Taimyr Peninsula may be an additional evidence of changes in the Earth's outer liquid core and a sharp rise of the plume from the core-mantle boundary under Siberia.

Thus, as a result of external cosmic influence on Earth's core in 1995, the inner core began to heat. The outer core started melting, which led to the rapid acceleration of the North Magnetic Pole's drift. The liquefaction of the outer core created the conditions for the core shift toward Siberia and the Taimyr Peninsula in 1997–1998. According to the hypothesis proposed by Dr. Yuri V. Barkin, the core shift caused an asymmetric heat transfer toward Siberia (Fig. 16). It is crucial to note that heat transfer within the mantle primarily occurs through convective mixing. This suggests that the core shift primarily triggered the ascent of magma toward Siberia. Later on, abnormal atmospheric heating began to be observed in this part of Siberia, and this heating is increasing every year.

Temperature Anomaly in Siberia in 2020

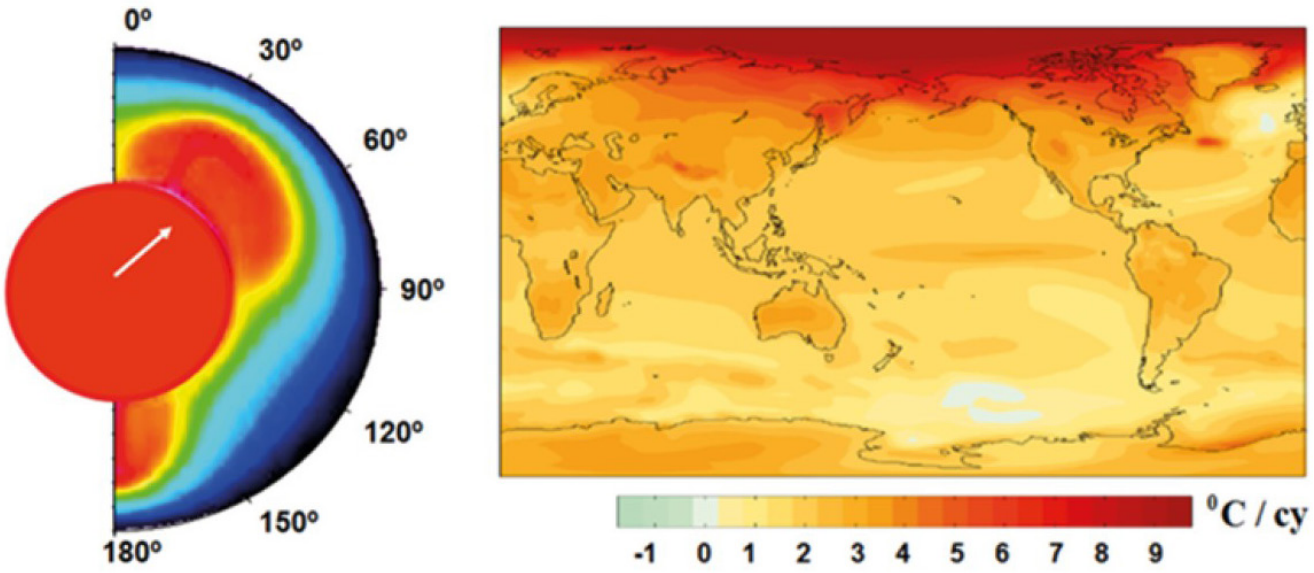

Fig. 16
Forced relative shift of the core and mantle, and the scheme of asymmetric heat supply to the upper layers of the mantle (on the left). Linear trends of surface warming (in °C per century) according to NCAR CCSM3 data averaged according to a special scenario http://www.realclimate.org/bitz_fig3.png) (on the right)
Source: Barkin, Yu.V. (2009). Ciklicheskie inversionnye izmenenija klimata v severnom i juzhnom polusharijah Zemli [Cyclic Inversion Climate Change in the Northern and Southern Hemispheres of Earth]. Geology of the Seas and Oceans: Materials of the XVIII International Scientific Conference (School) on Marine Geology. Vol. III. - Moscow: GEOS. pp. 4-8.

Siberia and the Siberian Arctic are Warming 3-4 Times Faster Than the Rest of the World

According to various organizations, the territory of Russia, in particular the Arctic region, is experiencing extreme heating.

As follows from data provided by the scientists of the Intergovernmental Panel on Climate Change (IPCC) for 2021, Russia is warming three times faster than the rest of the world, and its Arctic and Siberian regions are warming four times faster than the global average.

In 2022, Igor Shumakov, head of Roshydromet, cited data from the World Meteorological Organization[27] indicating that Russia's territory is warming at 2.5 times the global rate, with the country's northern polar region experiencing the fastest temperature increases, especially over recent decades. Siberia is among the regions experiencing the most intense warming globally (Fig. 17), an unprecedented trend over the past 7,000 years, as reconstructed from dendroclimatic studies.[28]

The US Woodwell Climate Research Center (WCRC)[29] carried out a large-scale study to assess how climate change has affected temperatures, soil moisture, snow cover thickness, precipitation levels, and other significant climatic parameters in various regions of the Arctic. To do this, scientists combined and systematized data collected via satellites, airplanes, drones, and ground-based meteorological stations over the past 40 years.

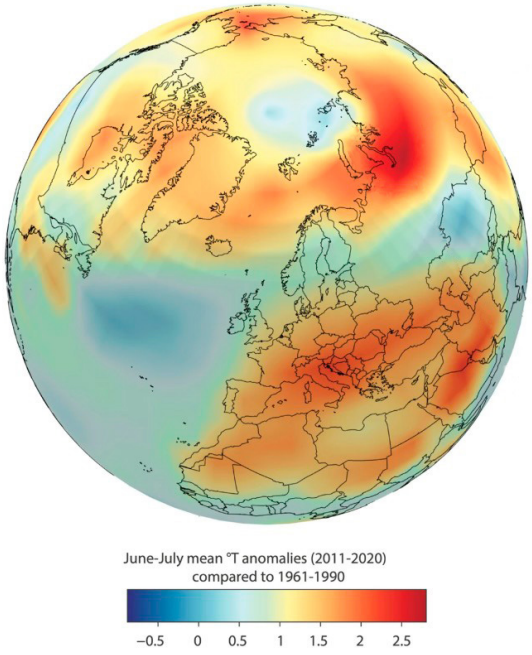

Fig. 17
Mean temperature anomalies in June–July for the Northern Hemisphere (Yamal and Taimyr Peninsulas) during the last decade of observations (2011–2020). Temperatures are expressed as anomalies relative to the baseline climate of 1961–1990 using the HadCRUT.5 dataset

Source: Hantemirov, R.M., Corona, C., Guillet, S., et al. Current Siberian heating is unprecedented during the past seven millennia. Nat Commun 13, 4968 (2022). https://doi.org/10.1038/s41467-022-32629-x

[27]TASS. (2024, January). Russia's territory is warming 2.5 times faster than the rest of the planet. TASS News Agency. https://tass.ru/obschestvo/16009287
[28]Hantemirov, R. M., Corona, C., Guillet, S., et al. (2022). Current Siberian heating is unprecedented during the past seven millennia. Nature Communications, 13, 4968. https://doi.org/10.1038/s41467-022-32629-x
[29]Watts, J. D., Potter, S., Rogers, B. M., Virkkala, A.-M., Fiske, G., Arndt, K. A., et al. (2025). Regional hotspots of change in northern high latitudes informed by observations from space. Geophysical Research Letters, 52, e2023GL108081. https://doi.org/10.1029/2023GL108081

Subsequent analysis of those data allowed the researchers to identify about two dozen climatic hotbeds. The most intensive warming has affected polar and central regions of Eastern Siberia where average annual temperatures rose by 1.1 degrees Celsius every decade, which is several times higher than the global warming rate. Temperatures rose even faster on the Taimyr Peninsula: 1.7 degrees Celsius per decade. Similarly, temperatures in the Siberian taiga have been rising at a rate of 0.6 degrees Celsius per decade since the late 1980s.

Heatwaves in Siberia have reached alarming new levels in recent years, particularly in 2020, when temperatures spiked sharply across the region (Fig. 18).

Temperatures in Siberia were more than 5°C (9°F) above average from January to June, with anomalies reaching up to 10°C (18°F) above average in June (relative to the 1981–2010 baseline). This exceptionally hot period broke local heat records, including at the Verkhoyansk meteorological station, which recorded an all-time high of +38°C (100.4°F) on June 20 (Fig. 19).

The Russian meteorological service stated that this temperature was the highest ever recorded north of the Arctic Circle.

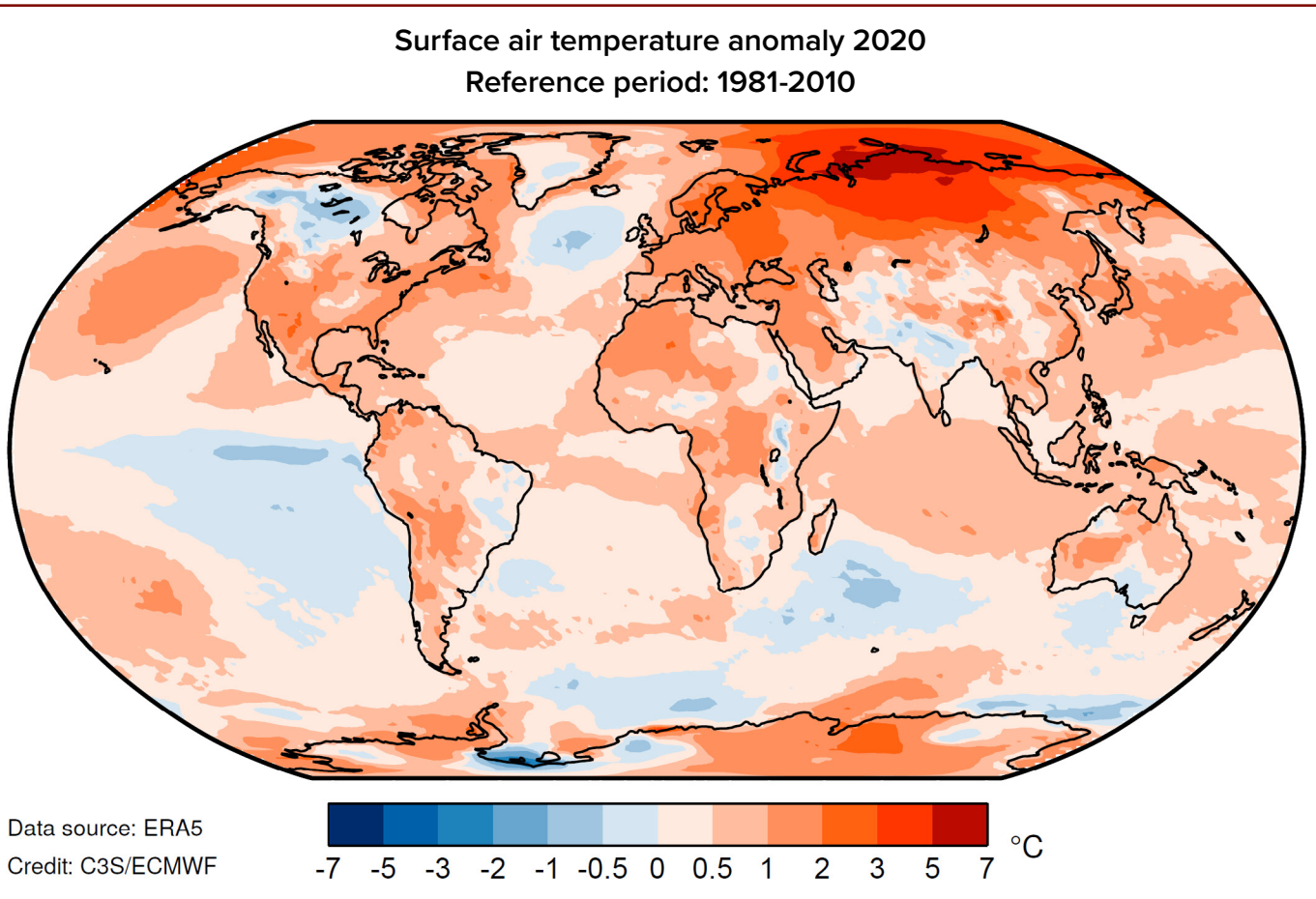

Fig. 18
Deviation of 2020 temperatures from the 1981-2010 average.
Source: Copernicus Climate Change Service, European Centre for Medium-Range Weather Forecasts (ECMWF)

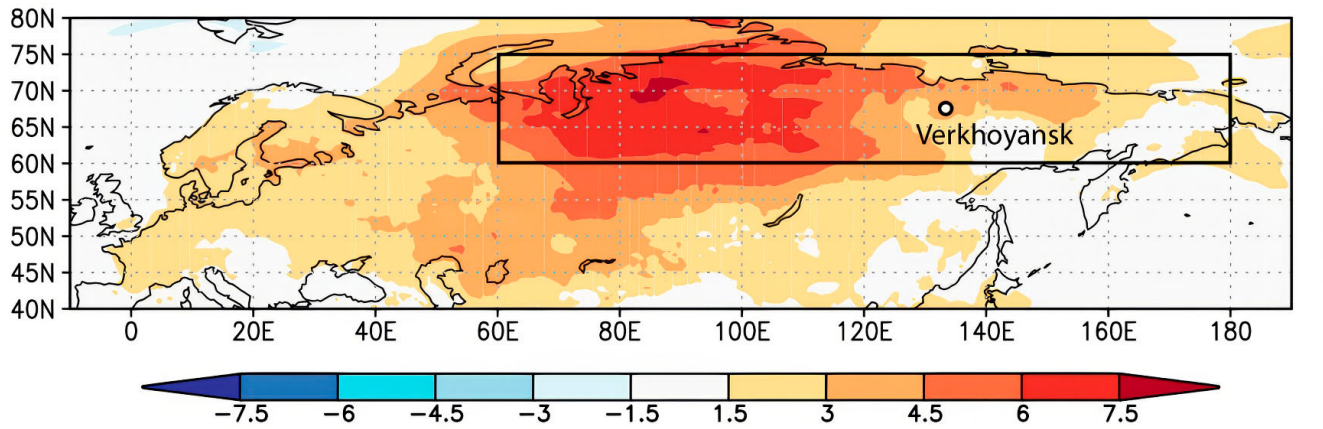

Fig. 19
Prolonged Siberian heat: Average temperatures from January to June 2020 compared to the norm (1981–2010) in the Siberian region, and the location of Verkhoyansk, where the record-breaking Arctic Circle temperature of +38°C was observed in June.

Source: Ciavarella, A., Cotterill, D., Stott, P., et al. (2021). Prolonged Siberian heat of 2020 almost impossible without human influence. Climatic Change, 166, 9. https://doi.org/10.1007/s10584-021-03052-w

These heatwaves do not persist in Siberia continuously, but occur in a pulsing pattern because magma inclusions causing the heatwaves have a wave-like character. In the atmosphere where air masses move and mix freely, heatwaves can subside within a few months as it happened in 2020, unlike heatwaves in aquatic environments.

According to 2022 research, the Siberian Arctic is warming nearly four times faster than the global average, a ratio higher than previously accounted for in climate models and one that has surprised scientists[30] (Fig. 20).

Notably, this Arctic warming is occurring specifically in the Taimyr Peninsula region. This anomaly in the oceanic zone of Siberia can be explained by the thinner oceanic crust which conducts heat more efficiently, and the higher heat capacity of water compared to the atmosphere. Ocean water, therefore, intensively absorbs and retains heat from the ascending magma plume, even though the plume is rising beneath the continental crust at a relative distance from the coastline.

[30]Rantanen, M., Karpechko, A. Y., Lipponen, A., Nordling, K., Hyvärinen, O., Ruosteenoja, K., Vihma, T., & Laaksonen, A. (2022). The Arctic has warmed nearly four times faster than the globe since 1979. Communications Earth & Environment, 3, 168. https://doi.org/10.1038/s43247-022-00498-3

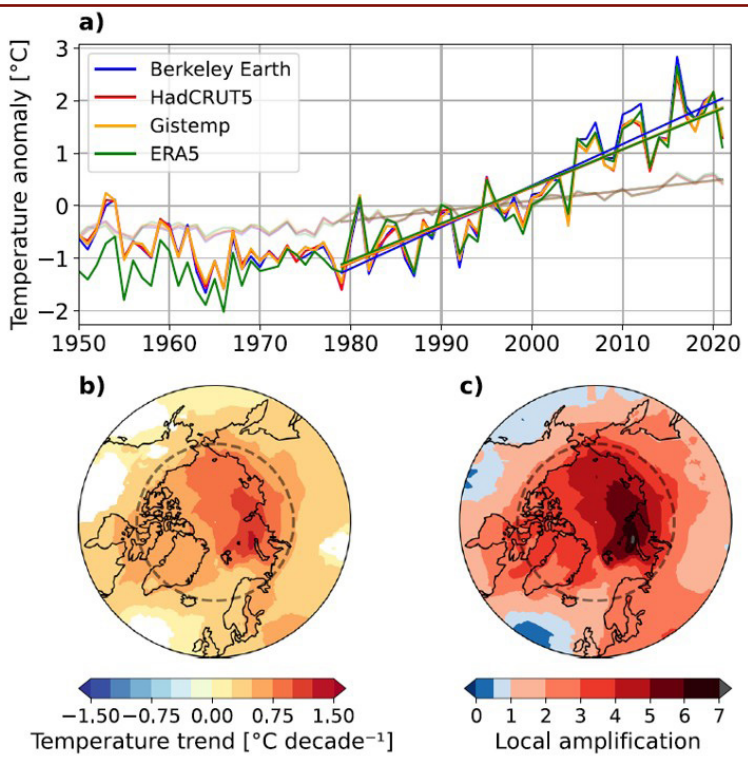

Fig. 20
Annual mean temperature evolution in the Arctic. a Annual mean temperature anomalies in the Arctic (66.5°–90°N) (dark colours) and globally (light colours) during 1950–2021 derived from the various observational datasets. Temperature anomalies have been calculated relative to the standard 30-year period of 1981–2010. The dashed line in (b) and (c) depicts the Arctic Circle (66.5N latitude)

Source: Rantanen, M., Karpechko, A. Y., Lipponen, A., Nordling, K., Hyvärinen, O., Ruosteenoja, K., Vihma, T., & Laaksonen, A. (2022). The Arctic has warmed nearly four times faster than the globe since 1979. Communications Earth & Environment, 3, 168. https://doi.org/10.1038/s43247-022-00498-3

Indirect Signs of the Siberian Plume Ascent

The intrusion of the magma plume into the Earth's crust beneath Siberia is causing not only atmospheric heating, but also a range of other anomalies: permafrost is melting from the bottom up; seismic activity in the region is increasing; hot water is rising to the surface, causing wells to boil, and unprecedented wildfires have erupted across Siberia, including under snow. The utmost localization of wildfires under snow has started manifesting in recent years in the south of the Taimyr, Yamal and Gyda peninsulas in the polar region. An important factor is that "zombie fires" — wildfires under snow — and boiling water in wells occur above the areas of deep faults (Fig. 21).

Winter fires under Distribution of fires and thermal springs in Western Siberia (as of 02.12.2021)

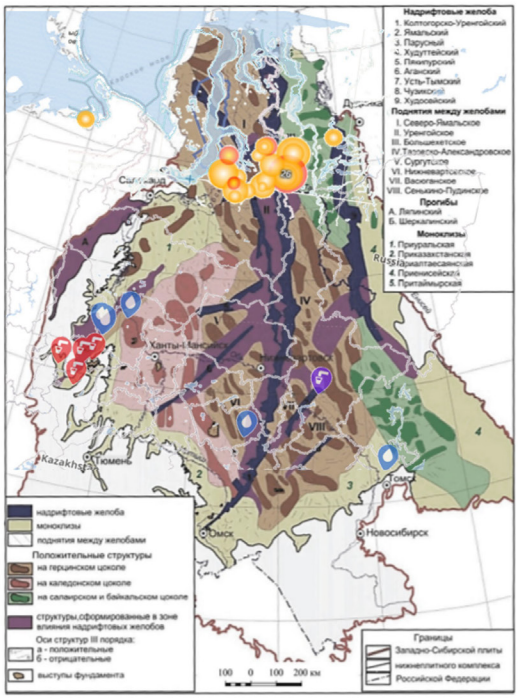

Tectonic structure map of the Lower Plate complex of the West Siberian Plate [Geological Structure..., 2005]"

Fig. 21
Map showing the localization of winter wildfires under snow beyond the Arctic Circle in 2021

Photographs of fires under snow in the Sverdlovsk region

In northern latitudes, methane and hydrogen emissions from the subsurface are increasing, the number of craters from natural gas explosions is growing, and mud volcanism is intensifying on the Arctic shelf. Heating from below causes degradation of permafrost and destruction of gas hydrates, which leads to a release of gasses, explosions of craters, and an increase in mud volcanism. The gas released from the planet's interior affects the state of the atmosphere, causing additional thermal, geochemical, and electromagnetic anomalies. Let's consider these processes in more detail.

Melting of Permafrost

Another marker of additional geothermal heat coming from the mantle plume is the condition of permafrost. The authors of the report analyzed data on the depth of seasonal melting of permafrost in Russia from 1994 to 2023. The database was compiled based on measurements carried out within the framework of the Circumpolar Active Layer Monitoring (CALM) program observing the response of the active layer and near-surface permafrost. The database is available on the website permafrost.su.

Currently, there are 58 sites in Russia that monitor permafrost by means of a standardized methodology, and 46 of the sites have been carrying out measurements for more than 10 years, making it possible to identify long-term trends. Analysis of the data array allowed researchers to identify sites where there is a steady trend of increasing depths of melting, which indicates additional heating in this area.

Two groups of data were identified: sites with a more pronounced trend of increased melting at depths from 40 cm (15.8 inches) to 200 cm (78.7 inches) (Fig. 22, a) and sites with a less intense rate of permafrost melting at depths from 40 cm (15.8 inches) to 140 cm (55.1 inches) (Fig. 22, b).

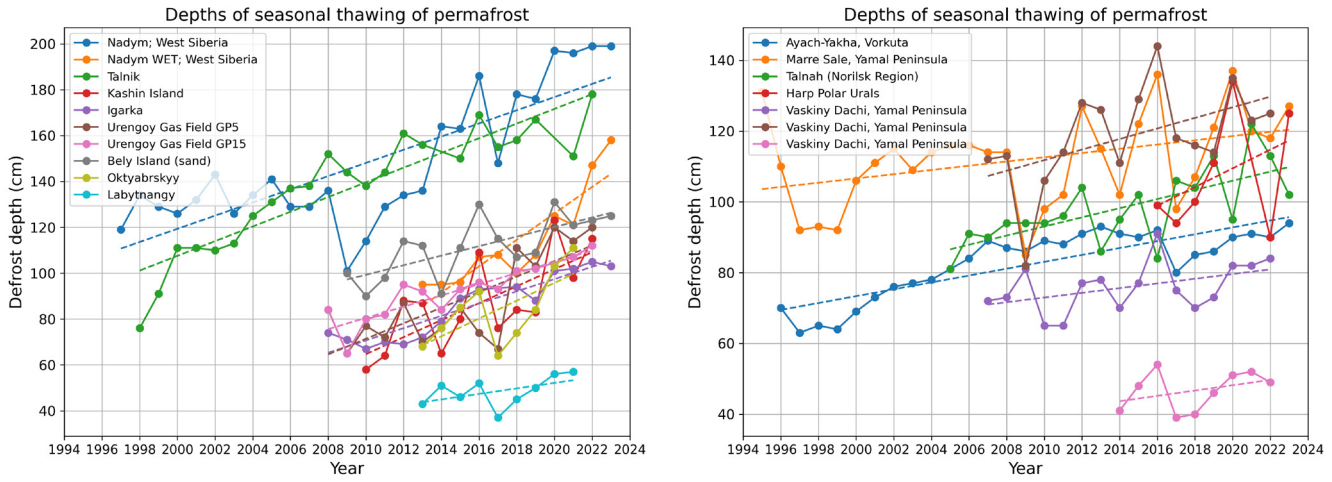

Fig. 22
Change in the depths of seasonal melting of permafrost in various regions with different intensity: a) with a more pronounced increase in the depths of melting; b) with a less pronounced increase in the depths of melting.

Data source: https://permafrost.su
Measurements are carried out within the framework of the Circumpolar Active Layer Monitoring (CALM) program: https://www2.gwu.edu/~calm

For clarity, all the monitored points were mapped and marked in orange and yellow, respectively (Fig. 23). It is noteworthy that these points are mainly concentrated in a certain region: in the north of Western Siberia, on the Yamal Peninsula, and south of the Gyda and Taimyr peninsulas.

Such localization of the areas of maximum permafrost melting corresponds to the area of reduced seismic wave velocities in the mantle, in the assumed zone of spreading of the magma plume head. This, in turn, is the cause of increased soil temperatures, including within the frozen layer.

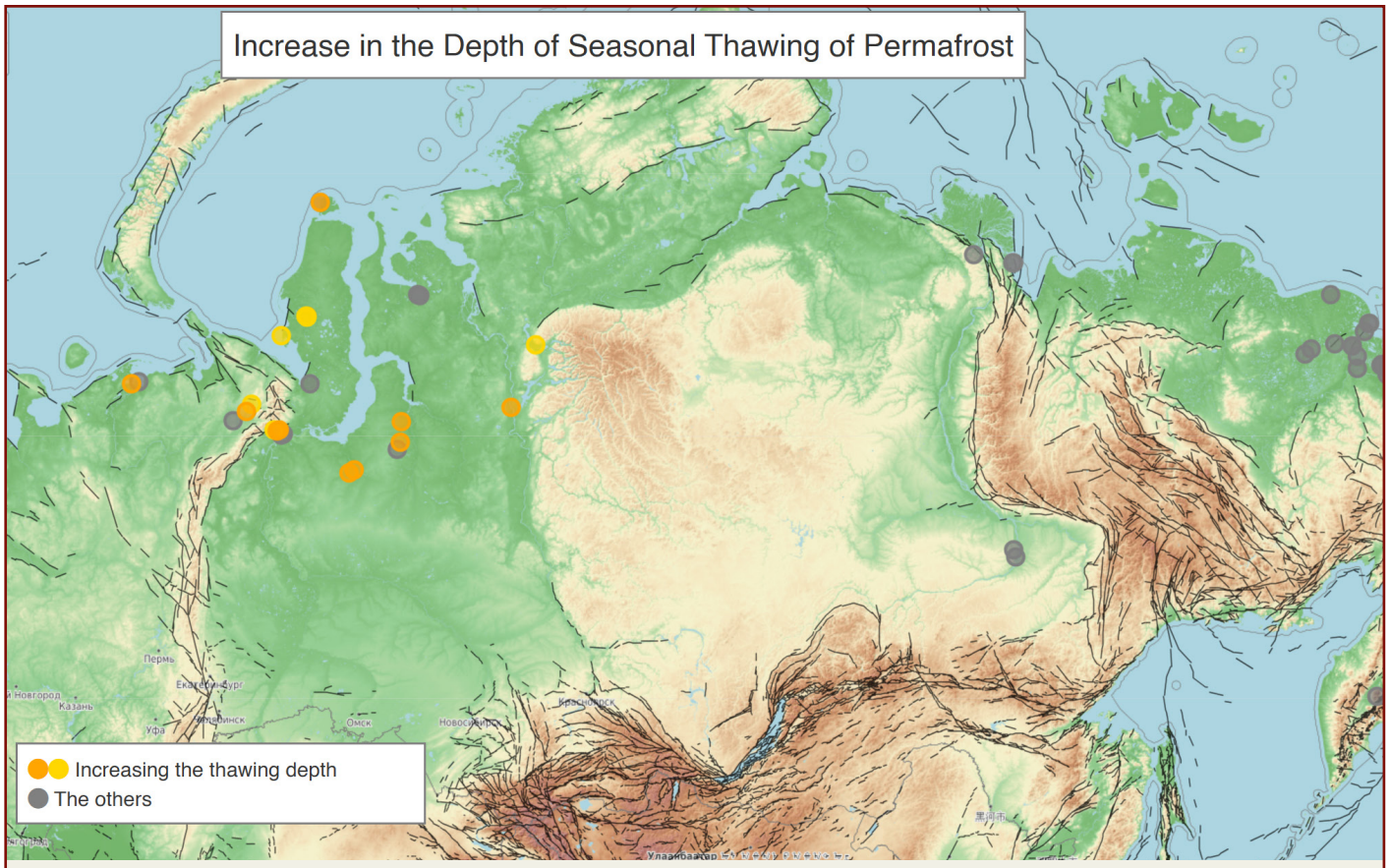

Fig. 23
Places with increased depths of seasonal melting of permafrost. Measurement sites are marked with dots: gray — places with no noticeable increase in seasonal melting, yellow — places where the depths of melting are increasing.

Data source: https://permafrost.su
Measurements are carried out within the framework of the Circumpolar Active Layer Monitoring (CALM) program: https://www2.gwu.edu/~calm

Manifestations of Mud Volcanism

Additional heating from rising magma results in degradation of permafrost and affects the gas hydrates preserved in the soils, releasing large volumes of gasses contained therein In addition, gas migrates from gas deposits and highly gas-saturated reservoir waters, reducing the elastic and strength properties of soils, promoting liquefaction of clays, and leading to possible processes of mud volcanism. Mud volcanism is a geological process of eruption of a mixture of gas, water and clastic material through cracks in the Earth's crust under the influence of internal geostatic pressure.

These processes have been discovered by researchers of the Russian Academy of Sciences (RAS) on the arctic Yamal Peninsula.[31] As a result of a complex of geological and geophysical studies using data from remote sensing of the Earth between 2014 and 2022, over 3,000 areas of powerful gas emissions with a formation of craters at the bottom of thermokarst lakes, rivers and the coastal part of the Kara Sea were identified (Fig. 24).

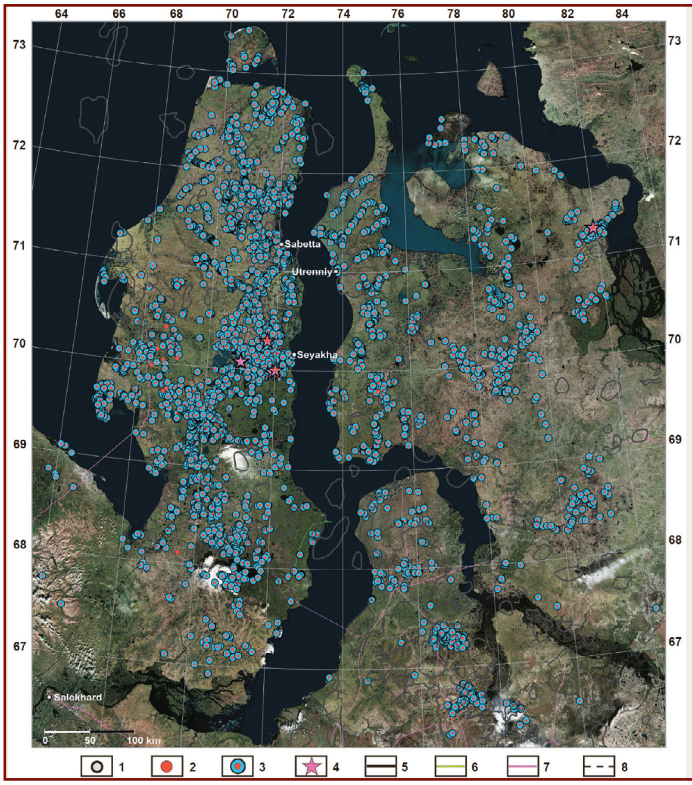

Fig. 24
Distribution of powerful gas blowout zones in the North of Western Siberia. Marks: 1 — settlements, 2 — isolated craters of gas blowouts, 3 — craters of gas blowouts on the water bottom, 4 — mud volcanic manifestations, 5 — contours of oil and gas fields, 6 — oil pipelines, 7 — gas pipelines, 8 — railway. The base map is a mosaic of satellite images by ESRI

Source: Bogoyavlensky, V. I., Nikonov, R. A. & Bogoyavlensky, I. V. New data on intensive Earth degassing in the Arctic in the north of Western Siberia: thermokarst lakes with gas blowout craters and mud volcanoes. AEE 13, 353–368 (2023). https://doi.org/10.25283/2223-4594-2023-3-353-368

[31] Bogoyavlensky, V. I., Nikonov, R. A. & Bogoyavlensky, I. V. New data on intensive Earth degassing in the Arctic in the north of Western Siberia: thermokarst lakes with gas blowout craters and mud volcanoes. AEE 13, 353–368 (2023). https://doi.org/10.25283/2223-4594-2023-3-353-368

In 2022–2023, remote sensing data revealed large mud volcanic structures for the first time on the floors of the thermokarst lakes Labvarto and Yambuto, occasionally exhibiting active mud volcanism[32] (Fig. 25). A thermokarst lake is a body of water formed by the thawing of permafrost. Thus, not only the thawing of the lake but also the liquefaction of clay deep beneath it indicates a deep-seated heat source.

According to the authors of the study, such distinct mud volcanic structures on the floors of thermokarst lakes had not been previously documented across the entire Circum-Arctic region.

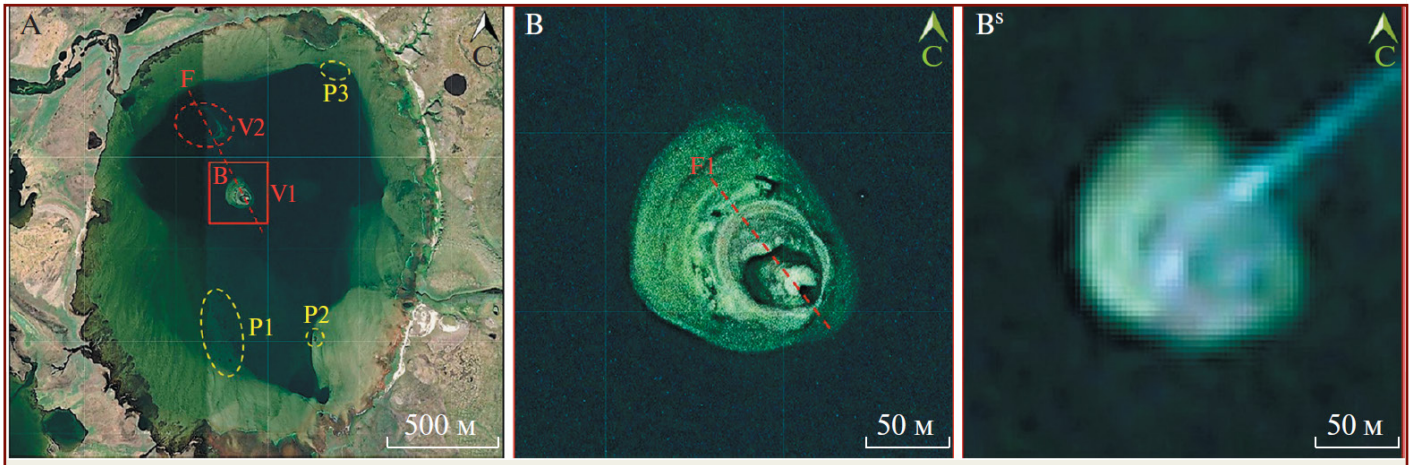

Fig. 25

WorldView-2 satellite image of the Labvarto thermokarst lake (A) and its enlarged fragment (B), supplemented with a fragment of the Sentinel-2 satellite image (BS). Marks: P1, P2, and P3 – pockmarks; V1 and V2 – mud volcanoes; F and F1 – predicted faults.

Source: Bogoyavlensky, V. I. New Data on Mud Volcanism in the Arctic on the Yamal Peninsula. Doklady Rossijskoj akademii nauk. Nauki o Zemle 512, 92–99 (2023). https://doi.org/10.31857/S2686739723601084

[32] Bogoyavlensky, V. I. NEW DATA ON MUD VOLCANISM IN THE ARCTIC ON THE YAMAL PENINSULA. Doklady Rossijskoj akademii nauk. Nauki o Zemle 512, 92–99 (2023). https://doi.org/10.31857/S2686739723601084

Soil Heating

Based on Roshydromet data from 2021–2023, soil temperature maps at depths of 80 cm, 160 cm, and 320 cm were analyzed. The most informative comparison was of temperature trends over the periods 1976–2021 and 1976–2023 (Fig. 26). Between 2021 and 2023, a distinct anomaly emerged on the trend map in the area south of the Gyda and Taimyr Peninsulas. This anomaly geographically coincides with the region of low velocities in the mantle identified by seismic tomography under the lithosphere of the Siberian region.

Given the significant depth of the measurements (320 cm) and the extensive coverage of observations (466 meteorological stations across Russia), it can be inferred that the detected temperature anomaly is associated with an increase in geothermal heat due to the rise of the magma plume.

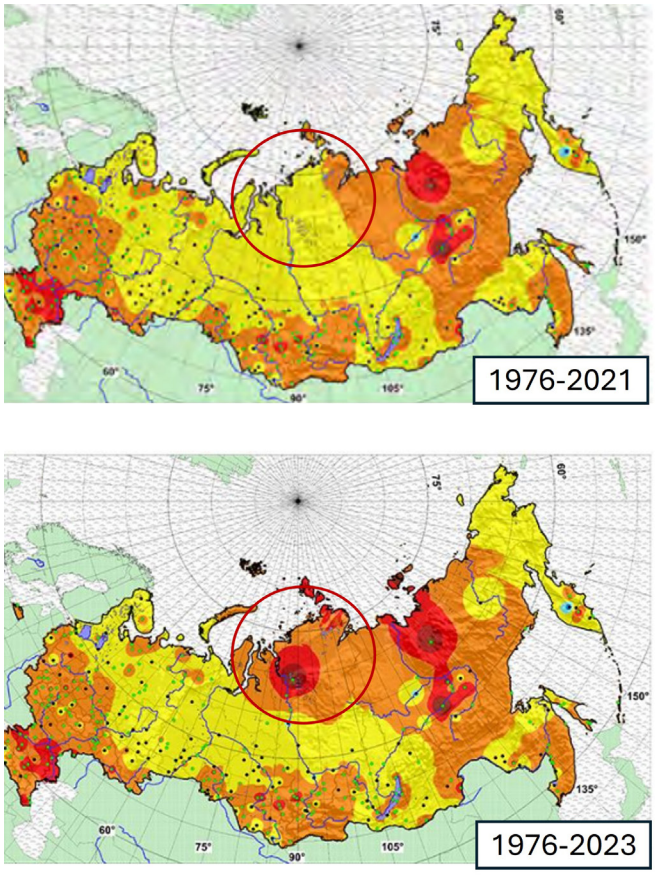

Fig. 26
Soil heating trend maps derived from Roshydromet data. Top: 1976–2021. Bottom: 1976–2023

Source:
Roshydromet. (2022). Report on climate features in the Russian Federation for 2021. Moscow: Federal Service for Hydrometeorology and Environmental Monitoring.
Roshydromet. (2024). Report on climate features in the Russian Federation for 2023. Moscow: Federal Service for Hydrometeorology and Environmental Monitoring.

Near-Surface Air Temperature

Temperature observations during the winter of 2023–2024 also reveal an anomalous pattern in near-surface air temperatures (Fig. 27). The map of average temperature anomalies from December 2023 to February 2024 shows a 2.0–4.5°C increase above the norm in the area of the Gyda and Taimyr Peninsulas.

Given the northern location of this region, such a significant winter temperature increase may be attributed to the thermal influence of the mantle plume.

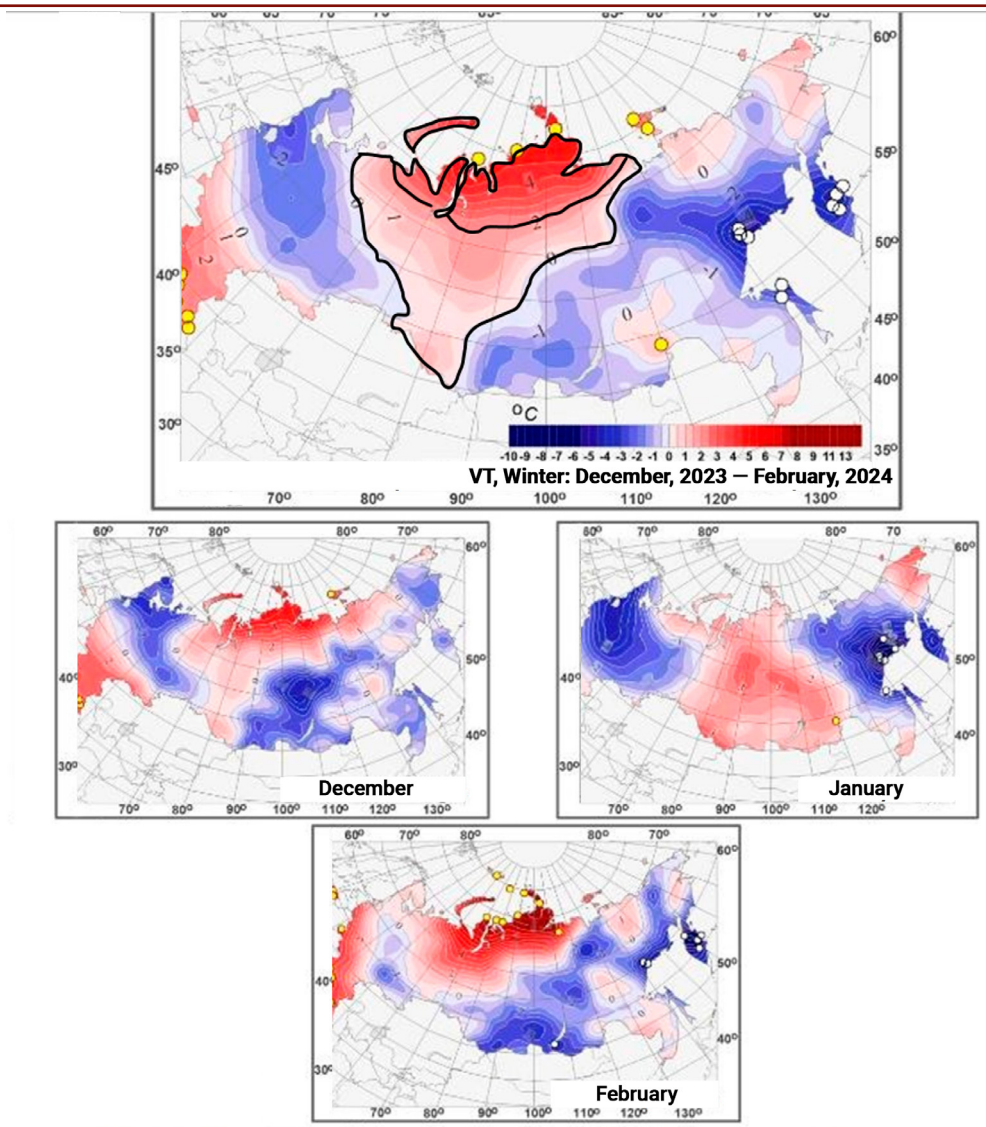

Fig. 27
Fields of average seasonal and monthly near-surface air temperature anomalies (°C) across Russia during the winter of 2023/24.
Source: Roshydromet. (2024). Report on climate features in the Russian Federation for 2023. Moscow: Federal Service for Hydrometeorology and Environmental Monitoring.

An analysis of monthly average temperature maps[33] for January and July over the period 2001–2022 shows a consistent temperature anomaly in the studied region (Figs. 28, 29). This indicates that the anomaly has not only been observed over the past two years but has persisted throughout the entire 23-year observation period, further supporting the conclusion that the plume's intrusion is influencing near-surface temperatures.

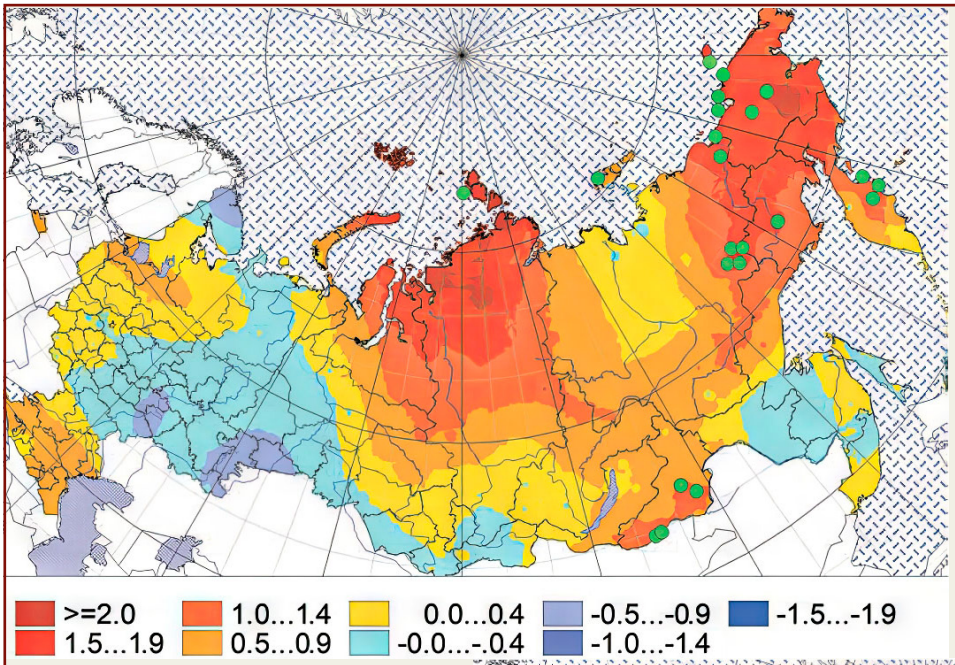

Fig. 28
Linear trend coefficients (°C/10 years) for average monthly air temperatures from 2001–2022 (within Russia's borders as of February 2022) — January.

Source: Sherstyukov, B. G. (2023). Global warming and its possible causes. Journal of Hydrometeorology and Ecology, 70, 7-37. https://doi.org/10.33933/2713-3001-2023-70-7-37

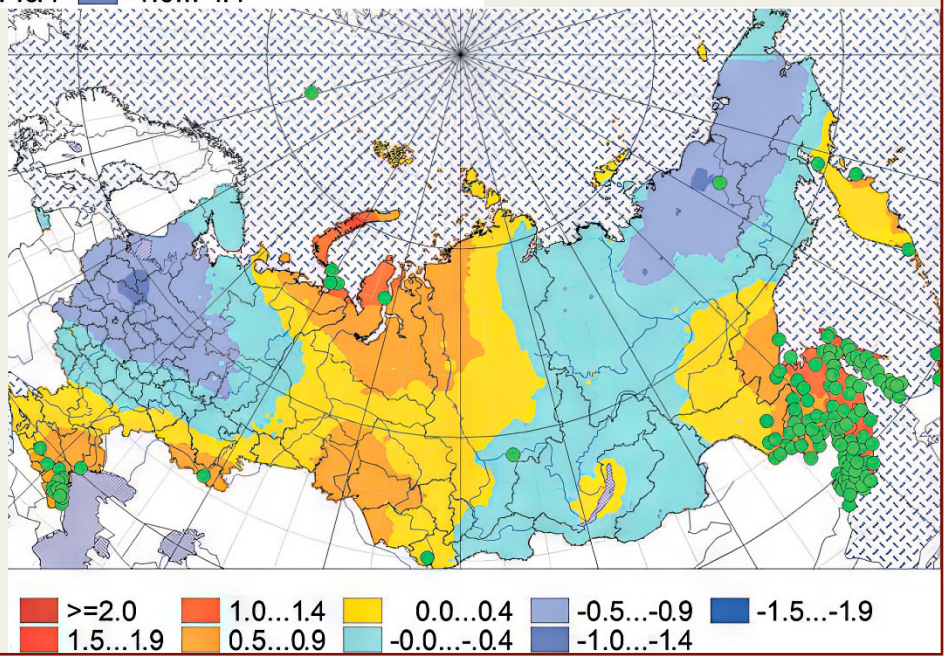

Fig. 29
Linear trend coefficients (°C/10 years) for average monthly air temperatures in Moscow from 2001–2022 (within Russia's borders as of February 2022) — July.

Source: Sherstyukov B. G. Global warming and its possible causes. Gidrometeorologiya i Ekologiya = Journal of Hydrometeorology and Ecology. 2023;(70):7—37. (In Russ.). https://doi.org/10.33933/2713-3001-2023-70-7-37

[33] Sherstyukov, B. G. (2023). Global warming and its possible causes. Journal of Hydrometeorology and Ecology, 70, 7-37. https://doi.org/10.33933/2713-3001-2023-70-7-37

Increase in Lightning Activity

The scientific community is increasingly concerned about the rise in thunderstorms and lightning strikes in the Arctic. The number of lightning strikes north of 65° N latitude has tripled between 2010 and 2020[34] (Fig. 30). Notably, the majority of these strikes are concentrated in northern Siberia, whereas they are nearly absent in northern Canada and Greenland (Figs. 31, 32).

Lightning activity is advancing toward the North Pole. In August 2019, multiple lightning strikes were reported just a few hundred kilometers from the Pole.[35] Most lightning events in the high Arctic (north of 80° N) occur during a few intense thunderstorm days each summer. However, these storms represent a new phenomenon for the region, as thunderstorms were rare in previous years.

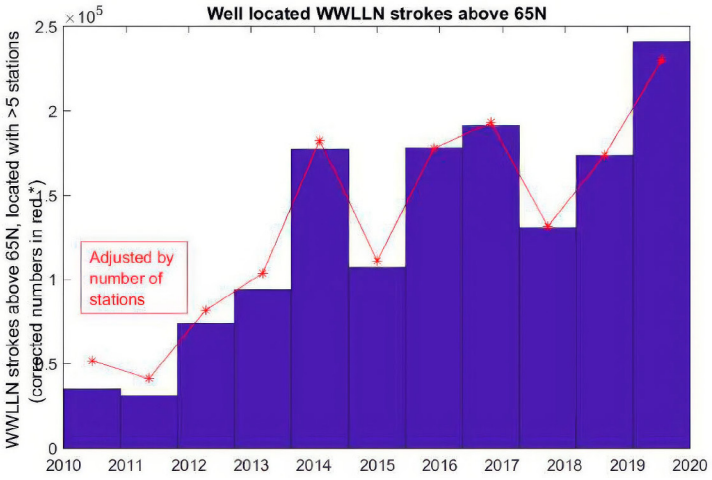

Fig. 30
Well located WWLLN strokes above 65°N (blue) and the red plot shows the adjustment based on total number of WWLLN stations. WWLLN, World Wide Lightning Location Network.

Source: Holzworth, R. H., Brundell, J. B., McCarthy, M. P., Jacobson, A. R., Rodger, C. J., & Anderson, T. S. (2021). Lightning in the Arctic. Geophysical Research Letters, 48, e2020GL091366. https://doi.org/10.1029/2020GL091366

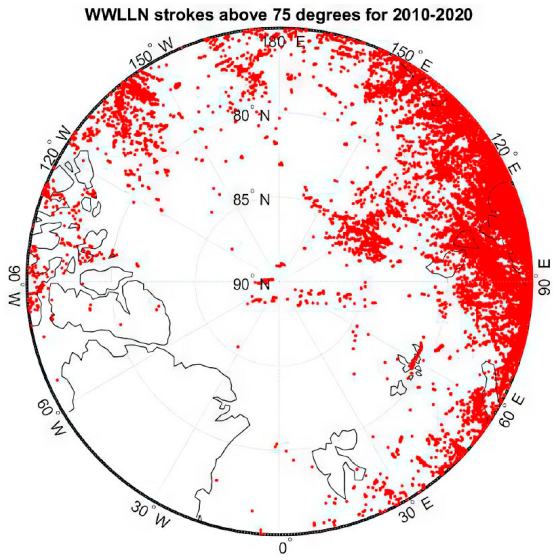

Fig. 31
Global distribution of WWLLN strokes in June July and August for 2010–2020 above 75°N. WWLLN, World Wide Lightning Location Network.

Source: Holzworth, R. H., Brundell, J. B., McCarthy, M. P., Jacobson, A. R., Rodger, C. J., & Anderson, T. S. (2021). Lightning in the Arctic. Geophysical Research Letters, 48, e2020GL091366. https://doi.org/10.1029/2020GL091366

[34] Holzworth, R. H., Brundell, J. B.,McCarthy, M. P., Jacobson, A. R.,Rodger, C. J., & Anderson, T. S. (2021).Lightning in the Arctic. GeophysicalResearch Letters, 48, e2020GL091366. https://doi.org/10.1029/2020GL091366

[35] Samenow, J. (2019, August 12). Lightning struck near the North Pole 48 times on Saturday, as rapid Arctic warming continues. The Washington Post. https://www.washingtonpost.com/weather/2019/08/12/lightning-struck-within-miles-north-pole-saturday-rapid-arctic-warming-continues/

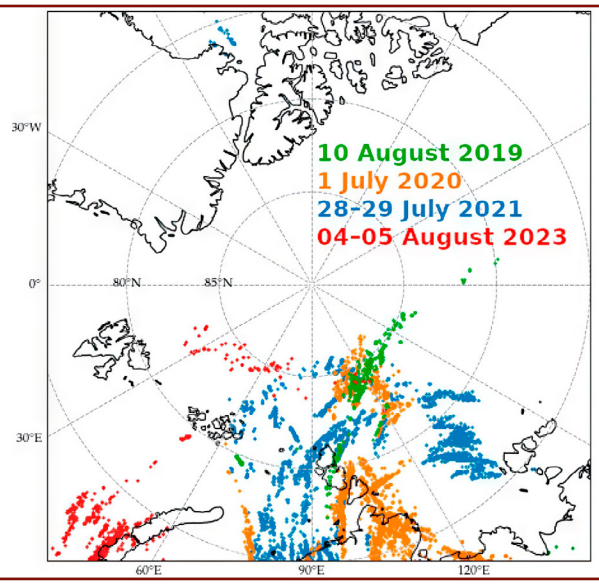

Fig. 32
Lightning locations detected by WWLLN during thunderstorms in 2019–2023. Green—2019, orange—2020, blue—2021, red—2023.

Source: Popykina, A., Ilin, N., Shatalina, M., Price, C., Sarafanov, F., Terentev, A., & Kurkin, A. (2024). Thunderstorms near the North Pole. Atmosphere, 15(3), 310. https://doi.org/10.3390/atmos15030310

The persistent location of these storms in recent years is attributed to extreme summer heat observed in northern Siberia, with temperatures reaching up to 35°C during the summer months. Additionally, it is hypothesized that an overall increase in atmospheric ionization in this region, due to magmatic plume intrusion, is also a significant factor contributing to the rise in lightning activity. This process involves the conversion of thermal energy into electrical energy via the Yutkin effect, occurring during deep-mantle explosive interactions when magma flows of different temperatures come into contact. As a result, vast amounts of energy are released from the Earth's interior, leading to an increase in surface static charge, alterations in surface potential, enhanced atmospheric ionization, and, consequently, a surge in lightning activity.

Additionally, significant volumes of gas are released through fractures in the Earth's crust. This process may influence cloud formation and local weather conditions. Magma intrusion is a key factor in surface warming, increased atmospheric moisture, and the development of thermal anomalies, all of which contribute to the formation of thunderclouds and lightning.

Since the formation of thunderstorms and lightning requires a combination of cold air, warm air, and convective instability, the location of the Siberian mantle plume provides optimal conditions for their development.

Ozone Layer Depletion

Magmatic activity within the Earth's interior is accompanied by the release of significant amounts of volcanic gases, including hydrogen, methane, and carbon dioxide. According to the research of V. L. Syvorotkin,[36] hydrogen emissions contribute to the degradation of the ozone layer. Since magma ascent occurs in a pulsatile manner, degassing and subsequent ozone layer destruction will also manifest sporadically, that is, as occasional events.

Ozone layer anomalies have been observed over northern Siberia since 1997–1998, coinciding with the shift of the Earth's core toward the Taimyr Peninsula. Episodes of ozone depletion were recorded in 2011, 2016, and 2020,[37] with the most severe ozone deficit occurring in 2016.[38] At the end of January 2016, for the first time since monitoring began in 1973, an ozone anomaly was detected over the northern Urals and Siberia, with total ozone content measuring 190–200 DU—40–45% lower than the long-term average. This anomaly persisted for up to one week (Fig. 33).

A significant reduction in total ozone content was also recorded using the Ozone Monitoring Instrument (OMI) aboard NASA's Aura satellite (Fig. 34).

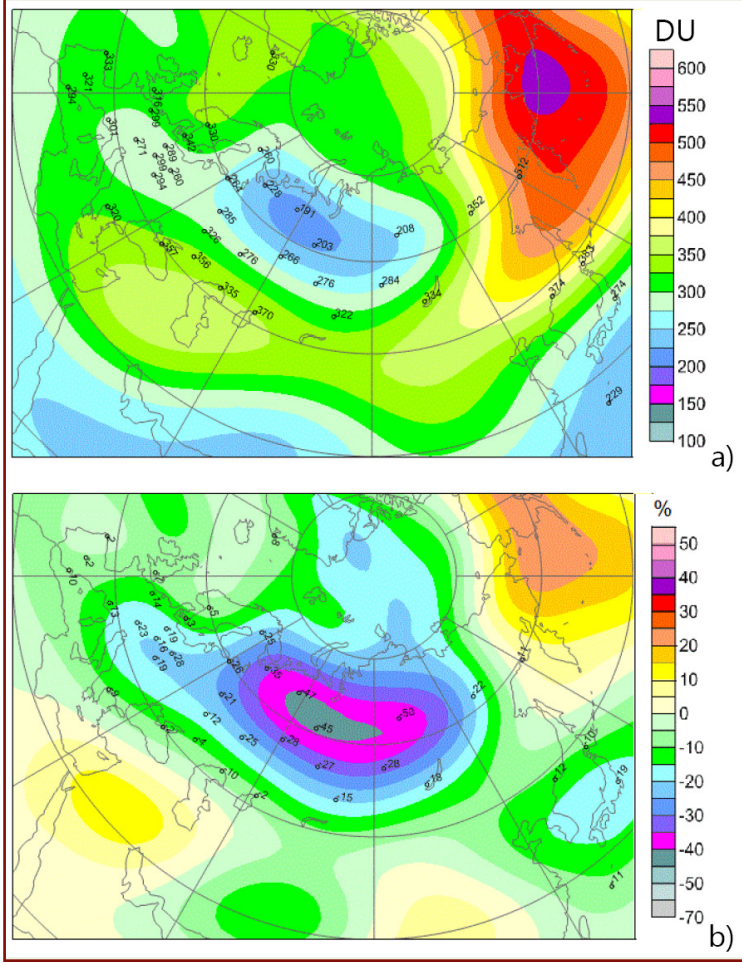

Fig. 33
Total ozone content (a) and its deviations from the norm (b) on January 28, 2016, based on WOUDC satellite data [http://woudc.org/]. The numbers on the map represent total ozone measurements from ground-based ozone monitoring stations.

Source: Nikiforova, M. P., Vargin, P. N., Zvyagintsev, A. M., Ivanova, N. S., Kuznetsova, I. N., & Luk'yanov, A. N. (2016). Ozone mini-hole over the Northern Urals and Siberia. Proceedings of the Hydrometeorological Research Center of the Russian Federation, 360, 168–180. In Proc. of the Hydrometeorological Conf., February 9–10, Vol. 4, 91–96. Voronezh: Nauchno-Issledovatel-skie Publikatsii.

[36]Syvorotkin, V. L. DEEP DEGASSING IN POLAR REGIONS OF THE PLANET AND CLIMATE CHANGE. APOG (2018) doi:10.29222/ipng.2078-5712.2018-23.art48
[37]Xia, Y. et al. Significant Contribution of Severe Ozone Loss to the Siberian- Arctic Surface Warming in Spring 2020. Geophysical Research Letters 48, e2021GL092509 (2021). https://doi.org/10.1029/2021GL092509
[38]Nikiforova, M.P. Extremely low total ozone values over the northern Ural and Siberia in the end of January 2016. AOO (2017) doi:10.15372/AOO20170102

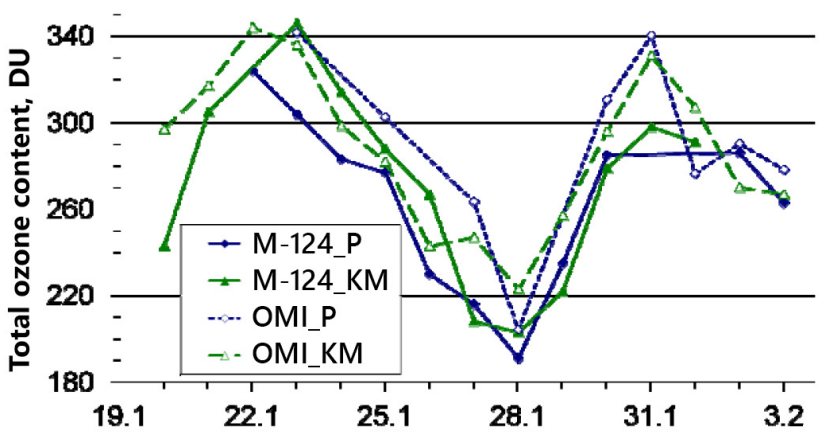

Fig. 34
Total ozone content measured using the ground-based M-124 ozonometer and the OMI instrument on the Aura satellite (USA) at the Pechora (P) and Khanty-Mansiysk (KM) stations from January 20 to February 3, 2016.

Source: Nikiforova, M. P., Vargin, P. N., Zvyagintsev, A. M., Ivanova, N. S., Kuznetsova, I. N., & Luk'yanov, A. N. (2016). Ozone mini-hole over the Northern Urals and Siberia. Proceedings of the Hydrometeorological Research Center of the Russian Federation, 360, 168–180. In Proc. of the Hydrometeorological Conf., February 9–10, Vol. 4, 91–96. Voronezh: Nauchno-Issledovatelskie Publikatsii.

It is important to note that the long-term seasonal cycle of total ozone content in the extratropical latitudes of the Northern Hemisphere typically reaches its minimum in September and its maximum in March–April. However, in 2016, ozone degradation occurred unusually early, in January, reaching the lowest recorded levels in the history of instrumental observations.

Thus, ozone layer depletion over the Siberian region may serve as an additional indicator of gas emissions through crustal fractures, resulting from the upward movement of the magmatic plume toward the surface.

Structure, Possible Dimensions, and Localization of the Magma Plume, Based on Published and Observational Data

The plume structure may be roughly visualized as a mushroom. It has a tail (stem) that carries heated material from the core-mantle boundary upwards. The upper part of a plume, which expands as it rises, forms the plume head. When a plume reaches the base of the lithosphere, it encounters a refractory layer of solidified rocks, causing the head to spread horizontally beneath the lithosphere, like a mushroom cap (Fig. 35).

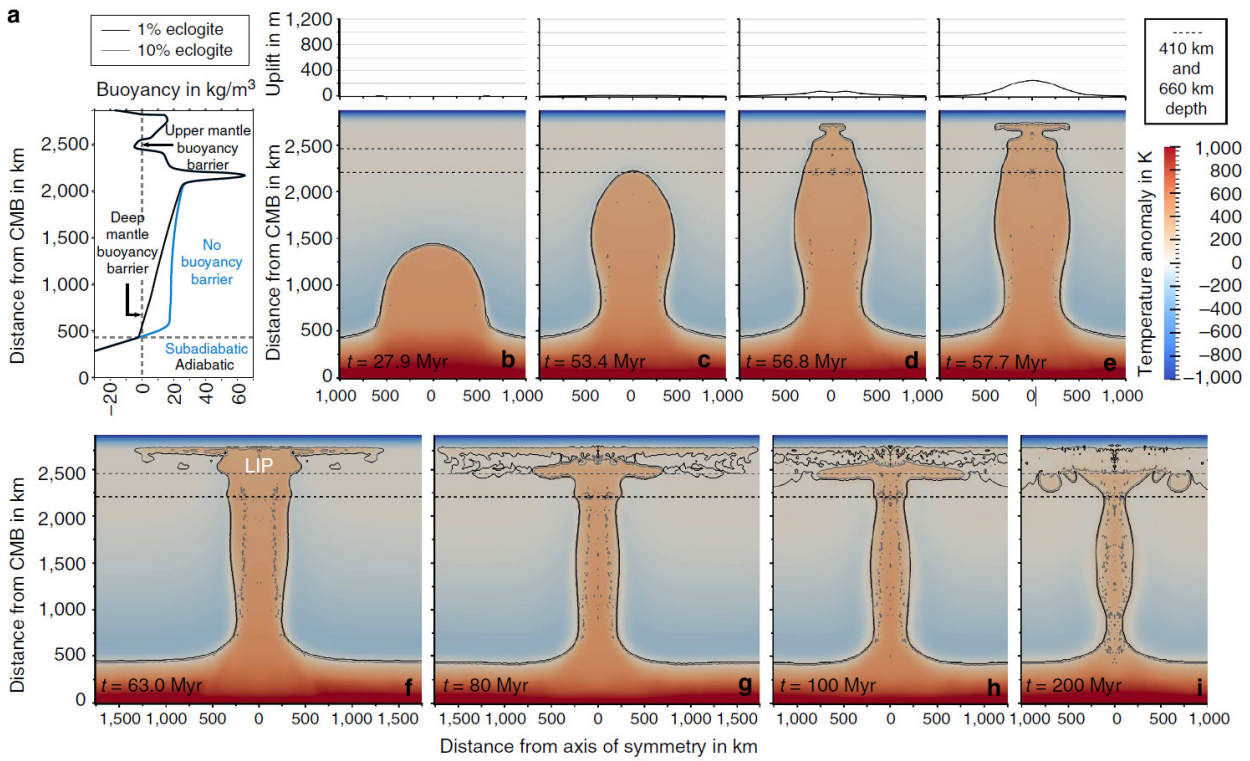

Fig. 35

The illustration presents a model of magmatic plume evolution, similar to the one that formed the Siberian Traps 250 million years ago.

The graph on the left (a) depicts how magma rises through different layers of Earth's mantle. The main section of the image (b–i) serves as a "timeline," showing the stages of plume development: Initially, a "column" of hot magma ascends from the mantle's base. Gradually, this column reaches the upper mantle, where it expands into a "mushroom-like" head. Over time, the plume becomes thinner and begins to fragment into separate structures. The colors in the diagram represent temperature: Red and orange areas indicate the hottest regions. Blue areas represent cooler regions.

Source: Dannberg, J., & Sobolev, S. (2015). Low-buoyancy thermochemical plumes resolve controversy of classical mantle plume concept. Nature Communications, 6, 6960. https://doi.org/10.1038/ncomms7960

According to research data, as the plume approaches the lithosphere, its radius doubles as it flows, and its ascent speed significantly decreases.[39] The rising hot material from the plume tail exerts pressure and burns through the lithosphere, forming cracks. In weak areas, secondary plumes are then formed — upper magmatic chambers within the Earth's crust. Such chambers exist, for example, under Yellowstone, Campi Flegrei, and other supervolcanoes. Those chambers are the sites where crustal breaches and massive magma eruptions can occur.

It is important to note that, according to existing models, the ascent of a plume to the surface may take tens of millions of years. However, these calculations are based on theoretical assumptions, while practical observations of the ongoing escalation of geodynamic processes suggest otherwise. Observations in Siberia indicate that the plume's ascent could occur within several decades.

Based on literature,[40] it is known that a similar magmatic superplume, which caused numerous basalt eruptions in Eurasia (in Siberia) at the boundary of the Permian and Triassic periods (250 million years ago), had the following dimensions: 4000 km from west to east and 3000 km from north to south. The head of the plume is assumed to have had a diameter of 1000 to 2000 km.

It is known that the West Siberian Plate is younger and thinner, with a thickness of 35 to 40 kilometers. Conversely, the East Siberian Plate (or platform), known as the Siberian Craton, is older, thicker, and colder, with a thickness of 40 to 45 kilometers. According to seismic tomography data,[41] scientists assume that small magmatic hotbeds are currently observed beneath the East Siberian Platform. Those hotbeds spread laterally under the Siberian Craton (Fig. 36) due to the plate's colder nature.

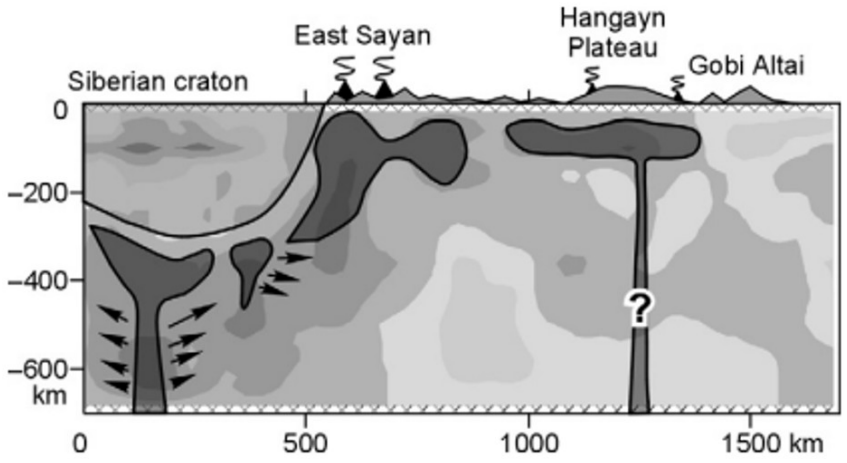

Fig. 36
Diagram from the article, illustrating how small magmatic hotbeds (shown with arrows on the left) flow round the Siberian Craton

Source: Koulakov, I. Y. (2008). Upper mantle structure beneath Southern Siberia and Mongolia from regional seismic tomography. Russian Geology and Geophysics, 49(3), 187-196. https://doi.org/10.1016/j.rgg.2007.06.012

[39] Ernst, R. E., & Buchan, K. L. (2002). Maximum size and distribution in time and space of mantle plumes: evidence from large igneous provinces. Journal of Geodynamics, 34, 309-342.
[40] Lvova, E. V. (2010). Tectonics of mantle plumes: Evolution of basic concepts. Moscow University Geology Bulletin, 5, 21-29.
[41] Koulakov, I. Y. (2008). Upper mantle structure beneath Southern Siberia and Mongolia from regional seismic tomography. Russian Geology and Geophysics, 49(3), 187-196. https://doi.org/10.1016/j.rgg.2007.06.012

According to the hypothesis, the modern Siberian plume is currently spreading beneath the base of the East Siberian Plate and partially beneath the West Siberian Plate. This spreading is thought to occur at depths of 50–60 km (31–37 miles), with the plume's "tail" most clearly observed at depths of around 100 km (62 miles). Secondary plume intrusions are likely already occurring at depths of approximately 40 km (25 miles).

Some seismotomographic models reveal low-velocity anomalies[42] (indicative of a more molten environment) at depths of 110–150 km (68–93 miles), consistent with a liquid mantle region beneath areas south of the Gyda and Taimyr Peninsulas (Fig. 37). These anomalies, as seen in velocity maps from an August 2024 study, are presumed to correspond to two inflows of magmatic material, referred to as the plume "tails" (Fig. 38).

If this model is accurate, the diameter of each plume tail rising beneath the East Siberian Craton is approximately 600–700 km (373–435 miles).

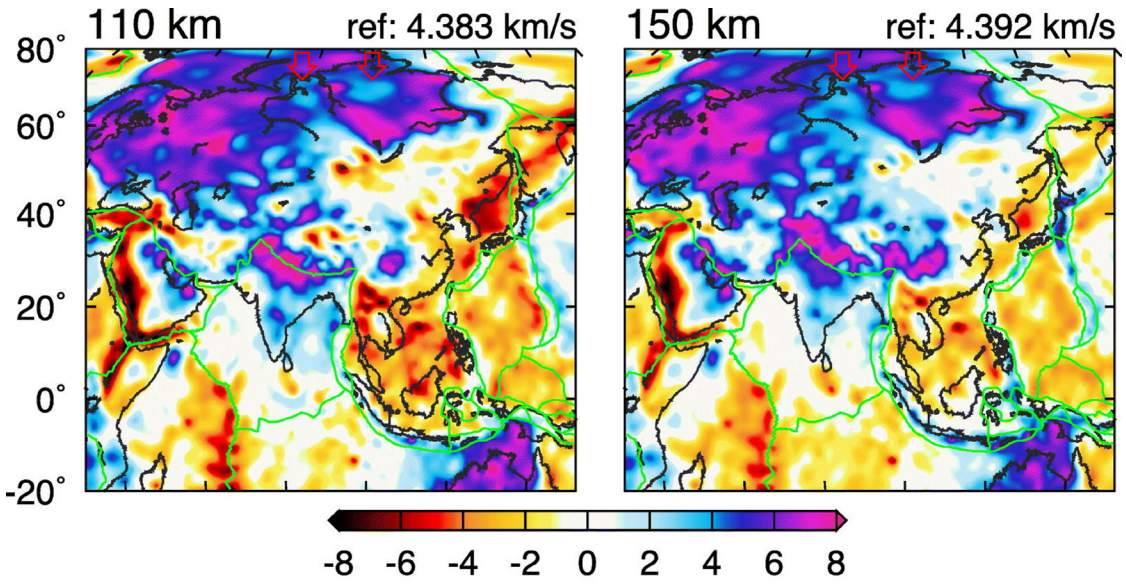

Fig. 37
The map shows regions of high seismic wave propagation speeds, represented in purple, which correspond to harder and denser rocks, while blue areas indicate zones of reduced speeds, suggesting the presence of more ductile or molten material. Low-velocity seismic waves anomalies corresponding to zones of more liquid mantle content are highlighted with two red arrows.

Source: Dou, H., Xu, Y., Lebedev, S., Chagas de Melo, B., van der Hilst, R. D., Wang, B., & Wang, W. (2024). The upper mantle beneath Asia from seismic tomography, with inferences for the mechanisms of tectonics, seismicity, and magmatism. Earth-Science Reviews, 255, 104841. https://doi.org/10.1016/j.earscirev.2023.104595

[42] Dou, H., Xu, Y., Lebedev, S., Chagas de Melo, B., van der Hilst, R. D., Wang, B., & Wang, W. (2024). The upper mantle beneath Asia from seismic tomography, with inferences for the mechanisms of tectonics, seismicity, and magmatism. Earth-Science Reviews, 247, 104595. https://doi.org/10.1016/j.earscirev.2023.104595

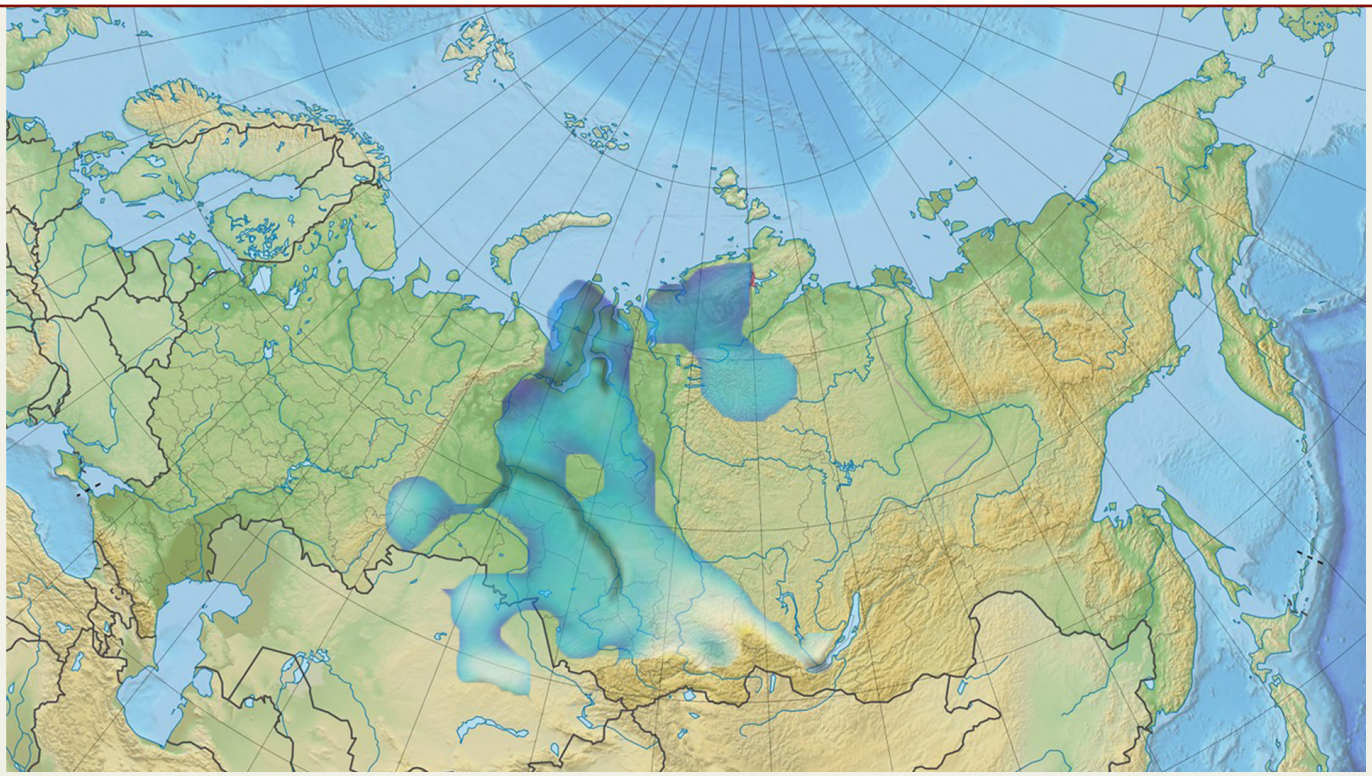

Fig. 38
Physical map of Russia showing and adapting low-velocity seismic waves anomalies based on data by Dou et al., 2024

It is important to note that the seismotomographic analysis presented in the Dou et al. (2024) study for Siberia relied on data from fewer than 10 seismic sensors (Fig. 39), all of which are positioned along plate boundaries with virtually no coverage within Western and Eastern Siberia. The analysis used data from all publicly available wide-range earthquake recordings from 1994 through September 4, 2023. For comparison, the red triangles on the map indicate the sensors used in the analysis for Asia, which number in the thousands.

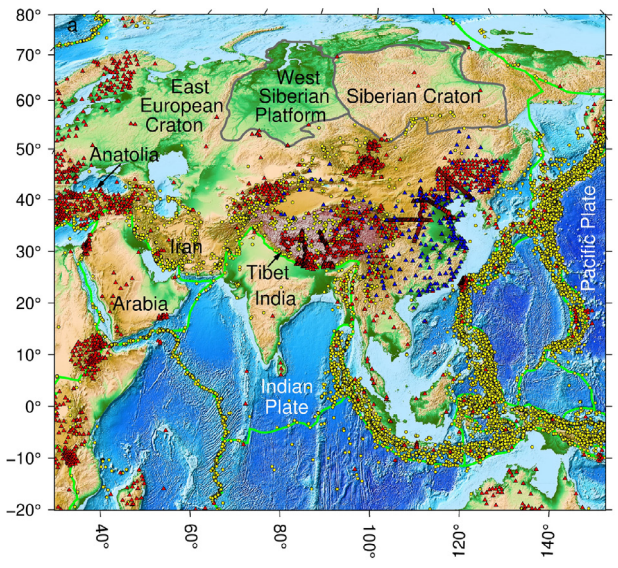

Fig. 39
Location of sensors (red triangles) used in seismic tomographic analysis

Source: Dou, H., Xu, Y., Lebedev, S., Chagas de Melo, B., van der Hilst, R. D., Wang, B., & Wang, W. (2024). The upper mantle beneath Asia from seismic tomography, with inferences for the mechanisms of tectonics, seismicity, and magmatism. Earth-Science Reviews, 247, 104595. https://doi.org/10.1016/j.earscirev.2023.104595

A 2023 study by Chinese researchers confirms that magma activity is currently melting and thinning the crust beneath Siberia[43] (Fig. 40). This ongoing process reduces the solidity of the lithospheric plate. The authors present mantle's electrical conductivity model for Northern Asia, derived from geomagnetic data, which highlights a major conductivity anomaly within the mantle transition zone beneath the Siberian Traps during their eruption. This anomaly is interpreted as a thermal irregularity with traces of melt, linked to the Permian anomaly in the region (Fig. 41).

Overall, seismotomographic models investigating depths of 40 to 110 km in the East Siberian Craton show differing results. There is a clear lack of seismological data for Siberia, which limits the accuracy of these models.

Modern tomographic models are based on seismic data collected over a long period—approximately 30 years. From the perspective of classical concepts of mantle plume evolution, which spans millions of years, a 30-year timeframe is considered extremely short. However, existing data indicate that significant structural changes have occurred in the Siberian plume during this period.

These observations highlight the need to revise current understandings of mantle plume development rates and the methodologies used to study them.

Fig. 40
White dots indicate the stations whose C-responses were used in this study. The Permian anomaly range is shown as a zone outlined by white lines. The current location of the Siberian Traps is marked in blue, while previous positions are marked in yellow, with dashed lines.

Source: Li, S., Li, Y., Zhang, Y., Zhou, Z., Guo, J., & Weng, A. (2023). Remnant of the late Permian superplume that generated the Siberian Traps inferred from geomagnetic data. Nature Communications, 14, 1311. https://doi.org/10.1038/s41467-023-37053-3

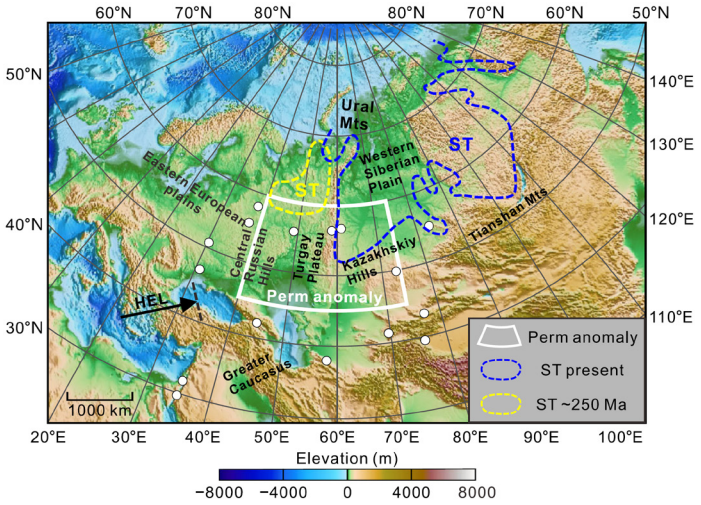

[43] Li, S., Li, Y., Zhang, Y., Zhou, Z., Guo, J., & Weng, A. (2023). Remnant of the late Permian superplume that generated the Siberian Traps inferred from geomagnetic data. Nature Communications, 14, 1311. https://doi.org/10.1038/s41467-023-37053-3

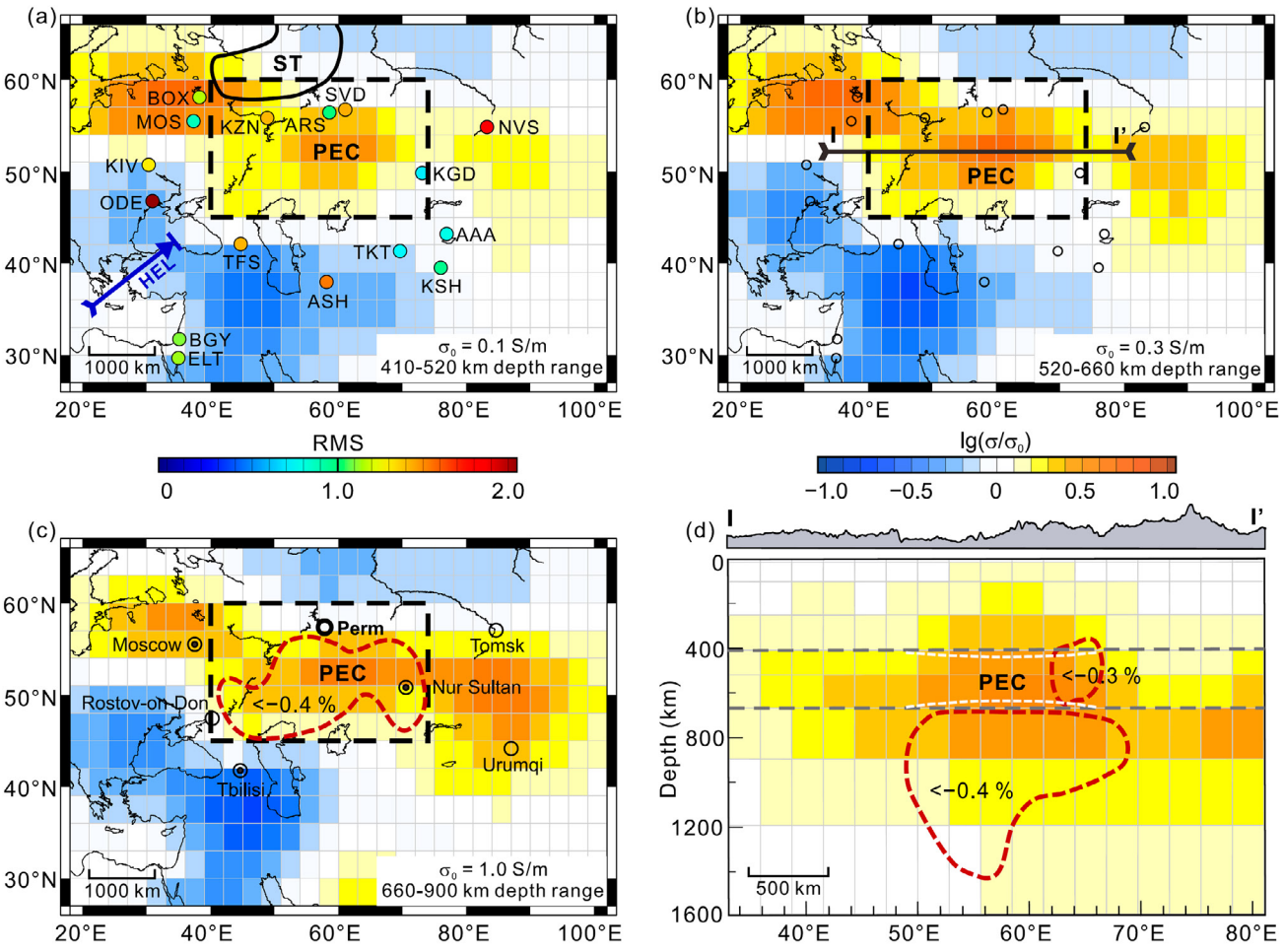

Fig. 41

Scientists from Jilin University and Shijiazhuang Tiedao University used geomagnetic field data from 16 stations in Northern Asia to calculate the electrical conductivity of the mantle at various depths. They discovered a noticeable increase in conductivity relative to the worldwide average conductivity in the region under the Siberian Traps (yellow and brown areas on the diagrams). Researchers have ascertained that these areas at depths from 400 to 900 km are on average 250 degrees hotter than the surrounding mantle. In these areas, there is a fraction of the molten mantle.

Source: Li, S., Li, Y., Zhang, Y., Zhou, Z., Guo, J., & Weng, A. (2023). Remnant of the late Permian superplume that generated the Siberian Traps inferred from geomagnetic data. Nature Communications, 14, 1311. https://doi.org/10.1038/s41467-023-37053-3

It is worth noting that previous eruptions 250 million years ago, at the boundary of the Permian and Triassic periods, also occurred in this region. The epicenter was located beneath the East Siberian Craton (beneath the Putorana Plateau), with effusions spanning both Western and Eastern Siberia (Fig. 42).

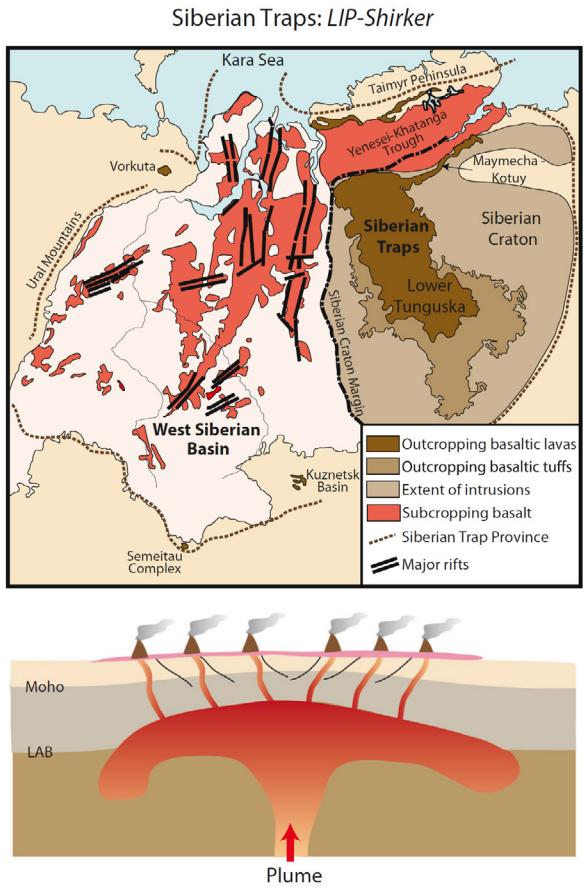

Fig. 42
The Siberian Traps as an example of a Large Igneous Province
The map shows eruptions in Western Siberia (red) and the traps in Eastern Siberia (brown), which erupted 250 million years ago. Hot material from the mantle plume rose and spread beneath the lithosphere-asthenosphere boundary, forming a mushroom-shaped structure. This led to extensive magmatic activity over an area of approximately 5 million km^2. The plume's influence resulted in the formation of the West Siberian Rift System, whose activity ceased roughly 10 million years later during the Middle Triassic.

Source: Koptev, A., & Cloetingh, S. (2024). Role of Large Igneous Provinces in continental break-up varying from "Shirker" to "Producer." Communications Earth & Environment, 5, 27. https://doi.org/10.1038/s43247-023-01191-9

Localization of the Magma Plume

By synthesizing the analysis of soil temperature anomalies, depth of permafrost thaw, near-surface temperature anomalies, low-velocity seismic waves anomalies in the mantle, and magnetic anomaly, it is possible to identify the current location and dimensions of the Siberian plume (Fig. 43).

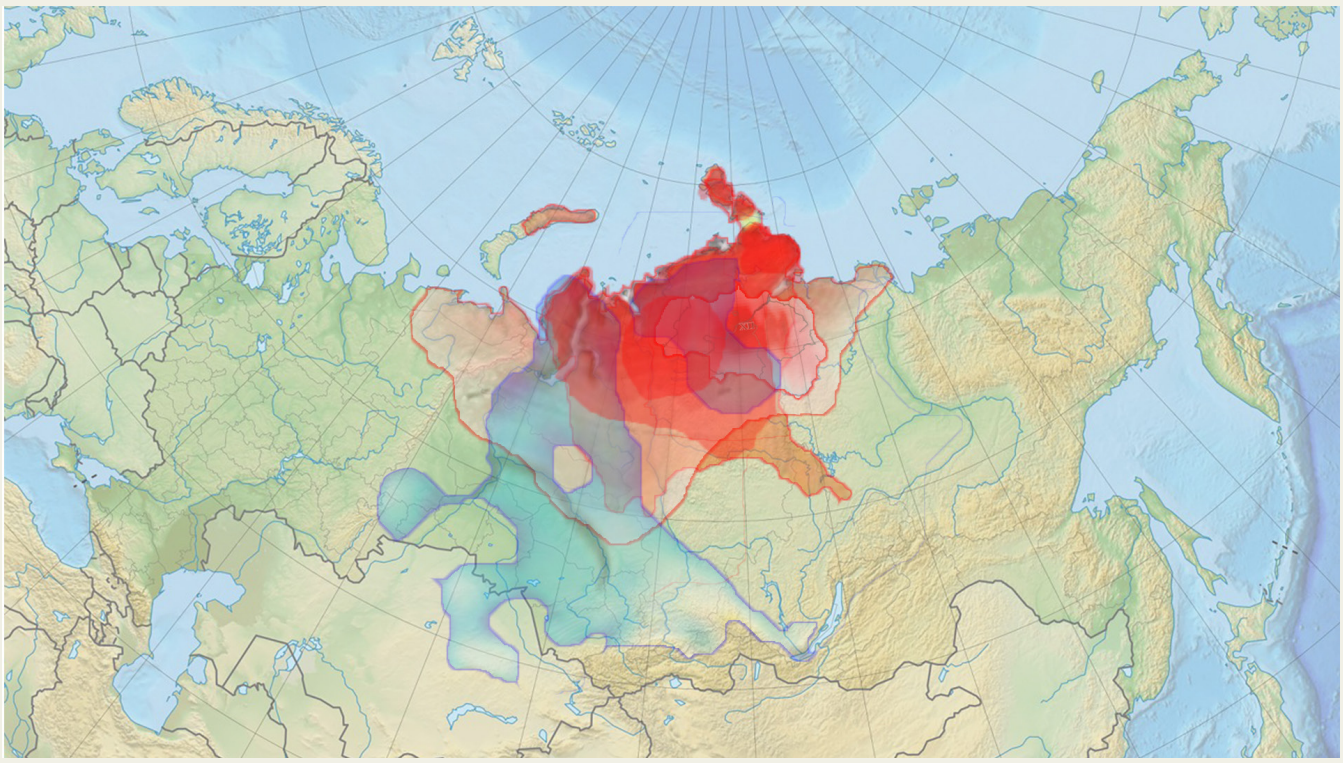

Fig. 43
A. Composite map overlaying key anomalies across multiple parameters, detailed below:

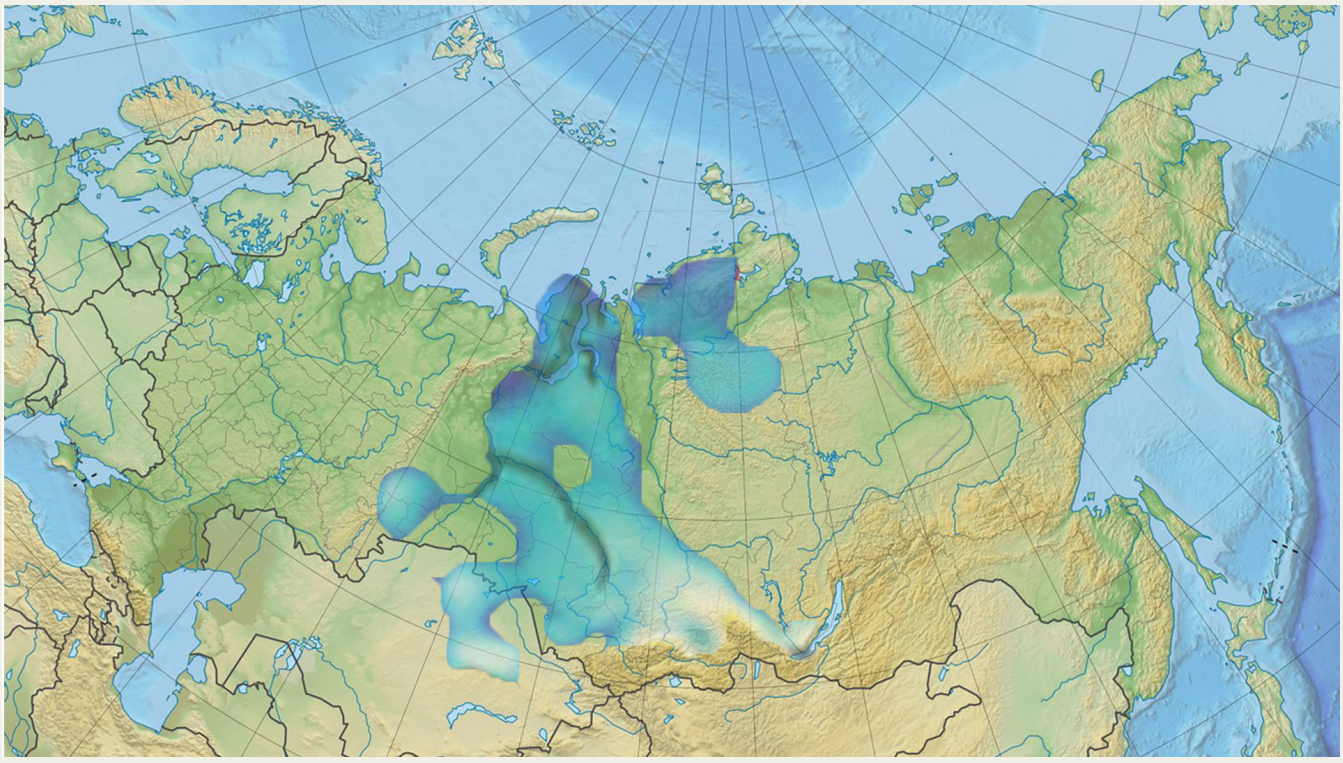

B. Map of low-velocity anomalies (indicative of more molten material) at a depth of 110 km, based on seismotomography from Li, S., Li, Y., Zhang, Y., Zhou, Z., Guo, J., & Weng, A. (2023)

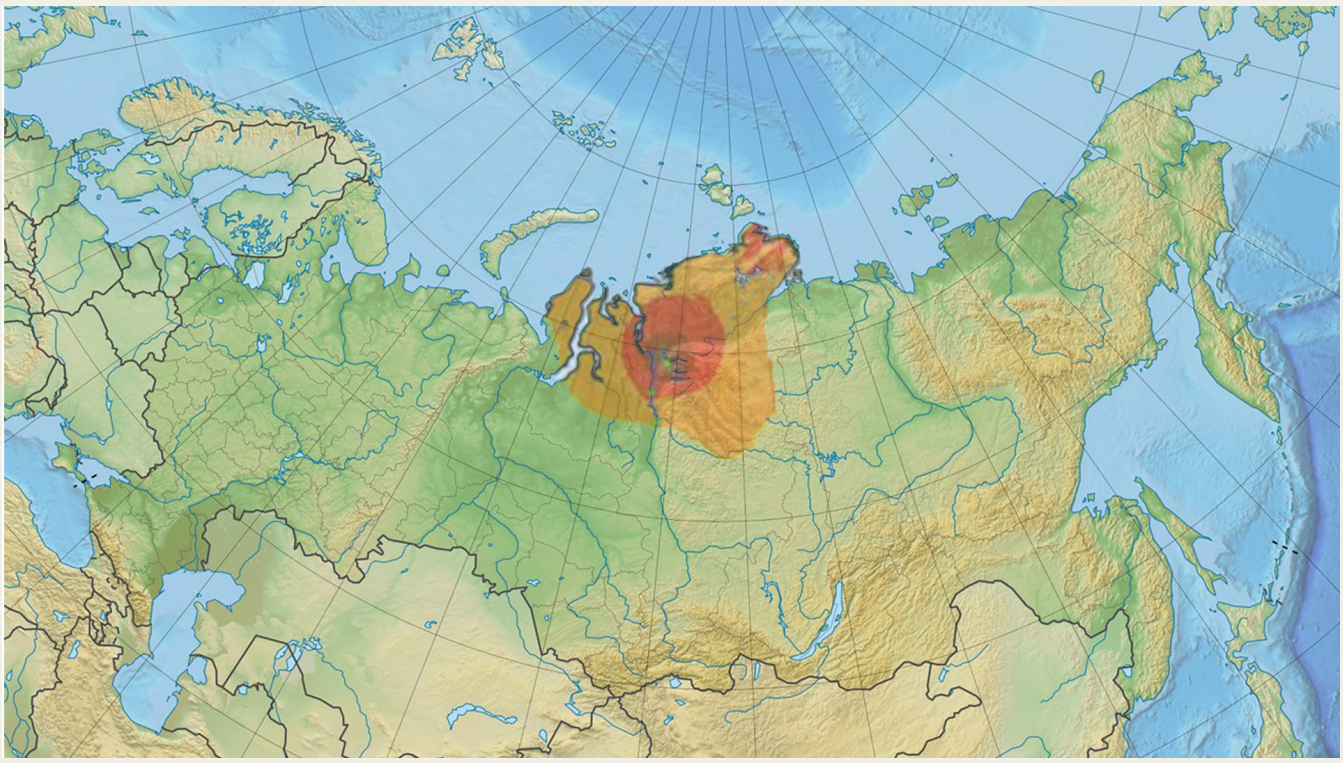

C. New soil heating anomaly trends comparing the periods 1976–2021 and 1976–2023, as reported by Roshydromet (2021, 2023).

D. Linear trend of average monthly air temperatures for January from 2001–2021, according to Sherstyukov (2023)

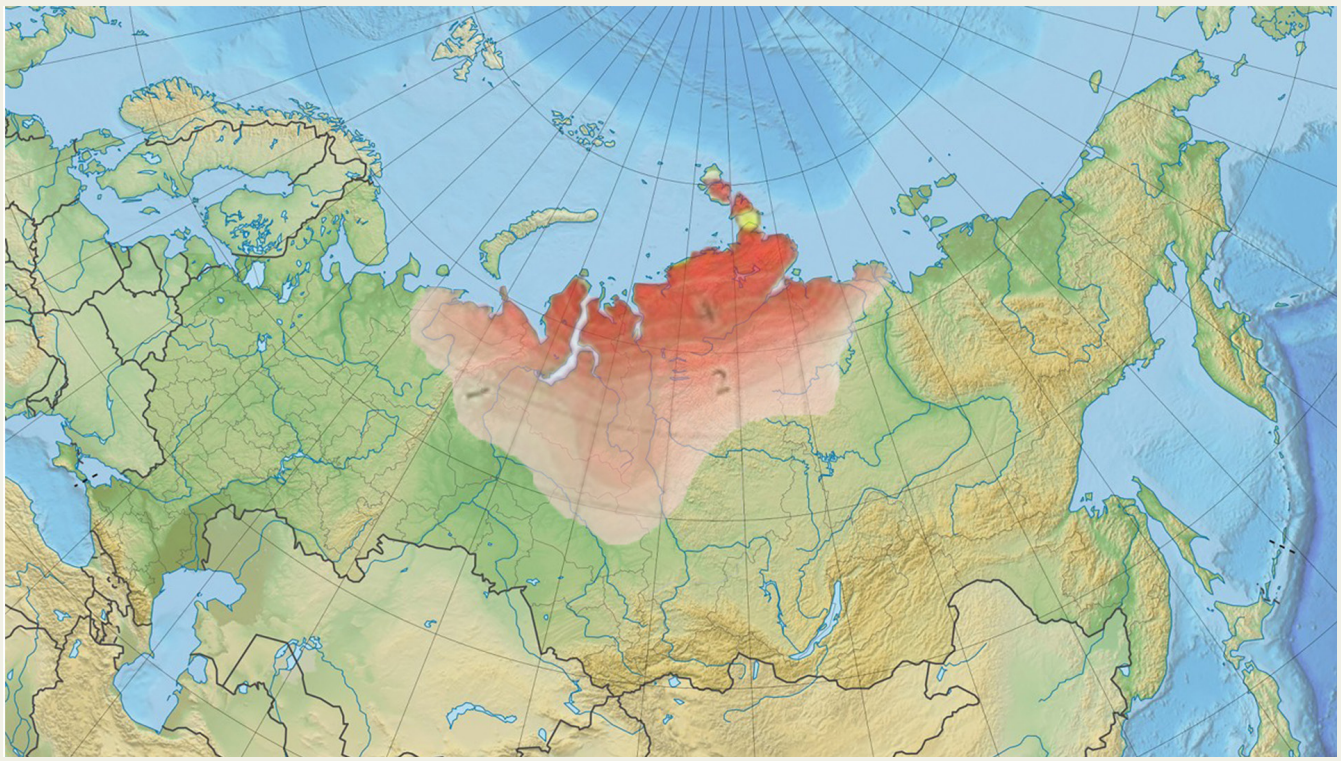

E. Seasonal average air temperatures from December 2023 to February 2024, based on Roshydromet data (2024)

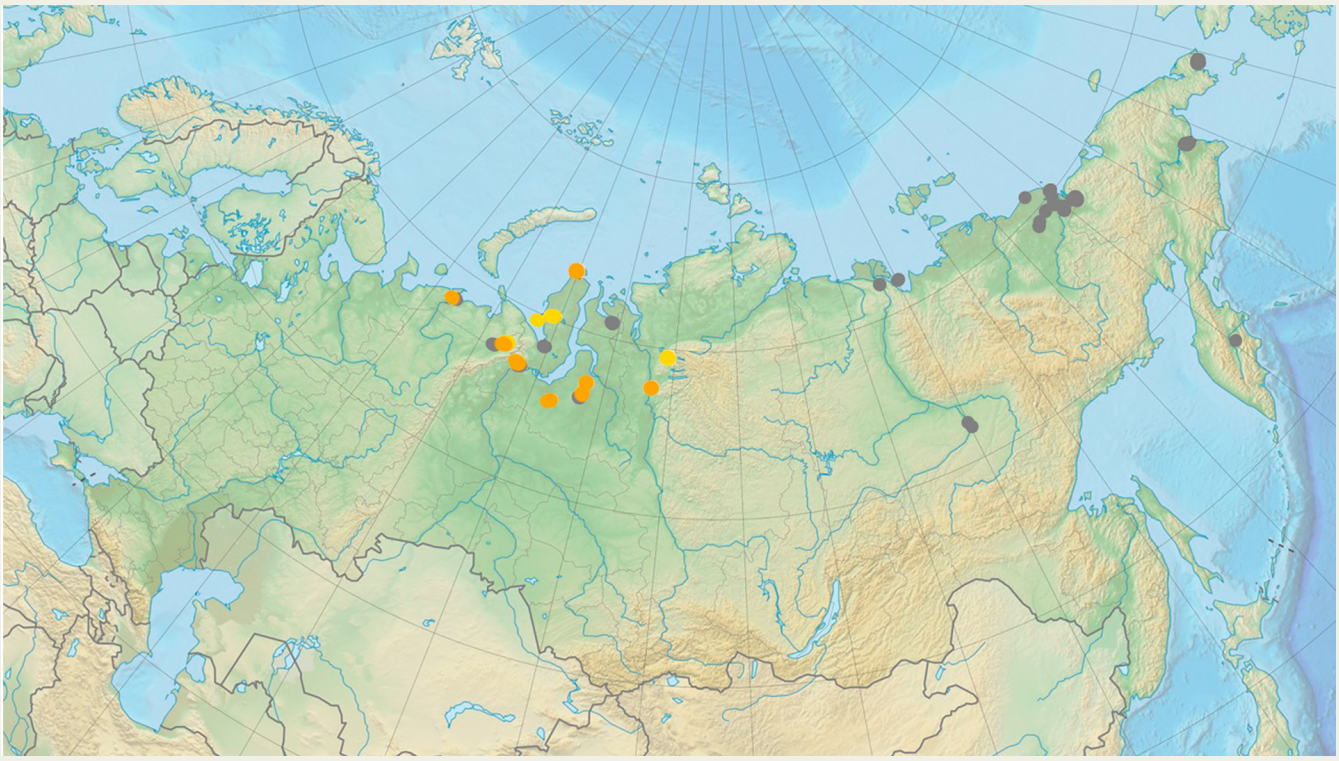

F. Areas of growing depth of seasonal thawing in permafrost layer. Data source: https://permafrost.su/

According to the hypothesis, the ascending section of the plume is located south of the Gyda and Taimyr Peninsulas and features multiple branches. The diameter of the plume head is estimated at 1,200–1,500 km, while the zone of magmatic flow dispersal may reach 2,500–3,000 km. This region encompasses structures of the West Siberian Plate and the East Siberian Craton.

Currently, the head of the plume is exerting influence on the base of the East Siberian Craton, spreading magmatic flows beneath its territory. This process is likely contributing to increased seismic activity along the plate margins, including areas such as Baikal and even the Urals. The cause of such anomalies specifically in the marginal parts of the plates is the destabilization of the plates due to the softening of the underlying asthenosphere and a slight uplift of the central part of the Siberian block of the Earth's crust, that is, the tectonic structures of the West Siberian Plate and the East Siberian Craton, together with the tectonic structure of the Verkhoyansk-Chukotka folded system.

Increase in Seismic Activity as an Indicator of Tectonic Plate Destabilization Due to the Siberian Magmatic Plume Activity

The methodology of seismic activity analysis included downloading and special processing of data obtained from the International Seismological Centre (ISC) website. Since the data contain different sources from different countries and research institutes, as well as different types of magnitudes (Mw, Ms, Mb, ML, MD, etc.), a certain algorithm of data processing was performed to select the appropriate type of magnitude from different sources (see Appendix 1). The main idea of the processing algorithm was to select the median value among the most common magnitude types for each of the events, since for each event different sources provided different magnitude types and values to the ISC database. On average, this processing leads to a small decrease in magnitude relative to the maximum value submitted, but as experience has shown the median-based algorithm produces results that align well with Gutenberg-Richter law and other patterns, and agrees quite well with data from other seismological resources such as IRIS and USGS.

The data obtained through the algorithm were filtered by event types in the ISC database (see Appendix 1) to exclude events caused by human activities during mining operations: explosions, suspected explosions, rockbursts, etc. Also, since there are many mining enterprises across Russia, the ISC database was cross-referenced with data from the Unified Geophysical Service of the Russian Academy of Sciences[44] as of January 2025, which lists all known explosions and rockbursts in Russia. These events were also excluded to ensure that the resulting dataset contained no events attributable to explosions.

[44] Federal Research Center, Unified Geophysical Service of the Russian Academy of Sciences http://www.ceme.gsras.ru/zr/contents.html

Let us now consider the results of the data analysis in the region of the rising magmatic plume and the peripheral areas of the major tectonic blocks it directly affects. Since the Siberian Craton is regarded as a relatively stable, aseismic platform, even a small number of earthquakes within its boundaries would be considered an anomaly.

Fig. 44 illustrates earthquake density distribution across Russia. In the Siberian region, the highest concentration of earthquakes is expectedly observed in folded areas: the Verkhoyansk Range in the east, the Gakkel Ridge, the Ural Mountains in the west, and the Altai-Sayan region in the south. Isolated events are also present within Siberia itself—several earthquakes with a magnitude of about 4.0 have been recorded south of the Taimyr Peninsula. Let us take a closer look at the dynamics of earthquakes in localized areas within Siberia. Let's have a closer look at the dynamics of local earthquakes in the area of the Siberian plume and adjacent regions.

M3+ Earthquakes Density on the Territory of Siberia

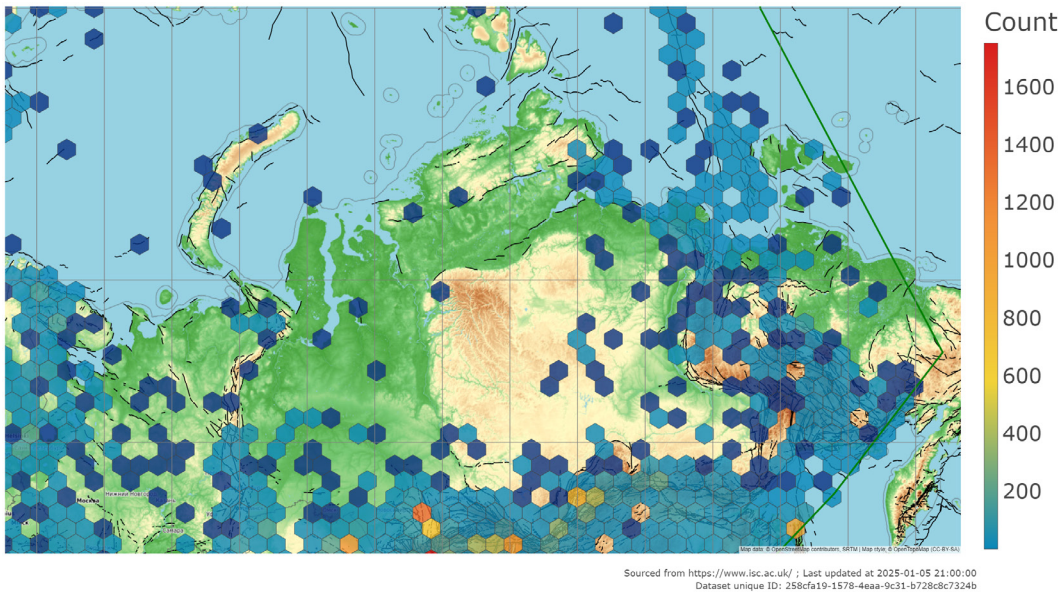

Fig. 44
M3+ earthquake density in Siberia from 1990 to 2024.

Source: ISC Database.

Based on geological structures, areas have been identified where the mantle plume can exert different influences (Fig. 45). The area of the plume itself was selected, where the impact may be associated with the intrusion and pressure of magma and the fluid phase (magmatic gasses). In the marginal parts of the East Siberian Platform and the West Siberian Plate, the influence of the plume on seismicity is likely to be caused by the destabilized position of dense blocks of the Earth's crust.

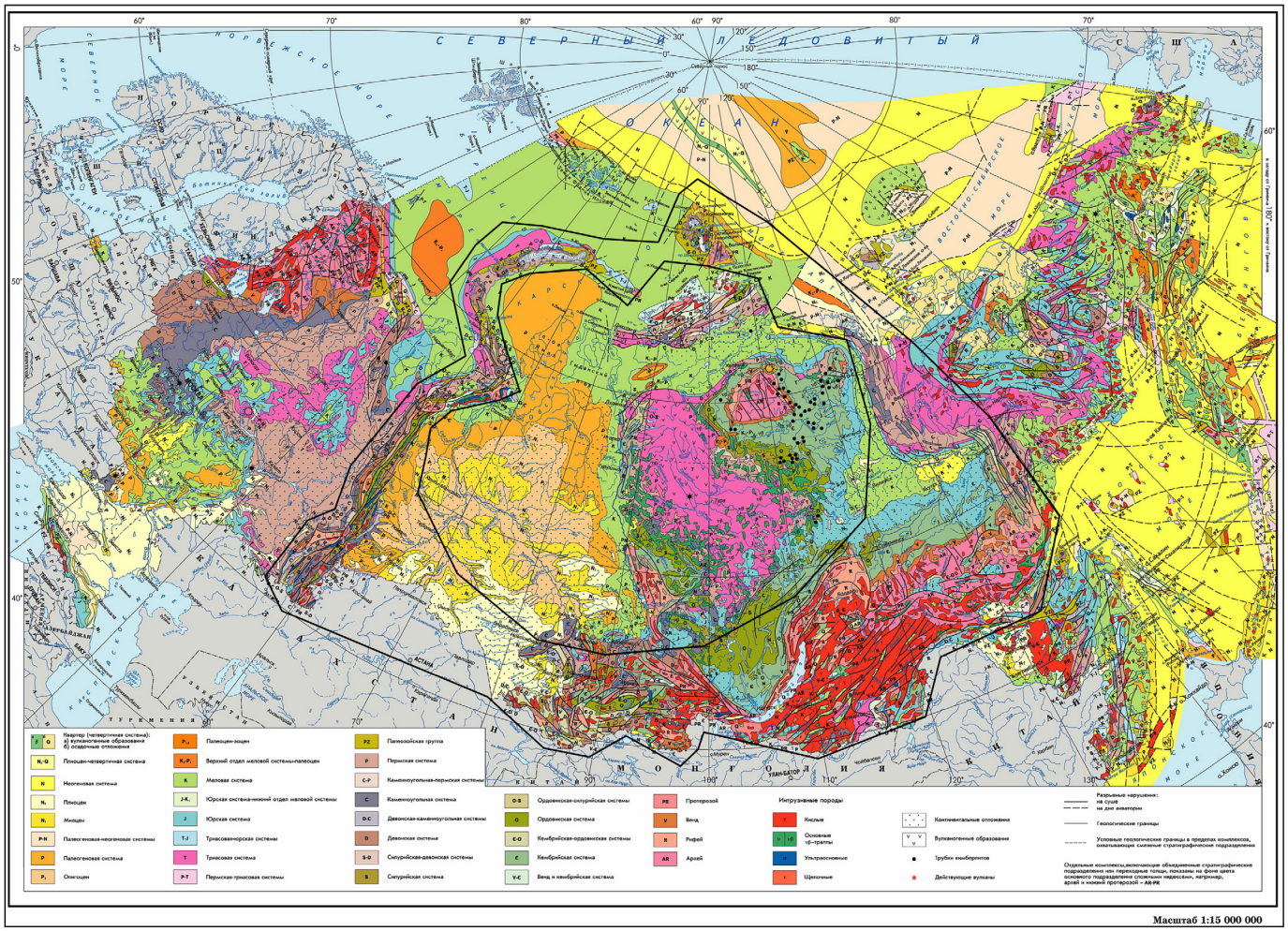

Fig. 45

The area delineated by geological structures in the area of intrusion and lateral spread of the Siberian plume (inner black site) for seismicity analysis. The outer black site corresponds to the area of marginal effects from the pressure of the Siberian plume on the plates.

Let us examine earthquakes in the central region of the Siberian Plume in greater detail. Figure 46 presents a map showing the distribution of earthquakes with magnitudes of 3.0 and above. Earthquakes are recorded in the southern area of the Taimyr Peninsula. Particularly concerning are two recent earthquakes that occurred in this region in August and September 2024, with magnitudes of 3.5 and 3.8, respectively. Similar magnitudes have been recorded in the southern part of the Gyda Peninsula (M3.5) and on the Yamal Peninsula (M3.7 and M4.2) at a depth of 10 km. These earthquakes were recorded in the zone corresponding to the localization of the head of the Siberian plume, which is an alarming trend that will be explained further.

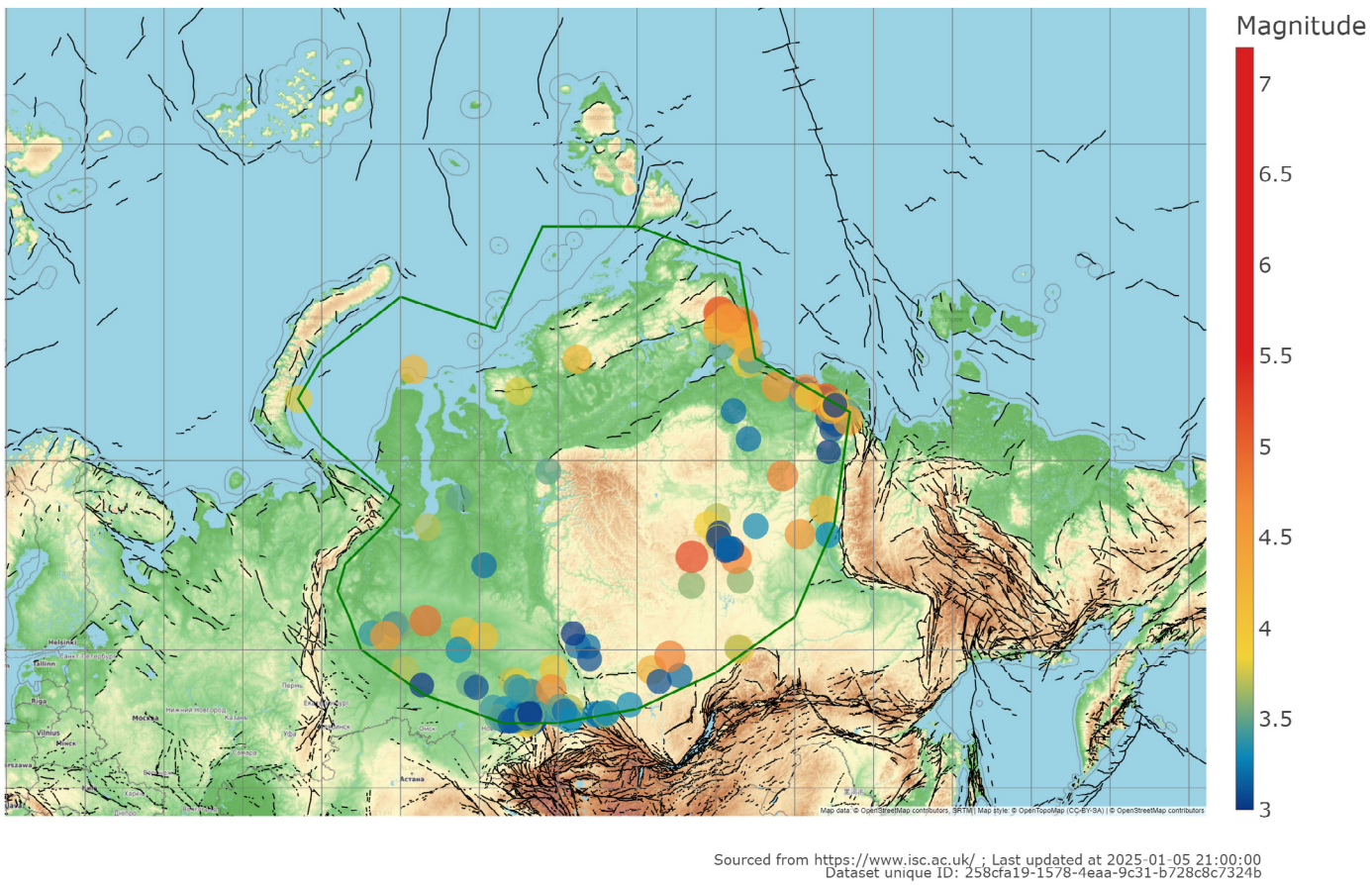

Fig. 46
Map of earthquakes with a magnitude of M3.0+ in the Siberian Plume region from 1990 to 2024.

Source: ISC Database.

In the highlighted Siberian Plume region, a total of 205 earthquakes with a magnitude of M3.0+ were recorded between 1990 and 2024. An increase in the number of earthquakes was observed in 1995 (Fig. 47), aligning with the global trend of increased seismic activity in 1995 associated with the growing magmatic activity. Since 2007, there has been a significant rise in the number of earthquakes, followed by a gradual decline in seismic activity. Starting in 2021, the number of earthquakes has sharply increased again, surpassing previous annual levels. Thus, wave-like growth in seismic activity is observed in the Siberian Plume region. In recent years, noticeably more events have been recorded than were typical for this area in the past.

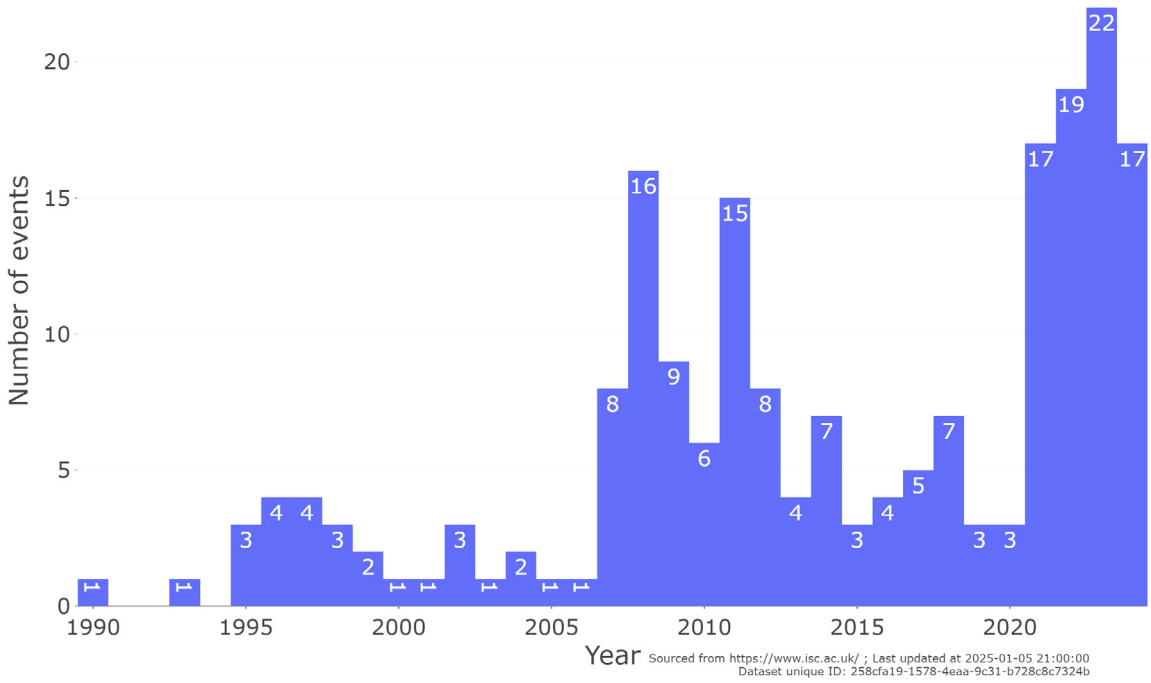

Fig. 47
Number of M3.0+ earthquakes in the Siberian Plume region from 1990 to 2024.

Source: ISC Database.

After an M5.0 earthquake in 1990, a gradual decrease in magnitudes and the number of earthquakes was observed (Fig. 48). From 1990 to 2007, only three earthquakes with a magnitude over M4.5 were registered. Since 2007, there has been a gradual increase in earthquake magnitudes. For the first time in recorded history, earthquakes with magnitudes of M5.1 and M5.2 occurred starting in 2019. All earthquakes of magnitude M4.5+ are located at the periphery of the plume (Fig. 49), with some occurring in stable areas where no known faults exist.

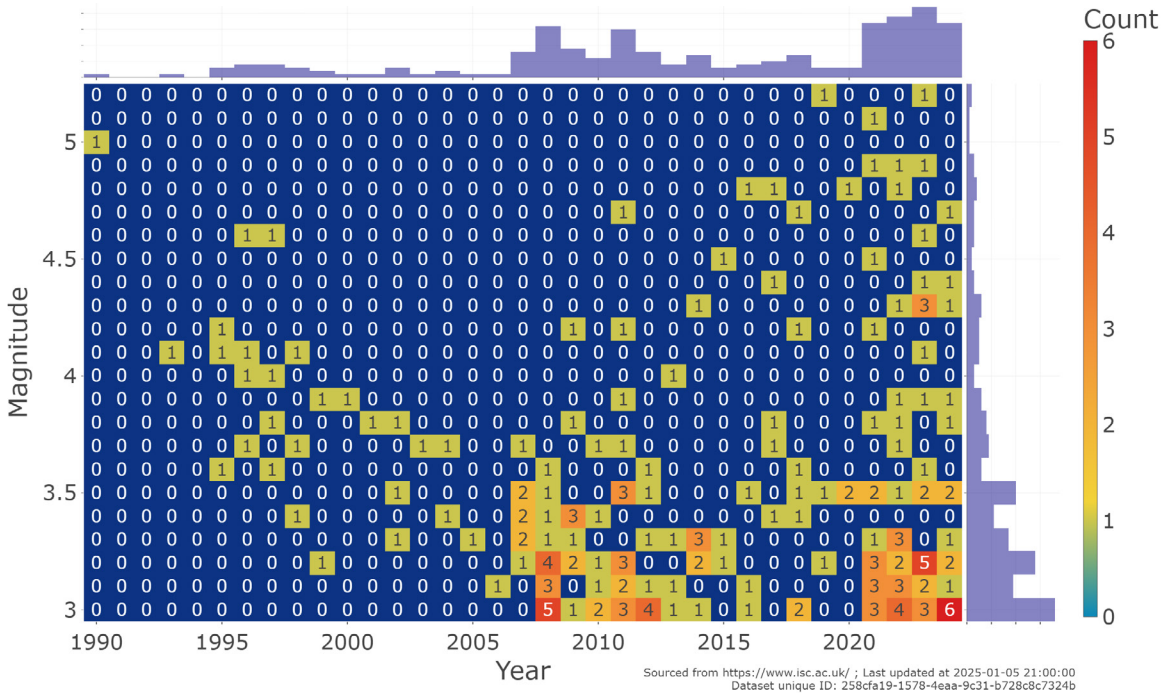

Fig. 48
Distribution of earthquakes that occurred in the Siberian plume region from 1990 to 2024 by magnitude.

Source: ISC Database.

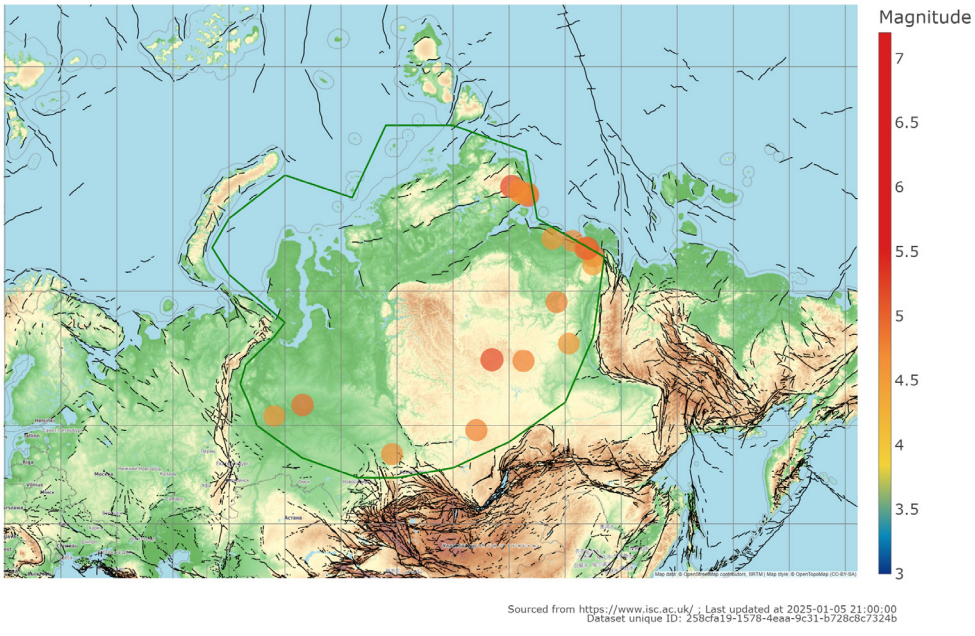

Fig. 49
Map of M4.5+ earthquakes in the area of the Siberian Plume from 1990 to 2024.

Source: ISC Database.

In the same year of 2007, an earthquake with a magnitude of 3.7 was recorded for the first time at a depth of 33 km near the Moho boundary (Fig. 50). After 2014, earthquakes at the base of the crust, at depths of 30–35 km, began occurring significantly more frequently, with magnitudes approaching 5.0. All of these are located along the periphery of the presumed plume site.

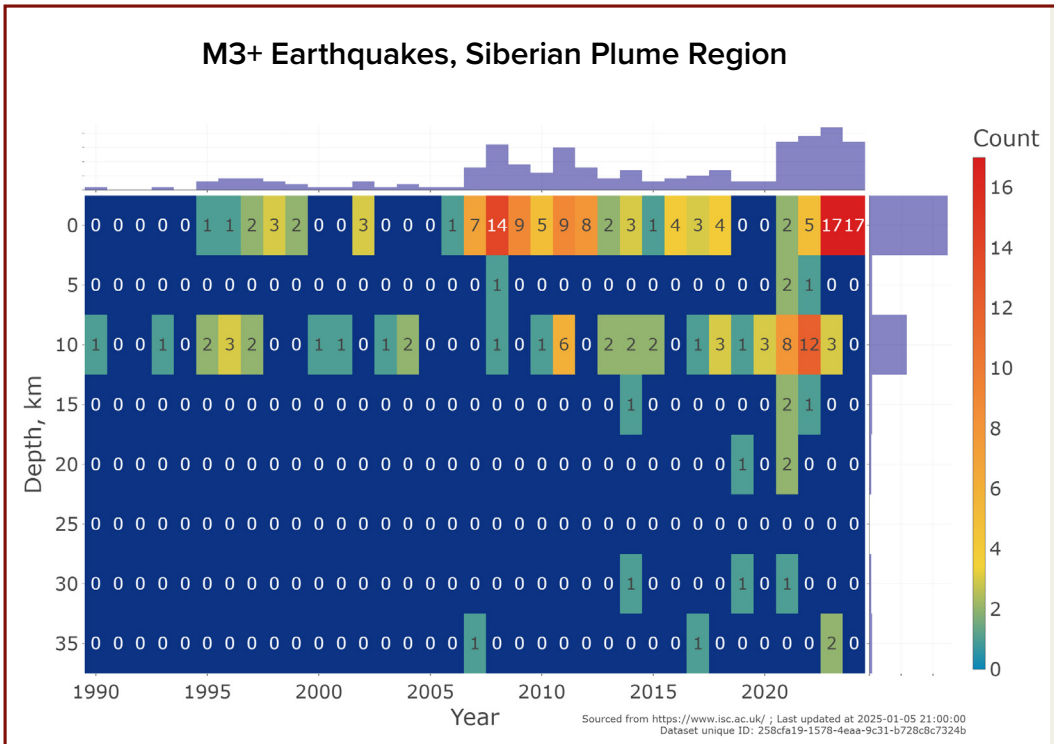

Fig. 50
Distribution of M3.0+ earthquakes between 1990 and 2024 in the Siberian Plume region by depth.

Source: ISC Database.

The analysis of earthquakes in the presumed Siberian Plume area demonstrates wave-like increases in seismicity: the number of earthquakes is rising, their magnitudes are increasing, and they occur at deeper levels. This indicates deformational processes of the plate under the immense pressure of magma from below. The progression of these processes will inevitably lead to an eruption of the Siberian Plume in the near future due to the following reasons.

The foundation of the East Siberian Craton is cemented with magmatic and metamorphic rocks, forming a dense, monolithic crust shaped by eruptions that occurred 250 million years ago. The emergence of strong earthquakes with magnitudes starting from 7.0 in this region would indicate that the platform structures of the Siberian Craton are undergoing deformations exceeding the strength limits of the rocks. To illustrate how the monolithic Siberian Craton could fracture under plume pressure, imagine how glass begins to crack just before it completely shatters. Thus, the appearance of strong earthquakes in this region could signal the onset of a plume breach to the surface within literally a day.

Currently, to understand the actual situation with the plume's advancement and the solidity of the Earth's crust in the Siberian magmatic plume area, it is critically important to install additional seismic sensors, preferably in boreholes several kilometers deep. This will enable a detailed seismic tomography analysis of the Earth's crust and mantle and allow for continuous monitoring of the plume's position and activity (see the section "Planned and Controlled Degassing").

Attention should be given to the distribution of earthquakes by depth in the Siberian Plume area and its peripheral zones (Fig. 51). Earthquakes at depths near the Moho boundary (greater than 30 km) and in the mantle occur mainly in folded regions, and they apparently outline the presumed location of the Siberian Plume.

M3.5+ Earthquakes, Siberian Plume Region

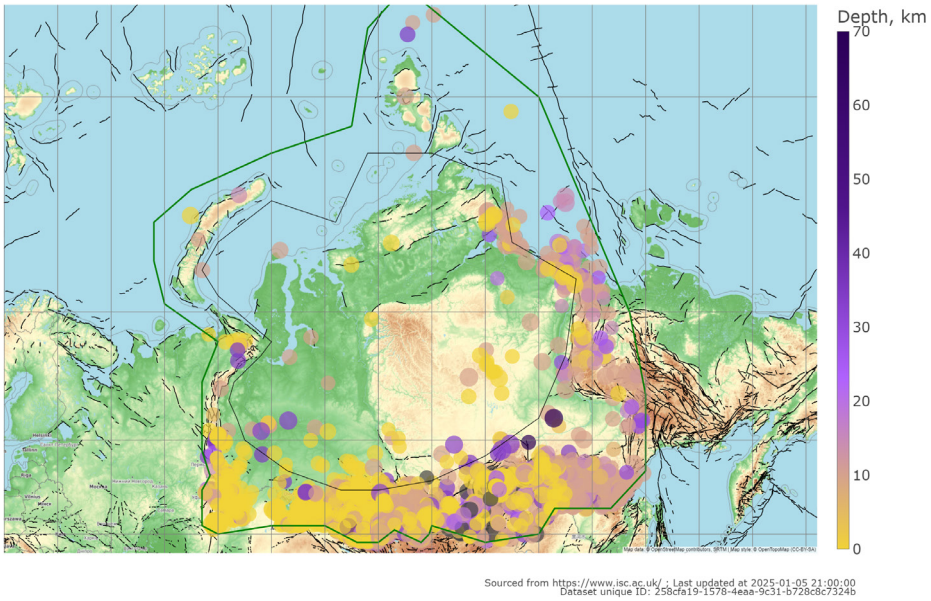

Fig. 51
Map of M3.5+ earthquakes in the Siberian Plume region from 1990 to 2024. The color scale corresponds to depth.

Source: ISC Database.

Let us examine the seismic activity specifically in the peripheral parts of the Siberian Plume. Geologically, these areas belong to folded belts and seismically active regions, where seismicity may be caused by both tectonic movements and the influence of the magmatic plume. The graph of the number of earthquakes shows a mixed picture of overlapping seismicity factors (Fig. 52). Significant spikes in seismic activity are visible in some years. For a better understanding of the nature of these processes, each region needs to be considered individually.

An analysis of the Verkhoyansk folded structures and fault zones on the floor of the Laptev Sea (Fig. 53) reveals notable surges in M3+ earthquakes, during the years 2013 and 2021-2022 (Fig. 54). Such spikes are characteristic of magma intrusion phases, which cause significant disruptions in the integrity of the Earth's crust and the release of fluid content through rock fractures and nearby faults. These phenomena are often accompanied by an increase in low-magnitude earthquakes, the occurrence of earthquake swarms, and sometimes even series of swarms.

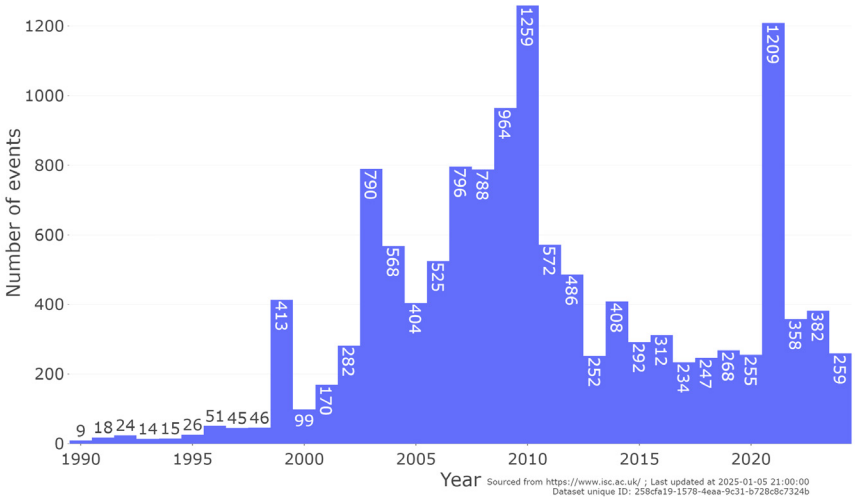

Fig. 52
Number of M3.0+ earthquakes in the peripheral areas of the Siberian plume from 1990 to 2024. Earthquakes within the Plume were excluded (Fig. 47).

Source: ISC Database.

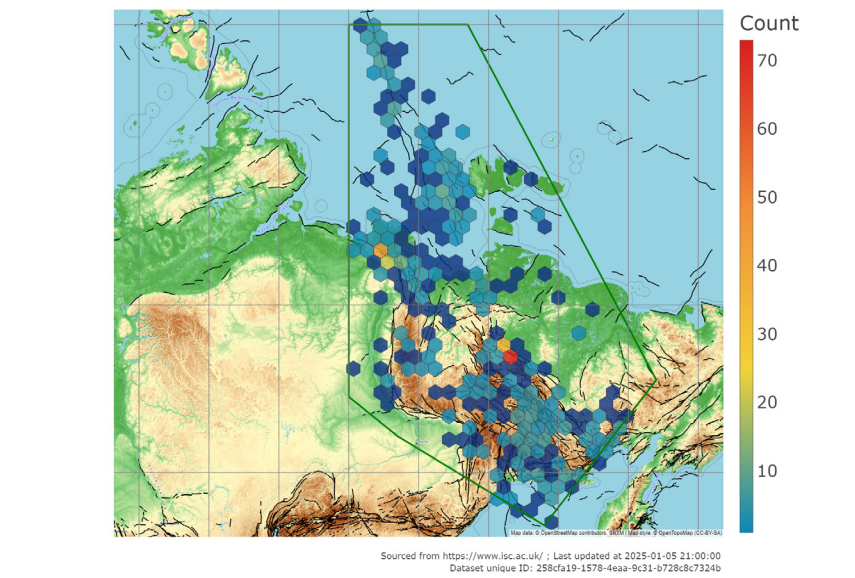

Fig. 53
M3+ Earthquake density in a selected section on the northeastern edge of the Siberian crustal block from 1990 to 2024. Fault lines are marked in black.

Source: ISC Database.

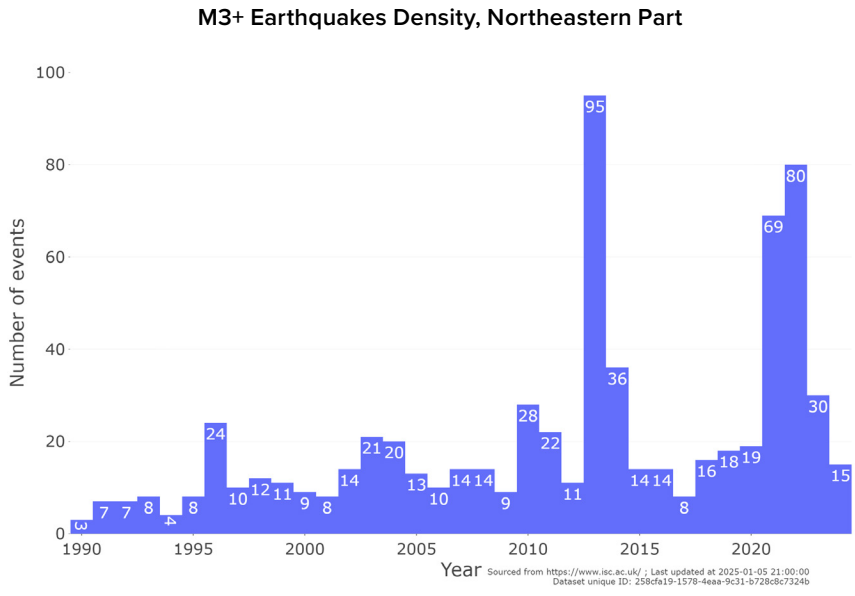

Fig. 54
Graph of the M3+ earthquakes number in a selected section on the northeastern edge of the Siberian crustal block from 1990 to 2024.

Source: ISC Database.

An analysis of earthquake magnitudes in this zone reveals a spike in the number of earthquakes with magnitudes from 2 to 3.5 in 2010, 2013-2014, and a significant increase from 2019 onward (Fig. 55). Since 2019, there has also been a notable rise in the number of earthquakes affecting the Earth's crust almost to its base, at depths reaching 35 km (Fig. 56). In 2013, the region experienced indicating either a prolonged phase of pressure accumulation or the release of accumulated magmatic fluids.

The group of earthquakes in the southeast direction from the Taimyr Peninsula (Fig. 57) should be reviewed separately.

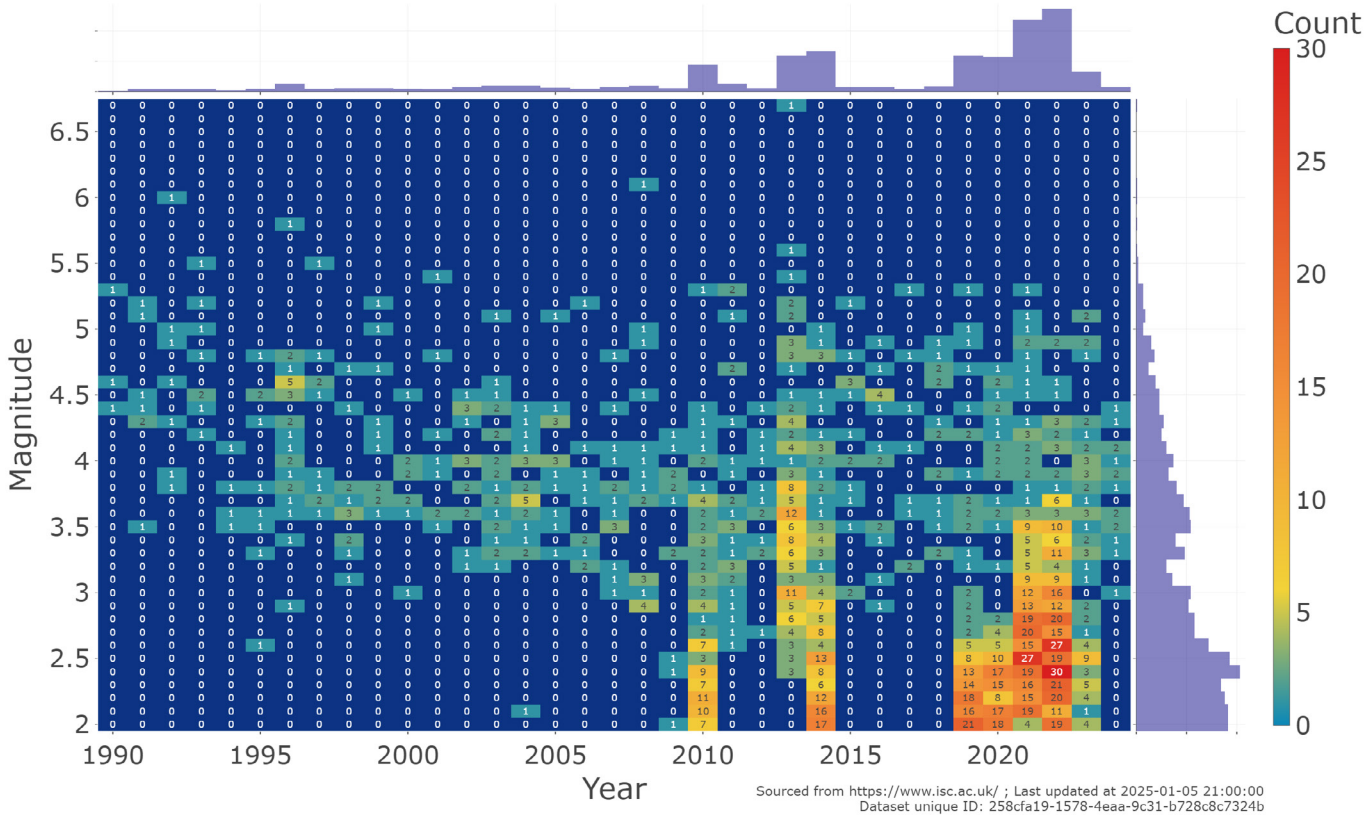

Fig. 55
Distribution of the number of earthquakes by magnitude in a selected section on the northeastern edge of the Siberian crustal block from 1990 to 2024.

Source: ISC Database.

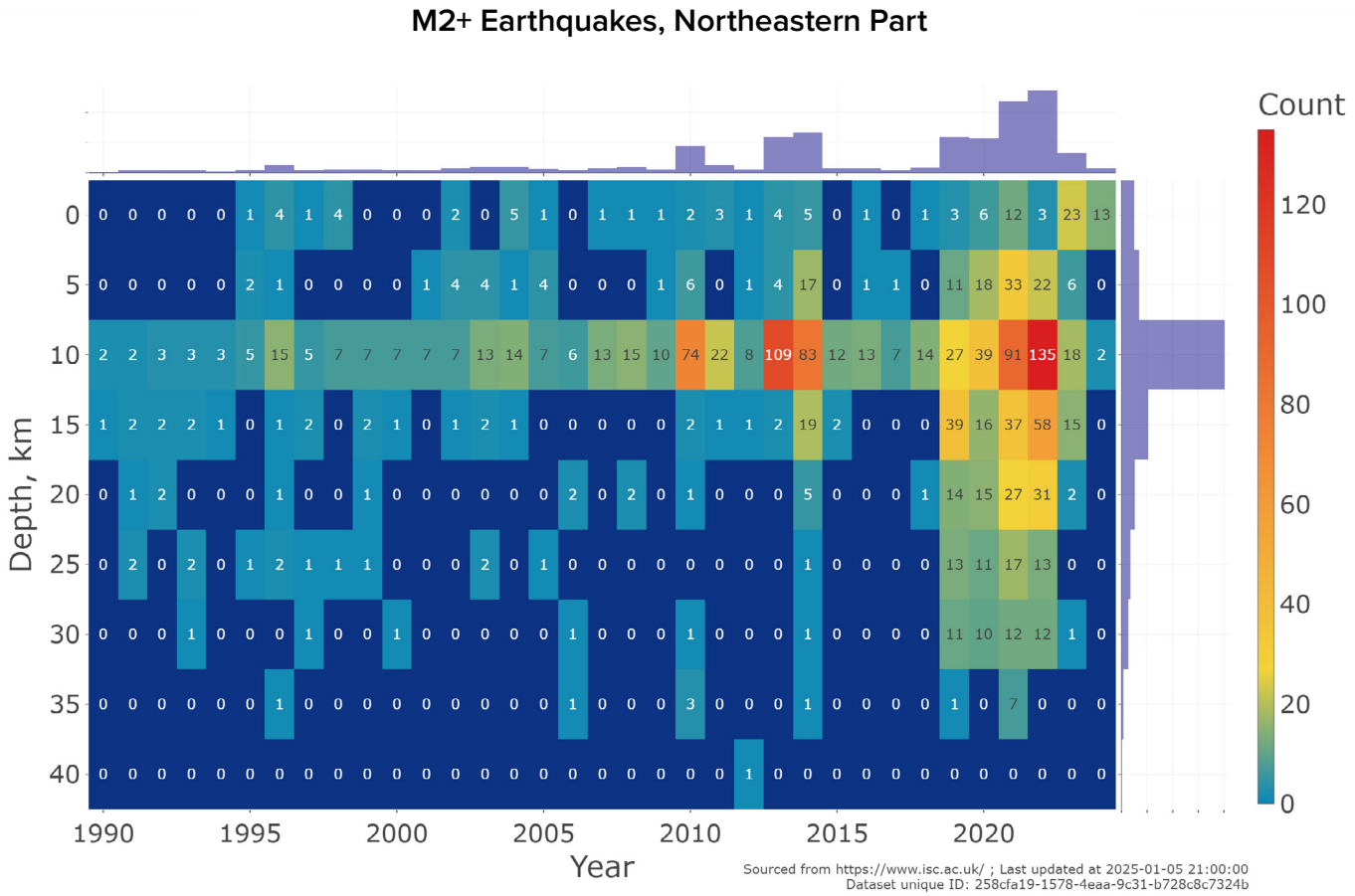

Fig. 56
Distribution of M2+ earthquakes by depth in a selected section on the northeastern edge of the Siberian crustal block from 1990 to 2024.

Source: ISC Database.

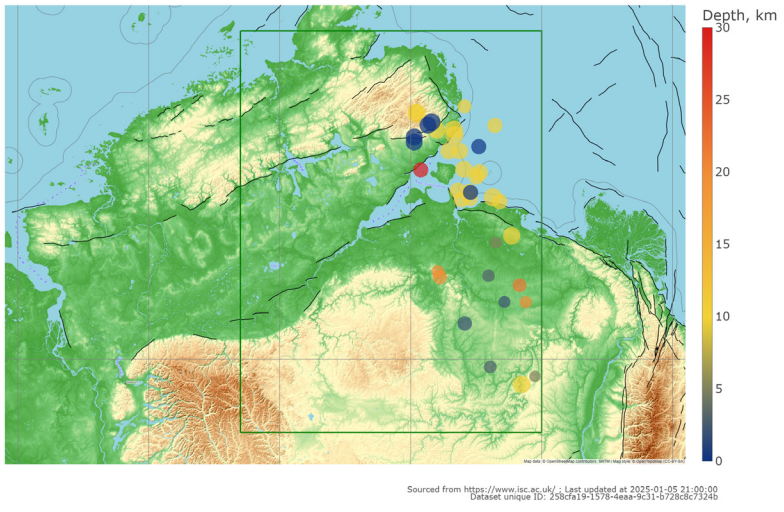

Fig. 57
Map of the distribution of M2+ earthquakes in the selected area northeast of the Taimyr Peninsula from 1990 to 2024.

Source: ISC Database.

In 2019-2020, this area also experienced a spike in seismic activity of low to moderate magnitudes (Figs. 58, 59).

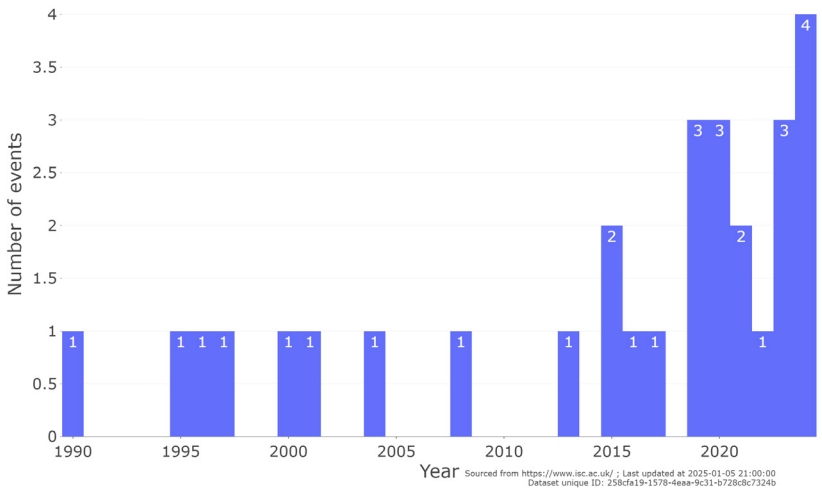

Fig. 58
Chart of the number of M3+ earthquakes in the selected area northeast of the Taimyr Peninsula.

Source: ISC Database.

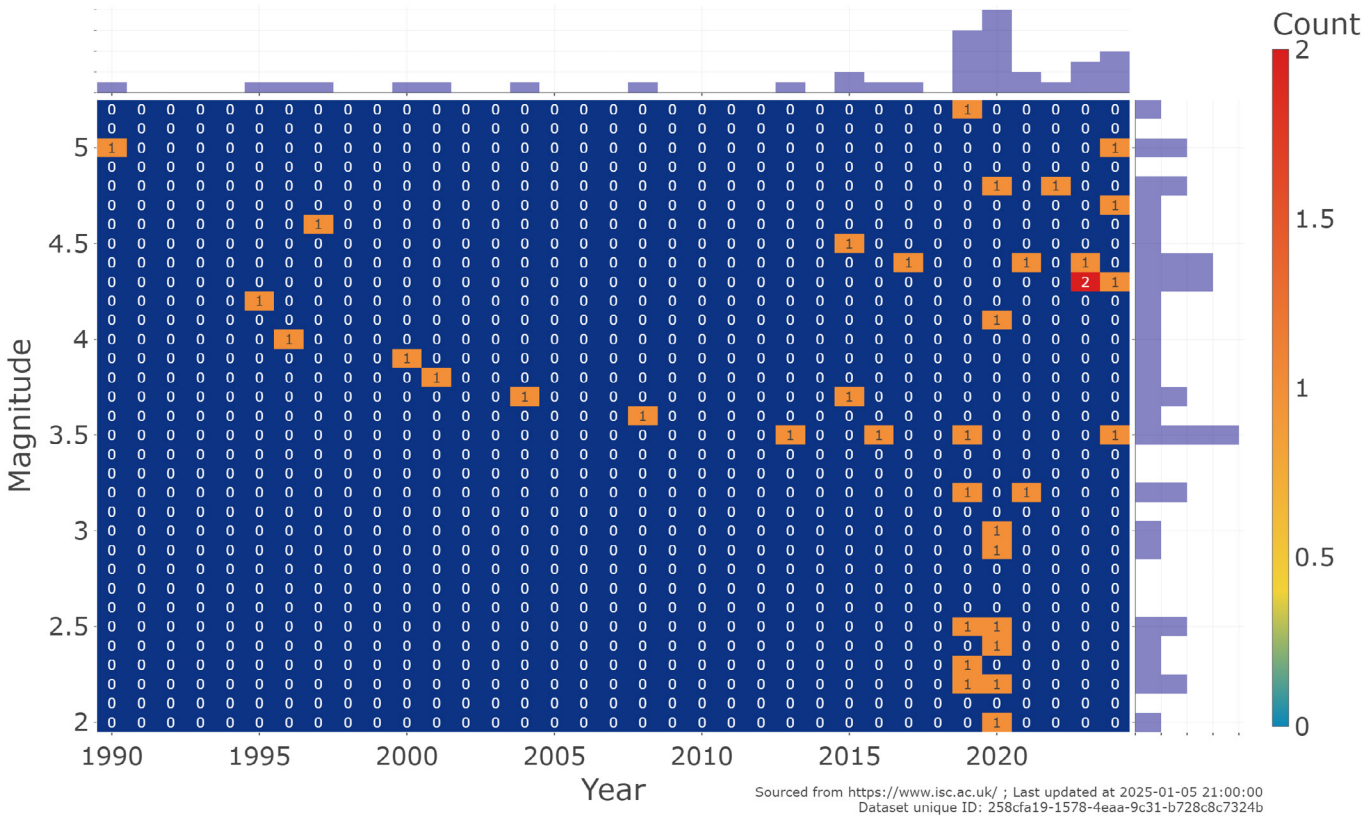

Fig. 59
Distribution of the number of earthquakes by magnitude in the selected area northeast of the Taimyr Peninsula from 1990 to 2024.

Source: ISC Database.

Between 2019 and 2020, there's a notable increase in terms of the depth of earthquakes that reach the base of the crust (Fig. 60) during the same periods as those observed in the Verkhoyansk folded structure area.

It should be emphasized that this zone is under the influence of the Siberian plume's head. Despite the relatively low number of earthquakes, the area exhibits a similar trend of increasing depth and frequency of earthquakes as in the Verkhoyansk folded structures, but starting from 2019.

The southern part of the examined territory includes the Altai-Sayan fold belt region and the Baikal area (Fig. 61). This is a tectonically mobile and seismically active region. Peaks in seismicity were observed in 1999 and 2021 (Fig. 62). Earthquake magnitudes began to grow in 2007, reaching M6.8 in 2021 (Fig. 63).

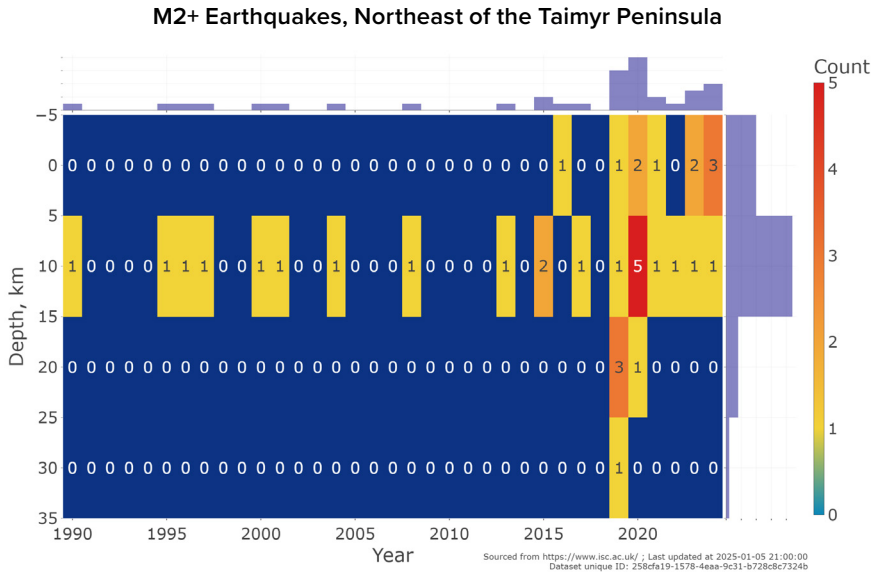

Fig. 60
Distribution of the number of M2+ earthquakes by depth in the selected area northeast of the Taimyr Peninsula.

Source: ISC Database.

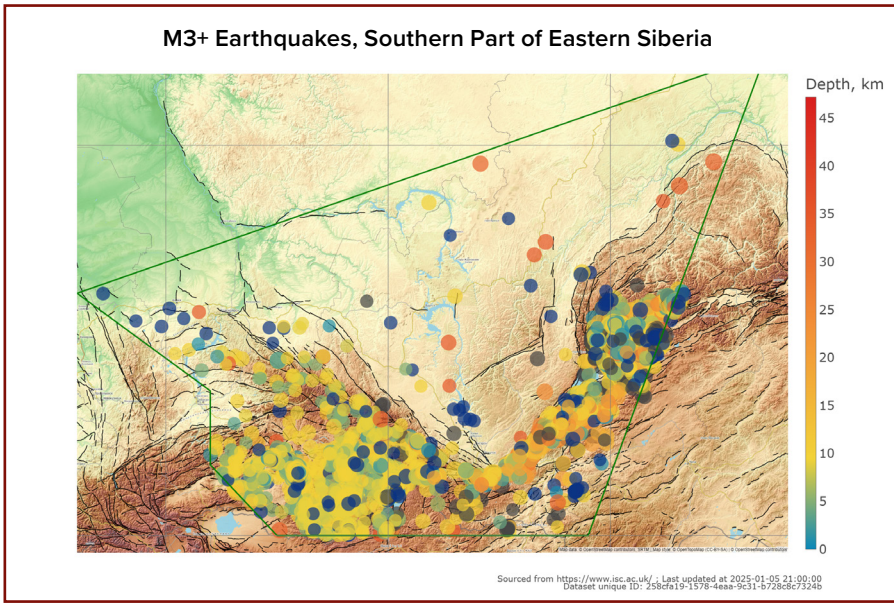

Fig. 61
Map of epicenters of M3+ earthquakes recorded from 1990 to 2024 in the selected area in the southern part of Eastern Siberia.

Source: ISC Database.

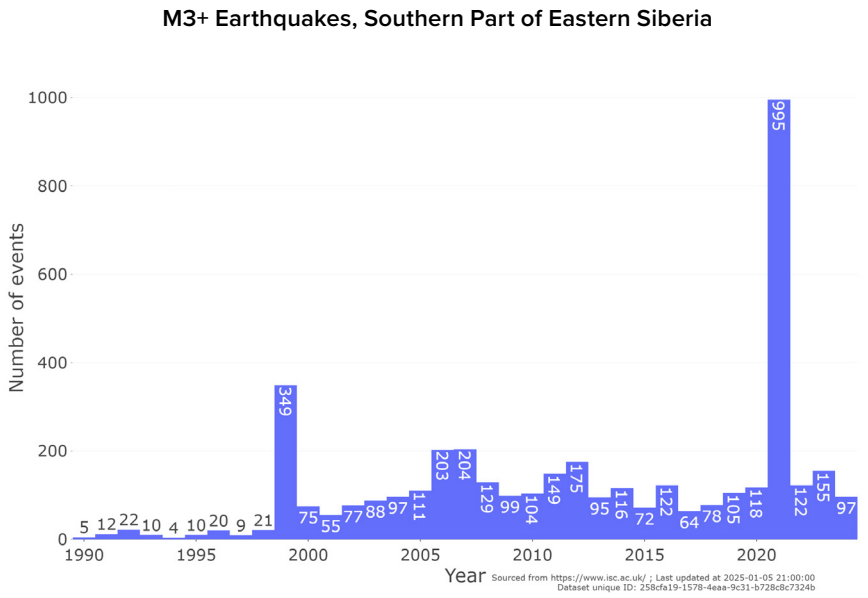

Fig. 62
Number of M3+ earthquakes in the southern part of Eastern Siberia.

Source: ISC Database.

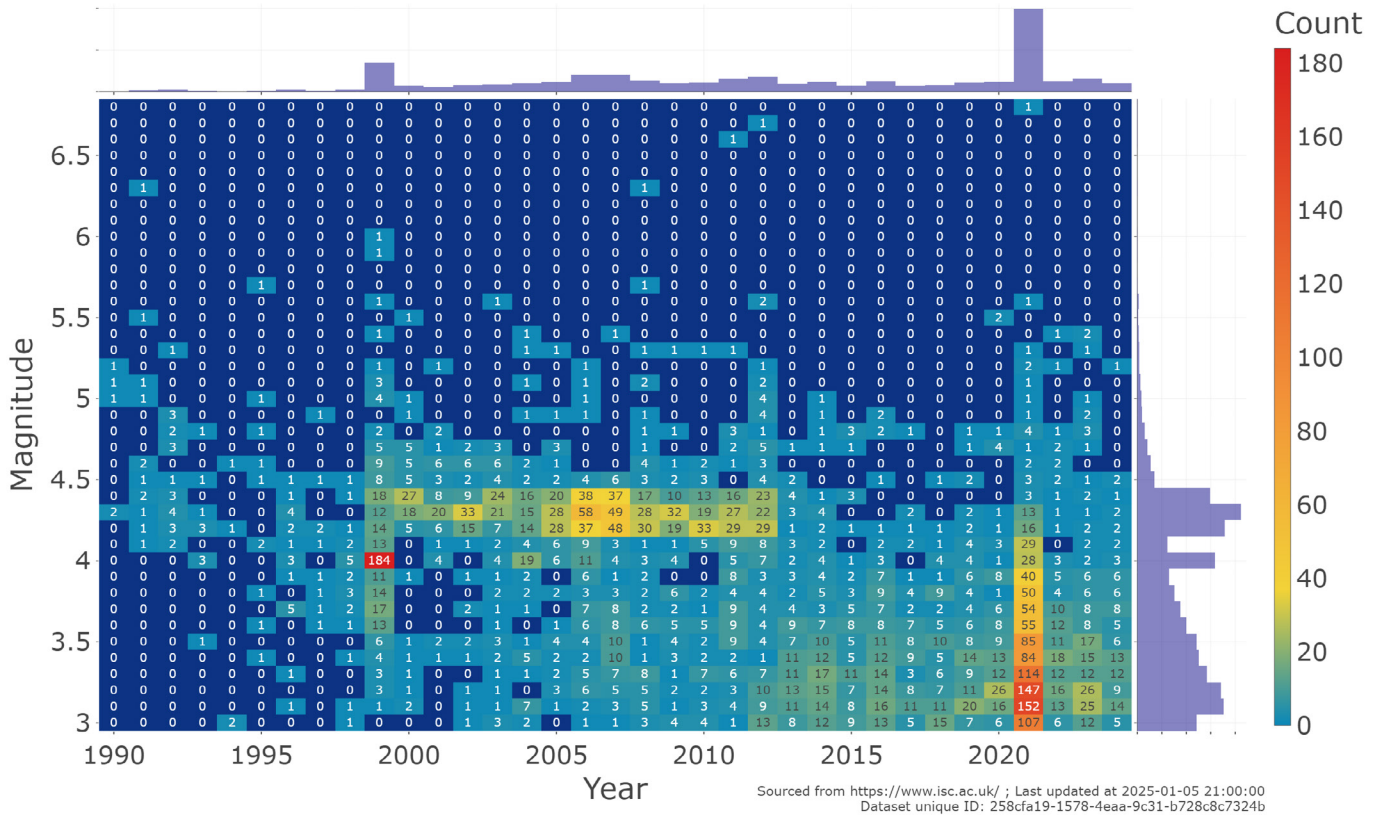

Fig. 63
Distribution of earthquakes by magnitude in the selected area in the southern part of Eastern Siberia from 1990 to 2024.

Source: ISC Database.

It is important to note the occurrence of mantle earthquakes beneath the Siberian Craton. As early as 1998, an earthquake with a magnitude of 3.3 was recorded at a depth of 211 km in the Vilyuy Syneclise area. This was an unexpected finding, but an even more unique event was a significant magnitude 5.1 earthquake at a depth of 627 km in the same region in 2023 (Fig. 64).

The very manifestation of deep-focus seismicity beneath the stable cratonic block of the Earth's crust is an exceptional event. Traditionally, it is assumed that such intramantle earthquakes occur in so-called subduction zones; however, the nearest subduction zone is located thousands of kilometers away and cannot influence this area.

The authors of this report suggest that the causes of these deep-focus earthquakes are intramantle explosions of immense power, which occur when relatively hotter magma flows come into contact with relatively cooler ones. According to the seismotomographic model, anomalies in seismic wave velocities are observed at the locations of both deep-focus earthquakes. These anomalies correspond to regions of relatively more viscous and fluid flows, which likely reflect their temperature differences. Thus, these two mantle earthquakes occurred at the interface of relatively cold and relatively hot mantle flows (Fig. 65), releasing significant amounts of energy that generated acoustic waves detected by seismic sensors as earthquakes. This clearly indicates substantial activity of mantle flows in this area.

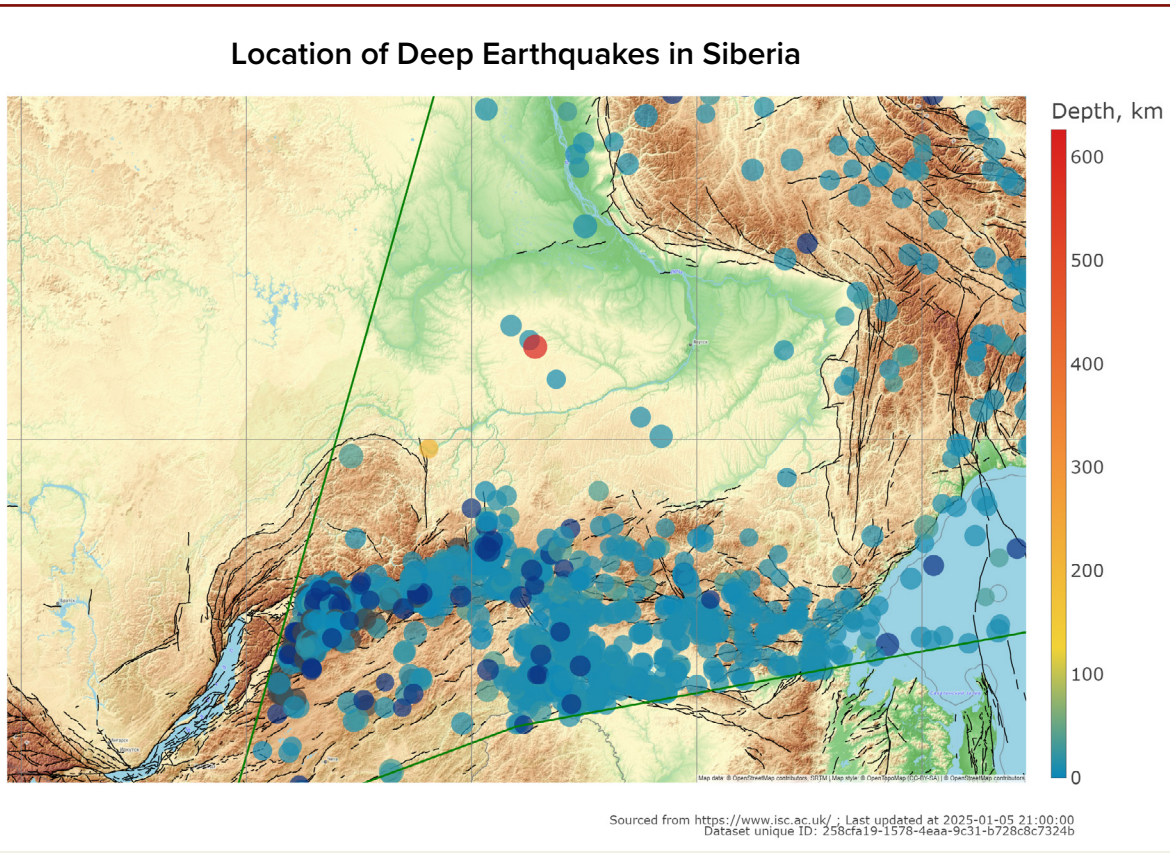

Fig. 64
The map marks the epicenter of the deep-focus M5.1 earthquake at a depth of 627 km beneath the Siberian platform in 2023, and the M3.3 earthquake at a depth of 211 km (marked in yellow).

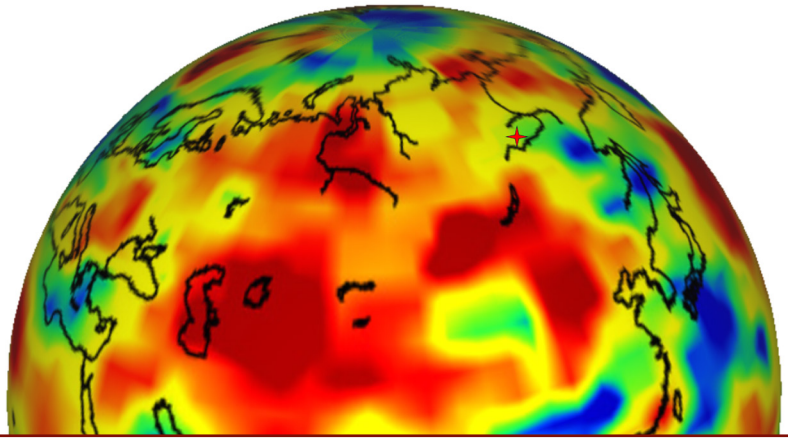

Fig. 65
Zones of low seismic velocities in the mantle at a depth of approximately 600 km. The hypocenter of the 2023 M 5.1 earthquake is located in the area of contact between relatively hot and relatively cold mantle regions.
Source: https://members.elsi.jp/~hiroki.ichikawa/gst/gallery/gallery.html

The oscillation of the peripheral sections of the Siberian Block is triggering an increase in seismic activity in the Ural region. Data for analysis were filtered to exclude seismic events associated with mining activities, considering only earthquakes with magnitudes of 3.5 and above to eliminate human-induced events (Fig. 66, 67). Consequently, the observed wave-like increase in seismicity reflects natural processes.

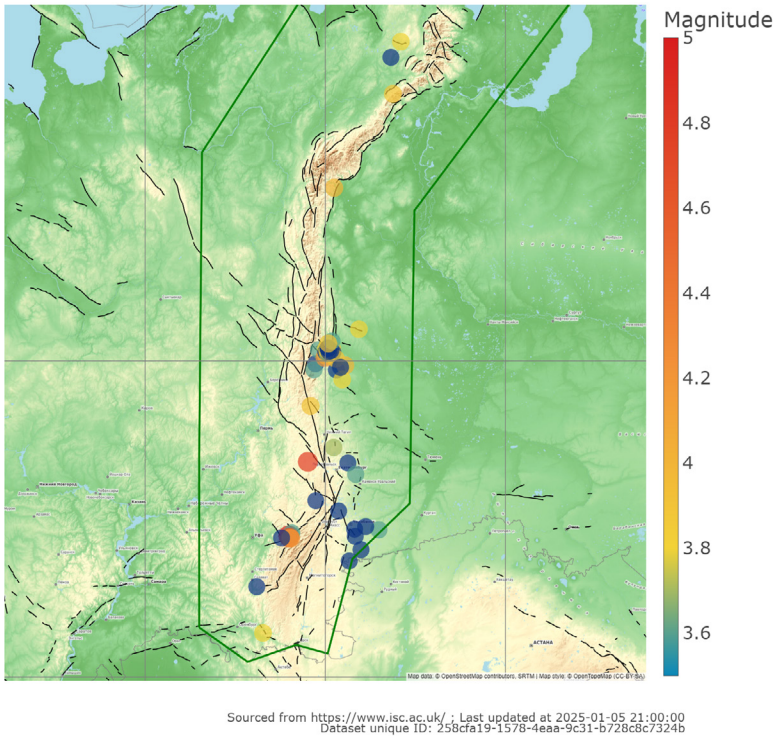

Fig. 66
Map of epicenters of M3.5+ earthquakes recorded in the Ural region from 1990 to 2022.

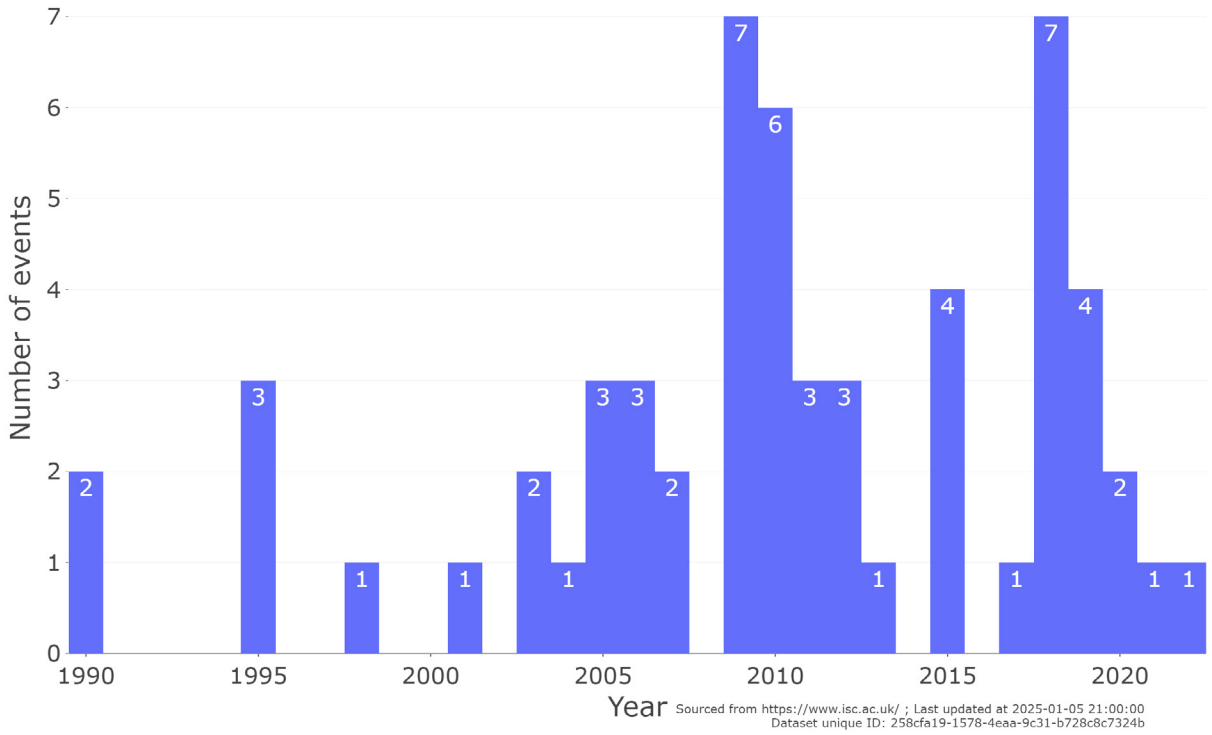

Fig. 67
Number of M3.5+ earthquakes recorded in the Ural region from 1990 to 2022.

Additionally, earthquakes with magnitudes ranging from 4.0 to 5.0 have appeared in the region, serving as further evidence of a natural increase in seismic activity (Fig. 68). The rise in seismicity in the Ural region does not occur steadily but rather in waves, which is a natural pattern.

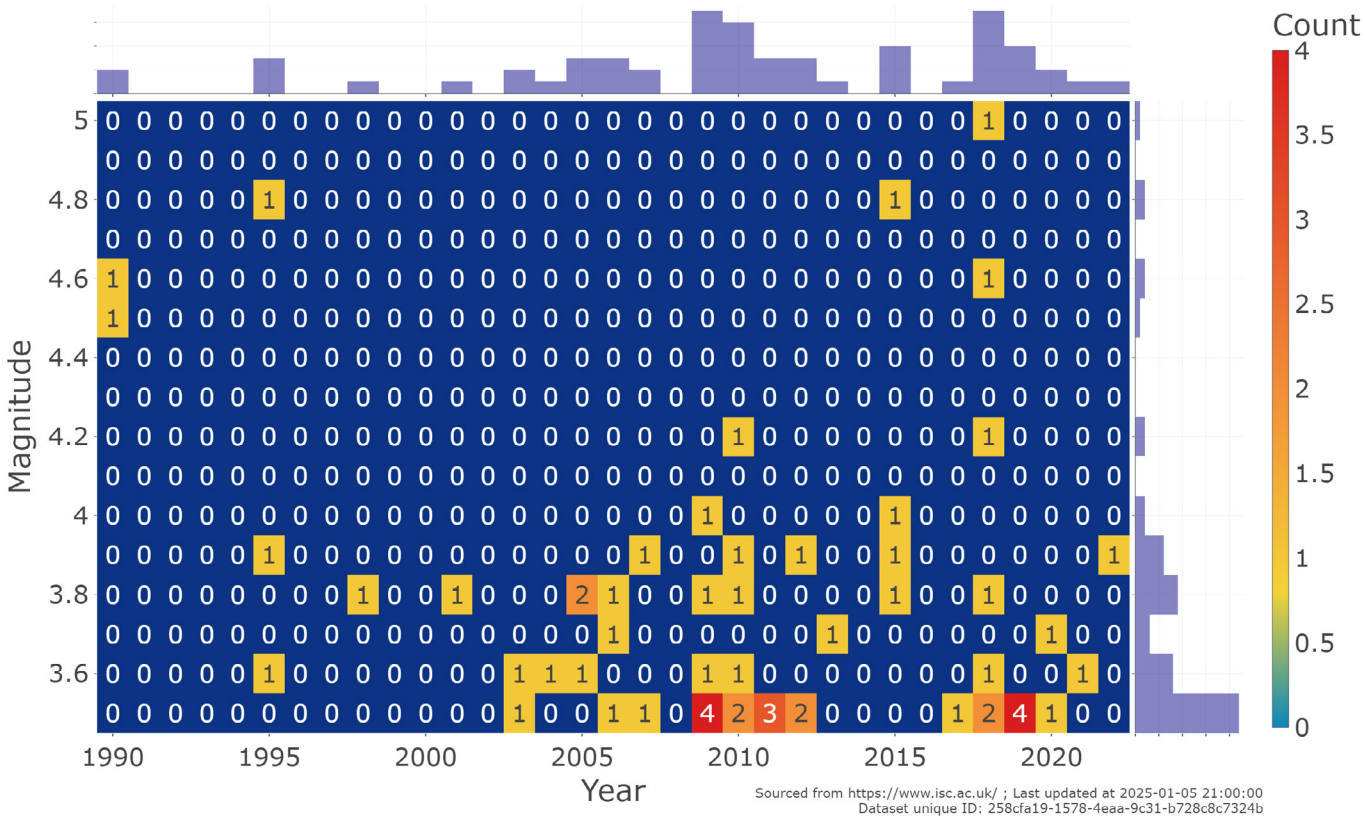

Fig. 68
Distribution of earthquakes recorded in the Ural region from 1990 to 2022 by magnitude.

Data source: ISC.

A graph is presented (Fig. 69) to compare the timing of peaks in seismic activity across different parts of the Siberian Plume area and its periphery. In 2021, seismic activity increased across all the regions examined, except for the Urals. We observe that activity is rising in all regions, and in recent years, it has been increasing in wave-like, 'pulsating' surges across different regions. At the same time, a certain pattern is observed, resembling the gradual oscillation of the plate from west to east and from north to south.

The emergence of wildfires in certain locations should also be considered. The increase in the area affected by fires in this region indicates heightened subsurface activity, as fires often arise in fault zones where combustible gases escape. These fires are difficult to extinguish and spread very quickly over large areas. In the Ural region, there has been a sharp increase in the area of natural fires since 2020 (Fig. 70). The graph is based on data from the Aerial Forest Protection Service (Avialesookhrana).

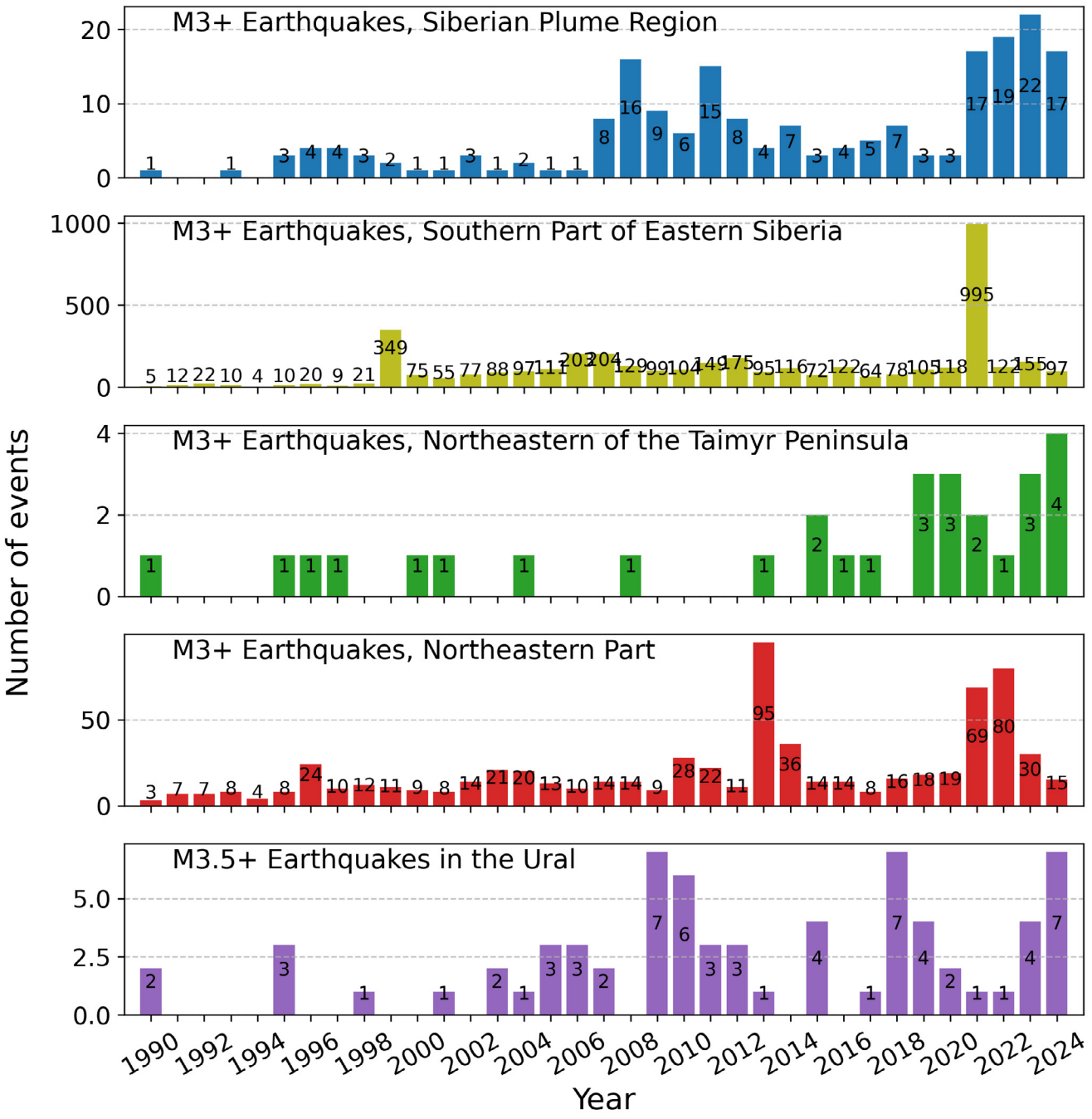

Fig. 69
Distribution of peaks in seismic activity in the Verkhoyansk region (east of the Siberian platform), the southern part of Eastern Siberia, the Ural region (west of the Siberian platform), and central Siberia (including the West Siberian Plate and the East Siberian Platform) by year. M3+ earthquakes.

Data source: ISC.

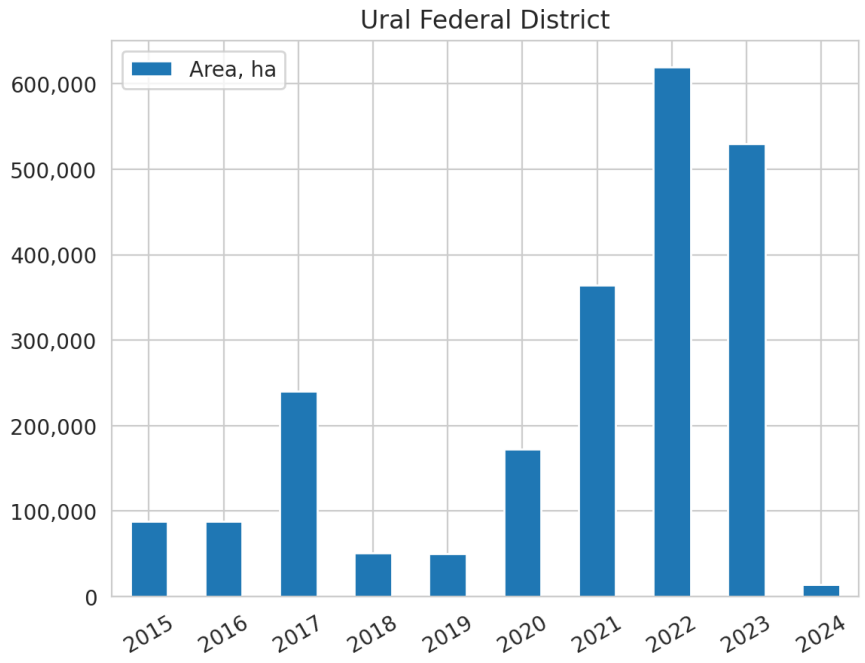

Fig. 70
Increase in the area of natural wildfires in the Ural egion since 2020. Graph based on data from the Aerial Forest Protection Service, Avialesookhrana.

The area affected by the fires in the Far Eastern region is also growing exponentially, as clearly illustrated in the graph (Fig. 71).

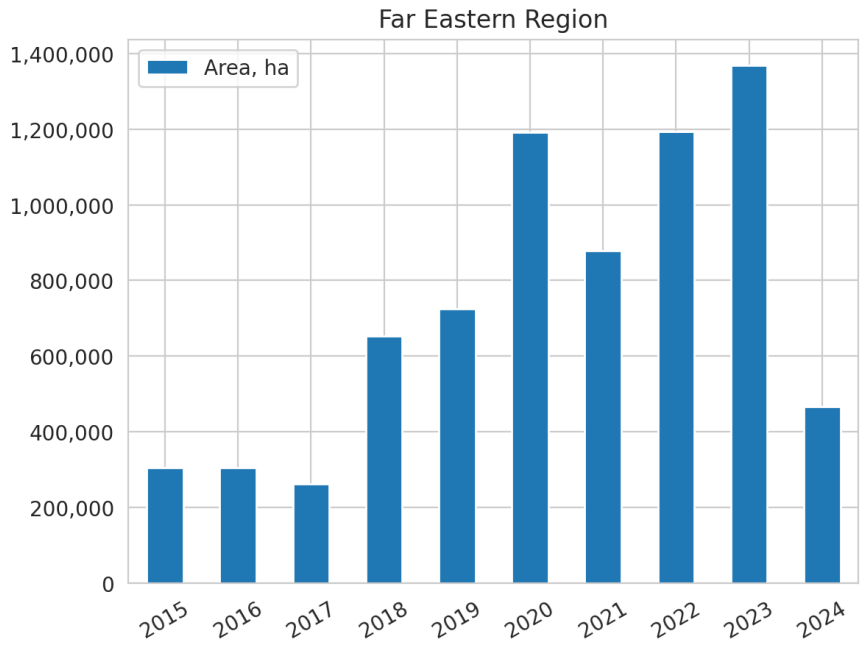

Fig. 71
Area of wildfire spread in the Far East: the graph includes data for Khabarovsk Krai, Kamchatka Krai, Magadan Oblast, Chukotka Autonomous Okrug, Sakhalin Oblast, and Primorsky Krai based on data from the Federal Forestry Agency (Aviolesookhrana).

(Data for 2024 are incomplete).

Thus, similar processes of increasing seismicity and wildfires occur on the opposite side of the Siberian and Far Eastern crustal blocks, along the boundary with the Pacific Plate.

Ilt is assumed that the intrusion of the Siberian plume also affects the Kuril-Kamchatka region as an ending region of a continental crustal block pressured by the plume. An analysis of seismic data in the Kamchatka and Kuril Islands region shows a noticeable increase in M4.0+ earthquakes (Figs. 72, 73). The region is part of the Pacific Ring of Fire (Fig. 74) and demonstrates a trend of increasing seismicity according to the patterns of this tectonic structure. However, most seismicity spikes are independent. This may indicate that the Siberian Plume exerts its own influence on the Kamchatka and Kuril Islands region.

M4+ Earthquakes Density in the Kamchatka Peninsula and Kuril Islands

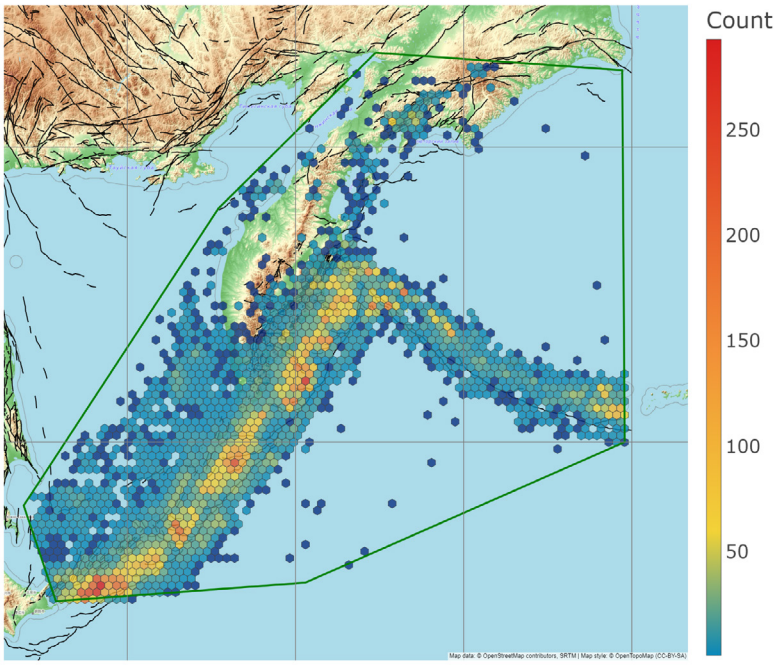

Sourced from https://www.isc.ac.uk/ ; Last updated at 2025-01-05 21:00:00
Dataset unique ID: 258cfa19-1578-4eaa-9c31-b728c8c7324b

Fig. 72
Earthquake density for M4+ earthquakes in the Kamchatka Peninsula and Kuril Islands region from 1979 to 2024.

Data source: ISC.

M4+ Earthquakes in the Kamchatka Peninsula and Kuril Islands

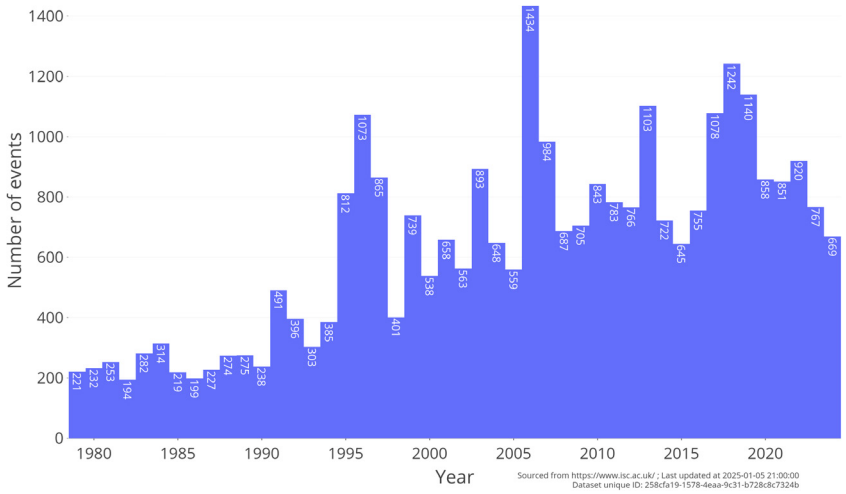

Fig. 73
Increase in the number of M4+ earthquakes in the Kamchatka Peninsula and Kuril Islands region from 1979 to 2024.

Data source: ISC.

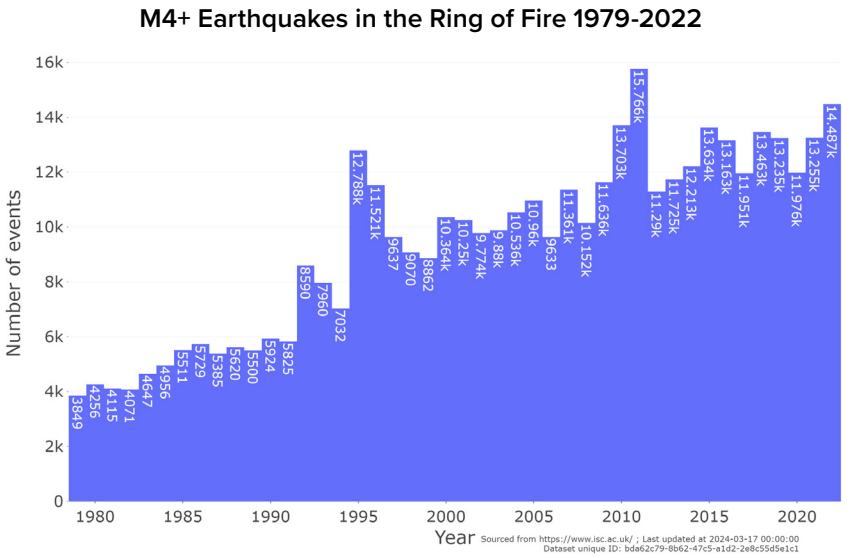

Fig. 74
ncrease in the number of M4+ earthquakes in the Ring of Fire region from 1979 to 2022.

Data source: ISC.

Remarkably, the depth of earthquakes in the Kuril-Kamchatka region is also increasing (Fig. 75). This indicates that the interaction between lithospheric plates is becoming more dynamic due to the influence of the Siberian mantle plume. An increase in volcanic activity in the Kuril-Kamchatka region is expected, along with the emergence of anomalies in the rapid ascent of deep magma and a swift shift in composition during volcanic eruptions to more mafic magmas. A similar compositional shift towards the deeper sources was demonstrated by the Bezymianny volcano during its 2017 eruption.[45]

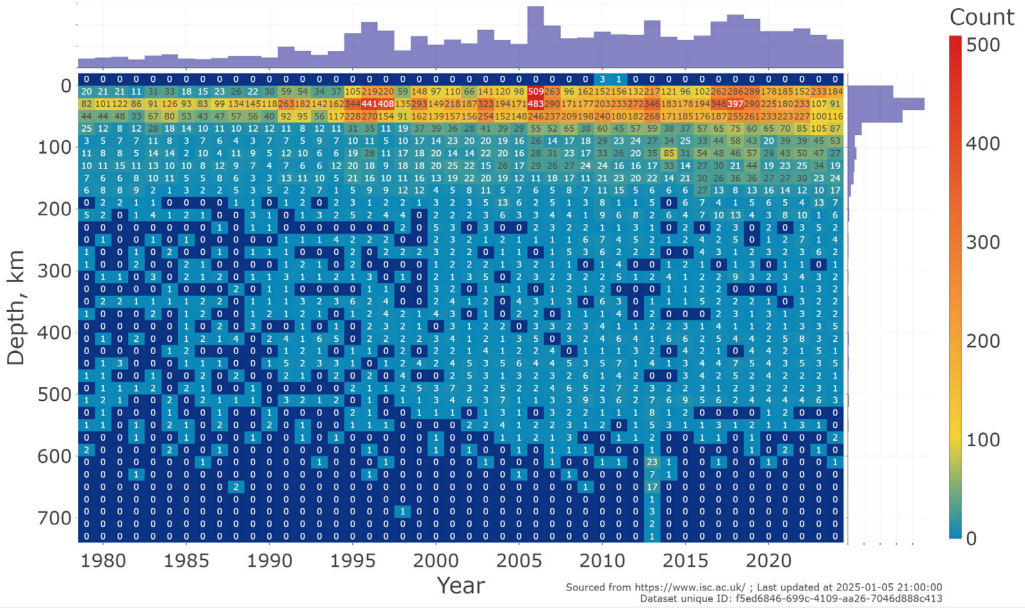

Fig. 75
Distribution of M4+ earthquakes recorded in the selected sector of the Kamchatka Peninsula and Kuril Islands region from 1979 to 2024 by depth. Data source: ISC.

[45] V.O. Davydova, V.D. Shcherbakov, P.Yu. Plechov, I.Yu. Koulakov, Petrological evidence of rapid evolution of the magma plumbing system of Bezymianny volcano in Kamchatka before the December 20th, 2017 eruption, Journal of Volcanology and Geothermal Research, Volume 421, 2022, 107422, ISSN 0377-0273, https://doi.org/10.1016/j.jvolgeores.2021.107422

The increase in seismicity, wildfires, and volcanic activity anomalies are edge effects of the uplift of the Siberian block of the Earth's crust, experiencing pressure from the Siberian Plume intrusion.

The rise in seismic activity not only in Siberia but especially along the edges of the West Siberian Plate and the East Siberian Craton suggests that the upward displacement of the plate due to pressure from the underlying mantle plume has already begun. This points to the significant and widespread impact of the magma plume on the plate.

Traditional models assumed that as mantle plumes rise and heat the overlying lithosphere, they should create a substantial surface uplift of up to 2 kilometers in height before magma breaks through. However, geological evidence of such dramatic uplift is absent in the region of the Siberian Traps, which formed as a result of a magma plume intrusion 250 million years ago.

Based on the study of magmatic rocks from the Siberian Traps, scientists from institutes in Russia, Germany, and France have determined[46] that, rather than ascending as a bubble, the plume gradually eroded the lithosphere from below (Fig. 76).

When the erosion at the contact zone between the molten plume material and the upper mantle rocks reached a depth of 50 kilometers (about 31 miles), large-scale lava outpourings and eruptions at the surface began.

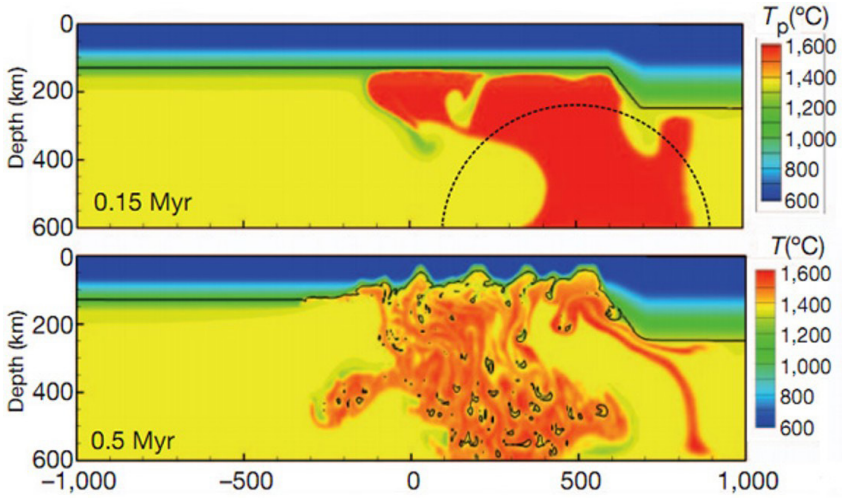

Fig. 76

A reconstruction of the initial stages in the formation of the Siberian Traps

The vertical axis shows depth (in km). Different colors indicate the temperature of the rock. The initial position of the mantle plume's apex is shown by a dashed semicircle. The plume approaches the lower boundary of the lithosphere—shown as a solid black line—and "spreads out" beneath it.

At the bottom: due to erosion by the plume's apex—visible are fragments of the lithosphere sinking into the depths—it has forged a path through the upper mantle toward the Earth's crust. This corresponds to the onset of the main phase of trap-related magmatism.

Source: Sobolev, S. V., Sobolev, A. V., Kuzmin, D. V., Krivolutskaya, N. A., Petrunin, A. G., Arndt, N. T., Radko, V. A., & Vasiliev, Y. R. (2011). Linking mantle plumes, large igneous provinces and environmental catastrophes. Nature, 477, 312-316.

[46] Sobolev, S. V., Sobolev, A. V., Kuzmin, D. V., Krivolutskaya, N. A., Petrunin, A. G., Arndt, N. T., Radko, V. A., & Vasiliev, Y. R. (2011). Linking mantle plumes, large igneous provinces and environmental catastrophes. Nature, 477, 312-316. DOI: 10.1038/nature10385

The modern activity of the plume likely follows the same mechanism. Therefore, significant localized surface uplift at a single point where the plume head intrudes is not anticipated. However, this mechanism does not rule out a widespread regional uplift of the entire East Siberian Platform by a small amount. According to tectonophysical modeling, even such minor uplift would suffice to trigger magma breakthroughs, releasing molten material under high pressure and causing a catastrophic event.

The presumed center of the plume head is located in the region north of the Putorana Plateau, approximately 225 km northeast of Norilsk. Additionally, breakthroughs would affect the entire thin West Siberian Plate, where old sutures—rifts and deep faults in the Earth's crust—are likely to reopen.

Evidence of the Inevitability of the Siberian Plume Eruption

The high risk of magma breakthroughs from the modern Siberian plume in the current period is driven by the following conditions:

Over the past 30 years, the Earth has experienced a gradual increase in geophysical anomalies, which are direct consequences of external forces intensifying thermal energy near the planet's core. However, the current situation differs significantly from the previous period. **By the end of 2024, the planet will enter a phase of heightened energetic influence on its core. Calculations indicate that by 2030, we will reach the peak of this phase.**

A critical factor exacerbating the situation is the global pollution of the oceans due to anthropogenic influences, including hydrocarbons, microplastics, and nanoplastics. This pollution has significantly altered the thermal conductivity of ocean water, impairing its ability to efficiently dissipate heat from Earth's interior. Historically, the ocean has acted as the planet's primary thermal regulator, but it has now lost a substantial portion of its heat-conducting capacity. As a result, there is an abnormal accumulation of thermal energy in the mantle, leading to its melting at an unprecedented rate in Earth's history.

Geophysical studies indicate a dramatic increase in the number of deep-focus earthquakes, which serve as direct indicators of active mantle melting. The expanding volume of molten magma exerts immense pressure on the Earth's crust. This process is analogous to inflating a balloon. Eventually, the pressure will exceed the strength of the crust, resulting in a rupture.

The Siberian region is particularly vulnerable to these processes due to its unique geological structure, as a powerful mantle plume—an ascending flow of molten mantle material—is rising beneath the area. This plume was triggered by the core's shift in this direction in 1997–1998. The increasing temperature anomalies in Siberia indicate that the volume of magma beneath the Siberian Craton continues to grow exponentially. Based on geological data and recent observations, there is a high degree of confidence that the Siberian plume has entered a critical phase of readiness for an eruption.

What is especially concerning is the simultaneous critical situation in the Mariana Trench, the deepest point of the ocean floor, where the crust is thinnest and most vulnerable. This region is also experiencing the rise of molten magma, accompanied by a significant increase in seismic activity. The threat of an oceanic rupture here poses a realistic scenario of planetary destruction.

Two potential scenarios may unfold. The first involves the eruption of the Siberian plume, which could occur at any moment due to the growing pressure of magma. The second involves a rupture in the Mariana Trench, which could precede the Siberian catastrophe. The Siberian plume would not erupt if the Mariana Trench rupture occurs first.

The geological history of Mars provides a stark example of the consequences of such a scenario—Mariner Valley serves as a silent testimony to a similar disaster, where the eruption of a plume beneath an ocean led to catastrophic outcomes for the entire planet.

According to calculations based on current trends in geophysical activity, the critical rupture point for the Mariana Trench may be reached by 2036. However, it is important to recognize that this timeline is conditional. The Earth's crust in Siberia could succumb to increasing pressure much earlier. Given the current trajectory of events, a rupture of the Siberian plume or the Mariana Trench appears to be an inevitable consequence of the processes occurring deep within the Earth. The only uncertainty lies in the exact timing and location of the catastrophe, not in the certainty of its approach.

Let's consider three potential scenarios for the development of the situation with the Siberian plume. The first scenario is a sudden, one-time breakthrough of the Siberian plume. The second scenario involves slow and gradual lava eruptions in Siberia, similar to the formation of the Siberian Traps. The third scenario occurs if humanity takes necessary measures to degas secondary magmatic hotspots of the Siberian plume within the Earth's crust.

Scenario 1:
Instantaneous One-Time Eruption of the Siberian Plume

A comparative analysis of historical geological events can be used to estimate the potential damage from a sudden eruption of the Siberian plume. However, it is important to consider that the current conditions on Earth—specifically, the convergence of the most intense 24,000-year cycle with anthropogenic pollution of the planet's primary cooling system, the oceans—are unprecedented. For this reason, a sudden breakthrough of the Siberian plume is considered the most likely scenario if no measures are taken by humanity to mitigate its risks.

To assess the magnitude of volcanic eruptions, the volume of ejected material is used. For example, during one of the most powerful eruptions of the Yellowstone supervolcano 2.1 million years ago, the volume of ejected magma was approximately 2,500 km^3 (600 mi^3), as determined from the study of tuff deposits in North America.[47] This eruption propelled ash and gasses to an altitude of 50 kilometers (31 miles), reaching the upper boundary of the stratosphere. A similar scale was observed in the eruption of the Toba supervolcano on the island of Sumatra, which occurred about 72,000–74,000 years ago and was the most powerful eruption in the last 25 million years.

[47] Swallow, E. J., Wilson, C. J. N., Charlier, B. L. A., & Gamble, J. A. (2019). The Huckleberry Ridge Tuff, Yellowstone: evacuation of multiple magmatic systems in a complex episodic eruption. Journal of Petrology, 60, 1371-1426. https://doi.org/10.1093/petrology/egz034

According to various estimates, the volume of ejected material during the eruption of the Siberian Traps around 250 million years ago ranged from 3 to 4 million km^3 (720,000 to 960,000 mi^3) of lava and tuffs[48] (Fig. 77). This means the Siberian Traps eruption was 1,000 times larger in terms of ejected material than the most powerful known eruptions of the Yellowstone Caldera or the Toba supervolcano.

Considering the sudden nature of a potential Siberian plume eruption, its activation could result in an event with a magnitude 1,000 times greater than these historical eruptions, such as those of the Yellowstone Caldera or the Toba supervolcano.

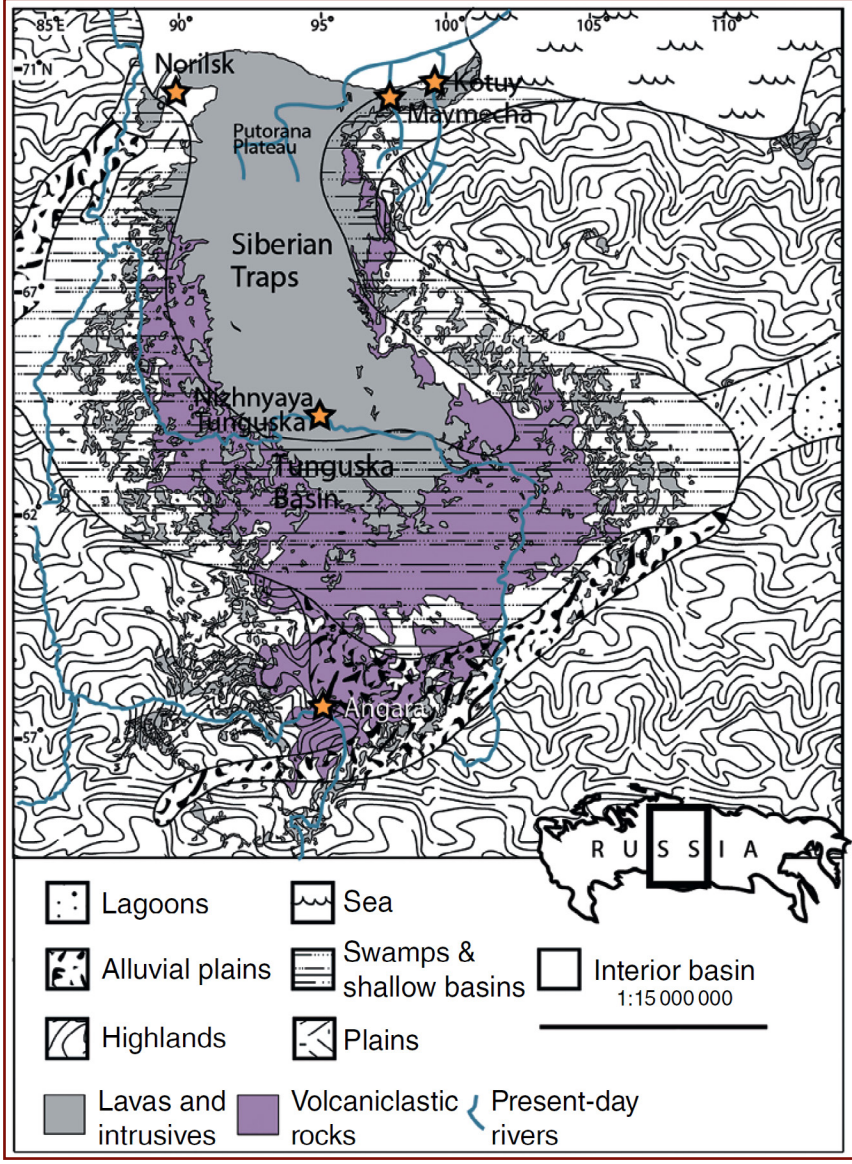

Fig. 77
Paleogeographic Map of the Siberian Traps that illustrates the scale of major volcaniclastic outflows and regions associated with the Siberian Traps. It is based on data from Malich et al. (1974), Polozov et al. (2010), and Black et al. (2015), with simplified Late Permian paleogeography adapted from Czamanske et al. (1998).

Source: Black, B., Mittal, T., Lingo, F., Walowski, K., & Hernandez, A. (2021). Assessing the Environmental Consequences of the Generation and Alteration of Mafic Volcaniclastic Deposits During Large Igneous Province Emplacement. In R. E. Ernst, A. J. Dickson, & A. Bekker (Eds.), Geophysical Monograph Series (pp. 117-131). Wiley. https://doi.org/10.1002/9781119507444.ch5

[48]Black, B., Mittal, T., Lingo, F., Walowski, K., & Hernandez, A. (2021). Assessing the Environmental Consequences of the Generation and Alteration of Mafic Volcaniclastic Deposits During Large Igneous Province Emplacement. In R. E. Ernst, A. J. Dickson, & A. Bekker (Eds.), Geophysical Monograph Series (pp. 117-131). Wiley. https://doi.org/10.1002/9781119507444.ch5

It is hypothesized that a sudden breakthrough of the Siberian plume would result in an explosive eruption, forming a single caldera. According to this hypothesis, the caldera created by the Siberian plume's breakthrough would cover an area of approximately 75,000 km^2 (29,000 mi^2), with a radius of about 150 km (93 miles) or dimensions of 380 km by 250 km (236 by 155 miles). During the eruption of the Siberian Traps 250 million years ago, the area inundated by lava, as documented in the literature[49], ranged from 4 to 7 million km^2 (1.5 to 2.7 million mi^2)[50]. A similar scale of land coverage could be affected in this event.

The notion that lava flows are the most dangerous volcanic phenomena is a misconception. In reality, ash often becomes the primary cause of fatal consequences. For supervolcanoes characterized by high explosivity, a significant portion of magma does not transform into lava. Instead, it fragments during the explosion, producing enormous quantities of fine volcanic ash—scalding fragments of sharp, jagged rock particles that disperse into the atmosphere. Inhalation of this ash forms a cement-like mixture in human lungs, leading to inevitable death.

It is estimated that during a Siberian plume eruption, the radius of dispersal for such scalding ash would reach approximately 9,000 km (5,592 miles), covering an area of about 255 million km^2 (98.5 million mi^2). Given that the total surface area of Earth is slightly over 510 million km^2 (197 million mi^2), the ash-affected zone, where breathing would become impossible, would encompass about half the planet, approximately 50% of Earth's surface.

Thus, a sudden breakthrough of the Siberian plume is expected to produce three life-threatening impact zones.

The first (central) impact zone is a region with a radius of 150 km (93 miles), centered in the northwestern part of the Putorana Plateau, where the caldera is expected to form (Fig. 78). This zone encompasses the cities of Norilsk, Dudinka, and Talnakh in the Krasnoyarsk Krai. Within this zone, the activation of the plume would result in the instantaneous destruction of all structures due to the shockwave and scorching pyroclastic flows during the initial phase of the eruption.

The second impact zone, extending to a radius of 1,500 km (932 miles) from the center, is the area affected by lava flows and heavy volcanic materials (Fig. 79). This zone would cover vast areas of northern Siberia, including the Yamalo-Nenets Autonomous Okrug, the Taymyr Peninsula, parts of the Khanty-Mansi Autonomous Okrug, northern Krasnoyarsk Krai, western Yakutia, and the northeastern European part of Russia. Major cities within this radius include Igarka, Novy Urengoy, Nadym, Salekhard, Vorkuta, Naryan-Mar, Mirny, Kogalym, Lesosibirsk, Surgut, Krasnoyarsk, Khanty-Mansiysk, Tomsk, and Nizhnevartovsk.

In the first hours of the eruption, this territory would be subjected to fast-moving flows of scorching gas, ash, and lava traveling at speeds of up to 700 km/h (435 mph). These flows would obliterate all life and infrastructure, burying the region under a thick layer of volcanic materials and consuming natural resources.

[49] Fedorenko, V. A., Lightfoot, P. C., Naldrett, A. J., Czamanske, G. K., Hawkesworth, C. J., Wooden, J. L., & Ebel, D. S. (1996). Petrogenesis of the Flood-Basalt Sequence at Noril'sk, North Central Siberia. International Geology Review, 38(2), 99-135. https://doi.org/10.1080/00206819709465327

[50] Ivanov, A.V., He, H., Yan, L., Ryabov, V.V., Shevko, A.Y., Palesskii, S.V., Nikolaeva, I.V., 2013. Siberian Traps large igneous province: Evidence for two flood basalt pulses around the Permo-Triassic boundary and in the Middle Triassic, and contemporaneous granitic magmatism. Earth-Science Reviews, 122, pp.58–76. Available at: https://doi.org/10.1016/j.earscirev.2013.04.001

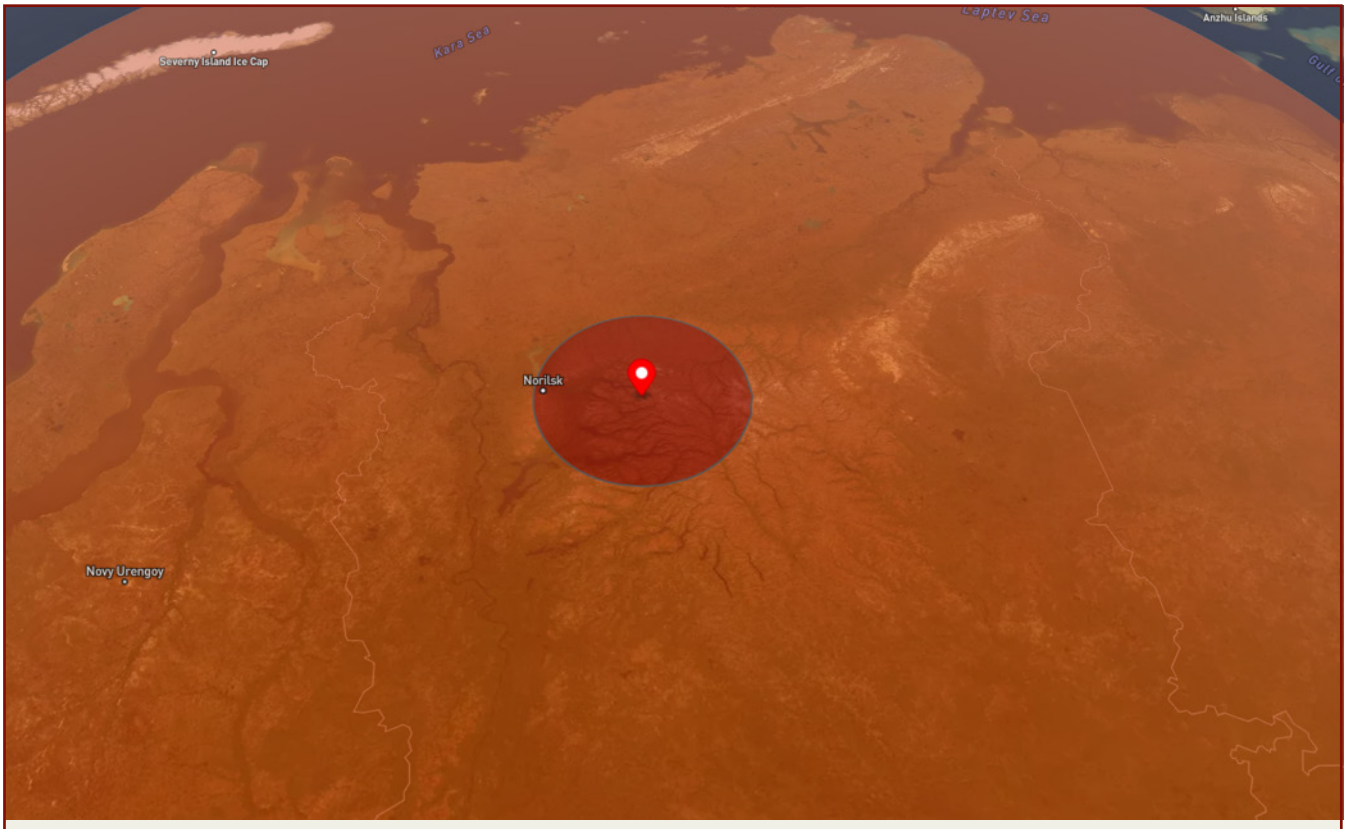

Fig. 78
The caldera formation zone is shown in red, with an approximate radius of 150 km

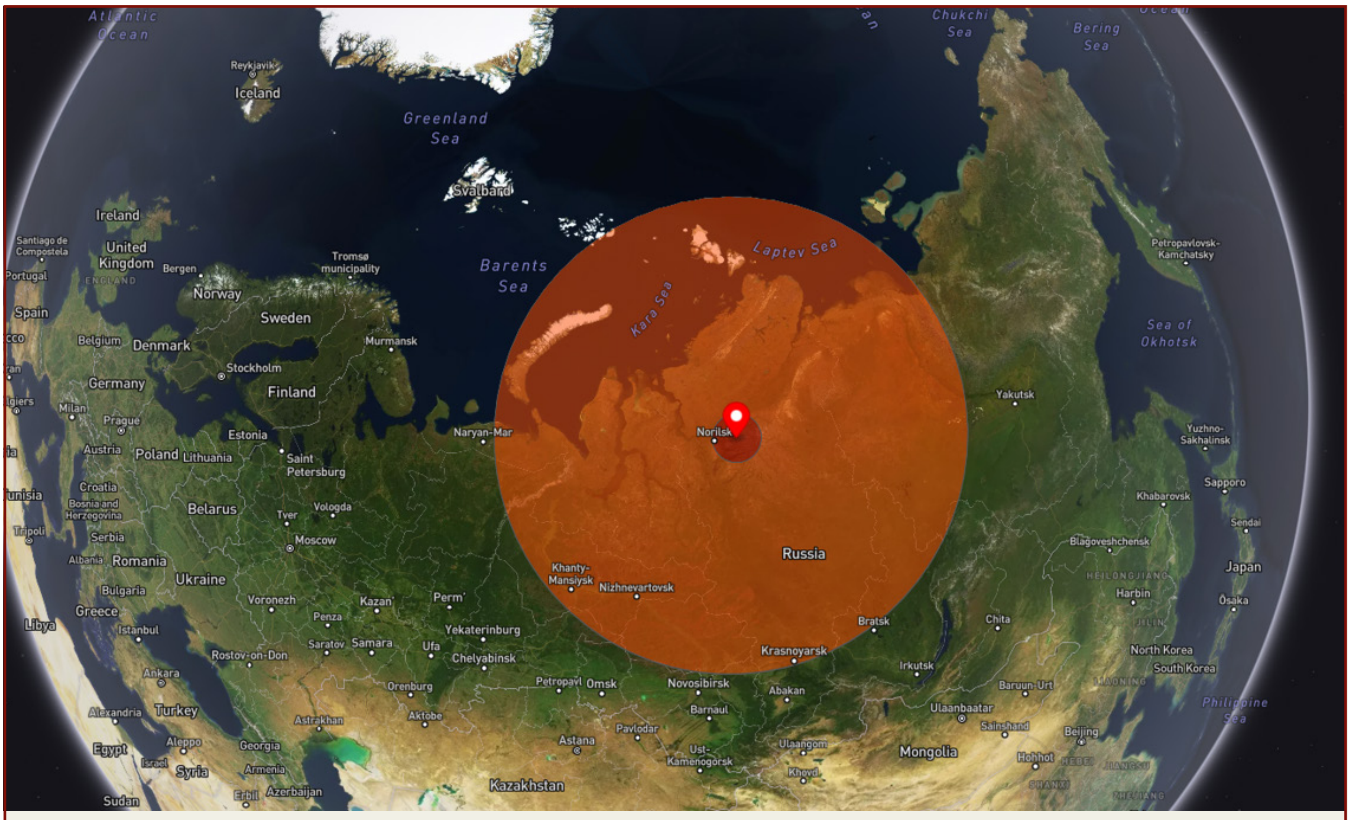

Fig. 79
The lava flow and heavy pyroclastic fallout zone is shown in orange, with an approximate radius of 1,500 km

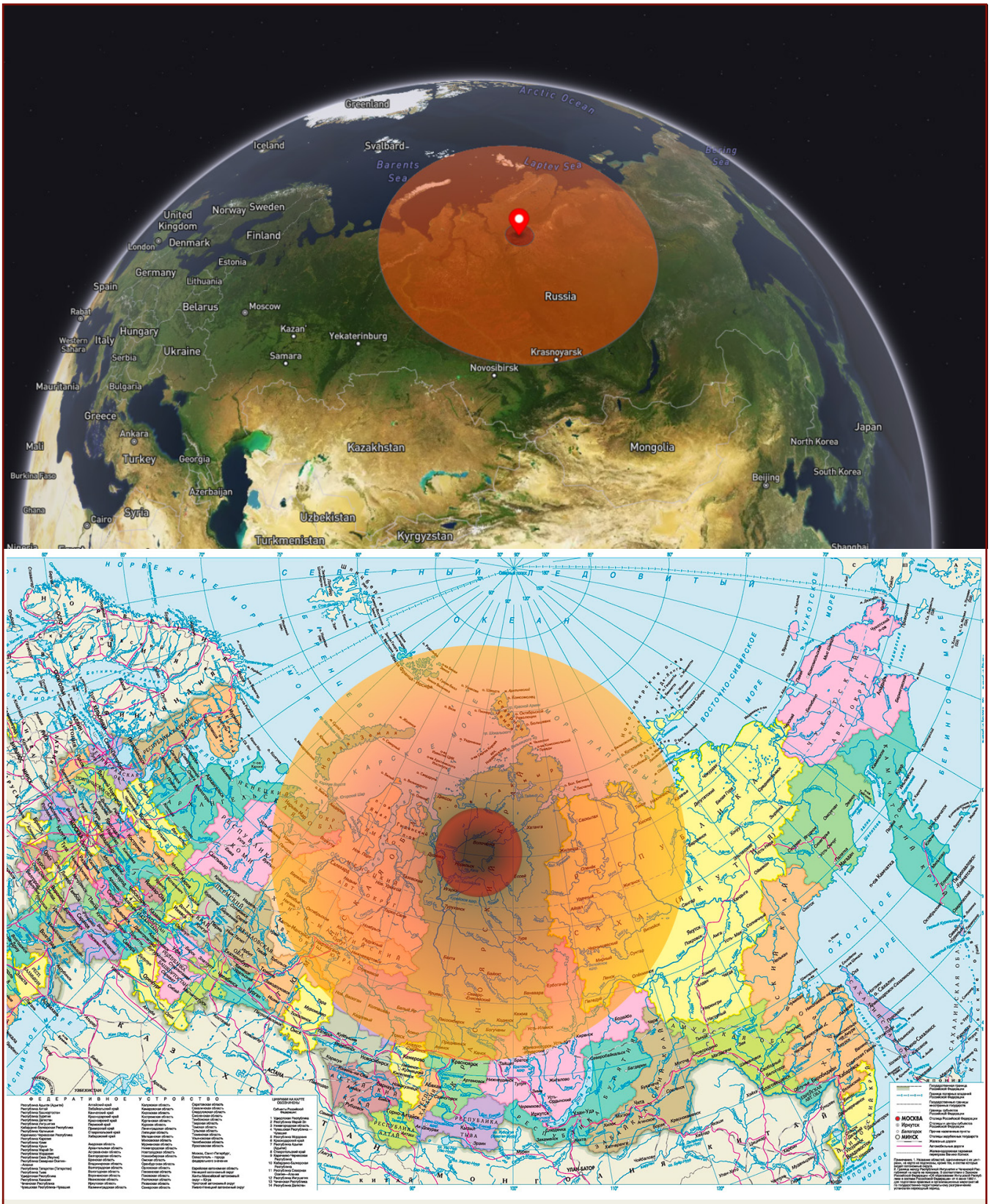

Fig. 79
The lava flow and heavy pyroclastic fallout zone is shown in orange, with an approximate radius of 1,500 km

The third impact zone, with a radius of approximately 9,000 km (5,592 miles), encompasses the dispersal area of fine pyroclastic materials and volcanic ash, covering roughly 50% of Earth's surface (Fig. 80).

During the initial phase (the first 24 hours after the eruption), the ash fallout will primarily affect the territories of the Russian Federation, continental Asia, Europe, the Arabian Peninsula, the northern part of the African continent, and North America. Over the following 7–10 days, the ash masses are expected to spread to the Australian continent, South America, and Antarctica.

Fig. 80
The dispersal area of fine volcanic ash is shown in yellow, with an approximate radius of 9,000 km

Fig. 80
The dispersal area of fine volcanic ash is shown in yellow, with an approximate radius of 9,000 km

Research into geological processes indicates that the activation of the Siberian plume would trigger a series of additional catastrophic phenomena. These include the generation of a powerful shockwave, the occurrence of powerful earthquakes (with magnitudes around 10), the formation of destructive tsunamis, and the potential awakening of other major volcanic systems on Earth. The energy released during the eruption could initiate a chain reaction, activating supervolcanoes and large volcanic regions across the planet. These conclusions are based on mathematical calculations of energy processes and their impact on the Earth's crust.

Next, we will examine additional risk factors threatening humanity as a result of the sudden breakthrough of the Siberian plume.

Shockwave

According to publicly available data, an eruption of the Yellowstone supervolcano could release energy equivalent to approximately 900,000 megatons and trigger an earthquake with a magnitude of 11.2. Since the magnitude scale is logarithmic (each whole number increase represents a 32-fold increase in energy), an eruption of the Siberian plume, estimated to be 1,000 times more powerful than Yellowstone, could result in an earthquake with a magnitude of 13.2. This would be 350,000 times more powerful than the strongest earthquake ever recorded—the Great Chilean Earthquake (magnitude 9.5, 1960)—and would rival the impact of a large asteroid collision.

The energy released, on the order of 10^{24} joules, would generate an immensely powerful shockwave on a global scale. At the center of the eruption, pressure would reach levels so extreme that rocks would instantly vaporize and be ejected into the upper atmosphere. A supersonic shockwave would devastate areas thousands of kilometers away within minutes, akin to the Tunguska meteorite impact, but far more powerful.

Massive wildfires would erupt in the Siberian taiga, burying vast regions under a thick layer of volcanic ash. Permafrost would rapidly melt across thousands of kilometers, releasing significant amounts of greenhouse gasses. The landscape would suffer extensive destruction with the activation of crustal fault lines. Seismic waves would propagate across the entire planet, triggering additional earthquakes with magnitudes exceeding 10.

In the Arctic Ocean, enormous tsunamis hundreds of meters high would form, threatening the coasts of Russia, Canada, Greenland, and Scandinavia. Secondary tsunamis would strike the shores of Indonesia, Japan, Australia, and both North and South America. Global atmospheric disturbances would lead to the formation of potent hurricanes and storms.

Activation of Supervolcanoes and Volcanic Systems

Seismic waves from the eruption of the Siberian plume would propagate not only through the atmosphere and Earth's surface but also deep into the mantle. Since all supervolcanoes are interconnected through the molten layers of the mantle, seismic waves of this magnitude are expected to trigger a chain reaction of eruptions within the first 24 hours (Fig. 81). The largest volcanic systems likely to become active include the Yellowstone and Long Valley calderas (North America), the Phlegraean Fields (Apennine Peninsula), Toba (Sunda Archipelago), the Aira Caldera (Japanese Islands), and the Taupo volcanic complex (New Zealand).

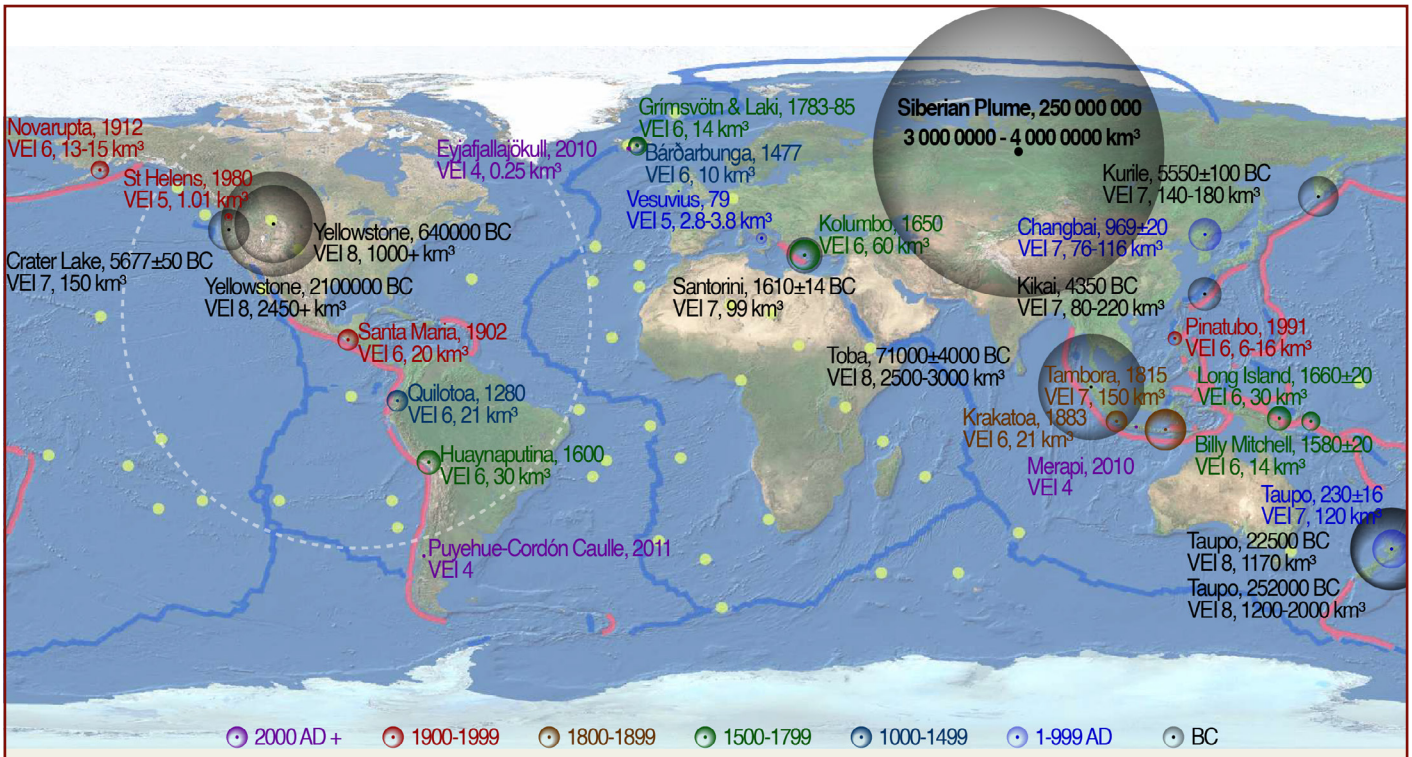

Fig. 81

The map shows a global distribution of major volcanic eruptions, classified by geological periods from the Precambrian to the present day

The size of the symbols is proportional to the volume of ejected material (in km^3). The map highlights the chronological sequence of eruptions with a Volcanic Explosivity Index (VEI) of ≥4, emphasizing events such as Toba (71,000 ± 4,000 BCE, 2,500–3,000 km^3), Yellowstone (640,000 BCE, >1,000 km^3), and Tambora (1815 CE, 150 km^3). Comparable eruptions are expected if the Siberian plume erupts, with an estimated output of 3–4 million km^3. Red lines indicate tectonic plate boundaries, illustrating the spatial correlation with the locations of major eruptions.

In addition to supervolcanoes, eruptions are likely to begin at many volcanoes along the Pacific Ring of Fire and other seismically active zones. There is a high probability of renewed activity at volcanoes such as Mount Fuji (Japan), Krakatoa and Merapi (Indonesia), Vesuvius and Etna (Italy), Popocatépetl (Mexico), volcanic groups in Kamchatka, the Andes, and the Alaskan volcanic belts, as well as subglacial volcanic systems in West Antarctica.

Dormant volcanic structures may also be reactivated, including stratovolcanos Ararat (Anatolian Plateau), Kilimanjaro and Nyiragongo (East African Rift System); the Elbrus volcanic massif (Caucasus region), the Laacher See volcano (Central Europe), and volcanic centers on the Arabian Peninsula.

Acid Rain

The catastrophic release of volcanic ash and sulfur dioxide during the eruption would cause precipitation worldwide to take the form of acid rain. To illustrate the scale of emissions, we can refer to the Yellowstone supervolcano eruption 630,000 years ago, which released approximately 500 megatons of sulfur dioxide into the atmosphere. Extrapolating this to the hypothetical eruption of the Siberian plume, emissions could reach an estimated 1,500,000 megatons (1.5×10^{12} tons) of sulfur dioxide—about a million times the emissions of Tambora in 1815, which caused the "Year Without a Summer." It is important to note that this estimate does not account for emissions from other volcanoes that could be triggered in a chain reaction.

Such a concentration of sulfur dioxide would lead to the formation of aerosol particles in the stratosphere, which would gradually be washed out over decades as acid rain. The primary period of acid precipitation is predicted to last 3 to 10 years, depending on climatic processes and atmospheric circulation. Regions closer to the epicenter, such as contemporary Siberia, would experience precipitation with a pH below 1.5, comparable to diluted sulfuric acid.

The effects would include the destruction of vegetation, such as roots, leaves, and branches, and the leaching of minerals from the soil, rendering it unfit to sustain life. Aquatic ecosystems would also suffer severe acidification, turning water bodies into toxic acid lakes with pH levels of 2–3. These conditions would be fatal for most life forms.

Additionally, acid infiltration into water supply systems would render drinking water unusable without advanced filtration systems. Infrastructure made of cement, marble, and metals would face accelerated corrosion from sulfate compounds.

While the peak intensity of acid rain would occur in the first months after the eruption, precipitation would gradually localize to specific regions. As volcanic winter sets in, much of the precipitation would transition to snow, reducing the immediate acid burden on ecosystems. However, by this point, the global destruction of flora and fauna caused by acid rain would already be irreversible.

The damage to ecosystems would have profound effects on natural and human processes long before global cooling begins.

Volcanic Winter

The cumulative impact of the Siberian plume eruption, amplified by the simultaneous activation of numerous volcanoes, would result in a catastrophic alteration of global climate and ecological conditions. Massive emissions of volcanic ash, gases (particularly sulfur dioxide, SO_2), and aerosols into the atmosphere would form an impenetrable barrier to solar radiation for decades.

The high concentration of sulfate aerosols in the stratosphere would reflect a significant portion of solar radiation, disrupting the planet's energy balance. This would lead to a dramatic reduction in heat reaching Earth's surface, resulting in extreme climate cooling—a state that could be termed a "hypervolcanic winter." Under such conditions, Earth would resemble an "ice ball," with habitable zones restricted to limited regions, primarily near the equator.

Projections of potential impacts are based on historical data from significant eruptions. For instance, during the maximum eruption of Yellowstone 2.1 million years ago, global temperatures decreased by an average of 3–5°C (5.4–9°F). For the Siberian plume eruption, whose magnitude would far exceed that event, it is estimated that the Earth's average temperature could drop by approximately 24–31°C (43.2 - 55.8°F).

In polar regions, temperature reductions are expected to reach 28–36°C (50.4–64.8°F) or more, resulting in the complete freezing of critical water bodies, including the North Atlantic and significant parts of the Pacific Ocean. Temperatures in mid-latitudes would decline by 24–31°C (43.2 - 55.8°F), eradicating all vegetation and triggering mass extinction of organisms.

Oceanic ecosystems would suffer catastrophic destruction. Freezing would begin at the surface and along coastal areas, leading to the extinction of marine biota on a global scale. In equatorial regions, temperatures are projected to drop by 20–27°C (36.0–48.6°F), rendering even tropical zones too cold to sustain life.

Virtually all land surfaces would become barren due to the global cold, darkness, and the cessation of photosynthesis. Food chains would collapse, causing the breakdown of agriculture and the mass extinction of flora, fauna, and a significant portion of humanity. Only isolated microbial ecosystems adapted to extreme conditions would remain viable.

Sulfate aerosols persisting in the stratosphere would continue to block sunlight for decades. However, the consequences of a hypervolcanic winter would be felt for far longer. Even after the ash and aerosols settle, given the frozen oceans, glacial expansion, and radical transformations in the biosphere, Earth would require hundreds or even thousands of years to restore its natural climate and ecological balance.

Conclusions on Scenario 1: Sudden Breakthrough of the Siberian Plume

A sudden eruption of the Siberian plume would constitute a catastrophic geological and climatic event, triggering global changes in the atmosphere, hydrosphere, and biosphere. A massive explosion on the Putorana Plateau would instantly annihilate everything within a 150 km (93-mile) radius, forming a giant caldera. Pyroclastic flows and lava would extend over a 1,500 km (932-mile) radius, turning Siberia into a scorched wasteland. Half of Earth's surface would be covered by ash.

An earthquake of up to magnitude 13.2 caused by the plume's explosion would generate destructive seismic waves that would spread across the planet, activating fault lines, secondary earthquakes, and mega-tsunamis hundreds of meters high, inundating the coastal zones of continents.

The release of 1.5 million megatons of sulfur dioxide (SO_2) would result in acid rain with a pH below 1.5, destroying soils, vegetation, and aquatic ecosystems. Water bodies would become uninhabitable, and land would rapidly lose its fertility. The collapse of photosynthesis and food chains would lead to the mass extinction of flora, fauna, and human civilization.

The massive activation of supervolcanoes, including Yellowstone, Campi Flegrei, and Toba, would exacerbate global climate changes by increasing emissions of volcanic ash, sulfur dioxide (SO_2), and aerosols. Their accumulation in the stratosphere would block sunlight, causing planetary cooling ("hypervolcanic winter") and temperature drops of tens of degrees. In polar regions, temperatures would plummet by more than 28–36°C (50.4–64.8°F); in temperate zones, by 24–31°C (43.2–55.8°F); and in the tropics, by 20–27°C (36.0–48.6°F). This would result in frozen oceans, halted oceanic circulation, ecosystem collapse, and the formation of massive glaciers on land.

The effects of a hypervolcanic winter would render Earth virtually uninhabitable, with natural conditions requiring thousands to millions of years for recovery. Such an event would mark the largest extinction in the planet's geological history.

Scenario 2:
Gradual Eruption of the Siberian Plume

The second scenario envisions a gradual series of eruptions and lava flows through fractures and weakened zones in the Earth's crust rather than a single explosive event. This process is comparable to the formation of the Siberian Traps in the same region at the end of the Permian period 250 million years ago.

The formation of the Siberian Trap provinces marked the largest manifestation of terrestrial volcanism. During this time, Earth experienced the greatest environmental catastrophe in its history—the Permian–Triassic mass extinction, in which up to 90% of marine species and 70% of terrestrial species disappeared (Fig. 82, 83).

Geological evidence[51] indicates that the Siberian eruptions may have been unusually explosive (Campbell et al., 1992), with pyroclastic deposits reaching thicknesses of up to 800 meters (0.5 miles) (Khain, 1985). The highly explosive nature of the eruptions expelled sedimentary rocks from depths of up to 10 km (6.2 miles).

Fig. 82
Artistic depiction of eruptions in Siberia during the Permian-Triassic extinction event

Illustration: Image by Tigran Nshanyan

Fig. 83
Artistic depiction of lystrosaurs, survivors of the mass extinction, dominating a desolate landscape, illustrating ecosystem changes after the Permian-Triassic crisis

Illustration: Julio Lacerda

[51] Beerling, D.J., Harfoot, M., Lomax, B. & Pyle, J.A., 2007. The stability of the stratospheric ozone layer during the end-Permian eruption of the Siberian Traps. Philosophical Transactions of the Royal Society A, 365, pp.1843–1866. Available at: http://doi.org/10.1098/rsta.2007.2046

Volcanic activity in the region occurred in several stages, drastically altering the geological landscape. Initially, magma intruded into the sedimentary layers, forming various intrusive bodies, such as sills. Later, the eruption style shifted to explosive, resulting in the release of massive amounts of pyroclastic material and the formation of thick volcanic deposits. The culmination of this process was the eruption of colossal volumes of basaltic lava, measured in the hundreds of thousands of cubic kilometers. The total volume of volcanic rocks, including intrusions, pyroclastic deposits, and lava flows, is estimated to be approximately 3 million cubic kilometers. It is important to note that this figure reflects only the rocks that have survived to the present day, and it can be confidently stated that the initial scale of the eruptions was much greater but has since been eroded.

The formation of the Siberian Traps led to colossal emissions of carbon dioxide (CO_2), sulfur (SO_2), chlorine (HCl), and other volatile compounds. These gases significantly intensified the greenhouse effect, causing rapid warming following a volcanic winter. CO_2 concentrations in the atmosphere reached 8,000 ppm, which is 20 times higher than current levels. As a result, the temperature of tropical seas rose from 22–25°C to 30°C, and the oceans began to acidify, killing organisms with carbonate skeletons.

The total sulfur emission amounted to up to 7800 gigatons, chlorine up to 8700 gigatons, and fluorine up to 13,600 gigatons[52].

Volcanic ash and aerosols blocked sunlight, disrupted photosynthesis, and caused mass deforestation and the collapse of food chains, exacerbating the extinction of both plant and animal species.

The ecological crisis of that era underscores the potential scale of consequences even with a gradual eruption of the Siberian plume.

Research indicates that the period of eruptions 250 million years ago was driven by the rise of a mantle plume—a massive magma flow ascending from deep within the Earth beneath the present-day Putorana Plateau. A recurrence of this scenario today would result in the formation of vast lava plateaus, among the largest geological formations on the planet, obliterating nearly all life within thousands of kilometers, encompassing Siberia and neighboring regions. The geological record reveals that such catastrophes, marked by the outpouring of enormous basalt fields,[53] have occurred repeatedly, each time triggering extensive mass extinctions (Fig. 84).

[52]Benjamin A. Black, Linda T. Elkins-Tanton, Michael C. Rowe, Ingrid Ukstins Peate, Magnitude and consequences of volatile release from the Siberian Traps, Earth and Planetary Science Letters, Volumes 317–318, 2012, Pages 363-373, ISSN 0012-821X, https://doi.org/10.1016/j.epsl.2011.12.001

[53] Witze, A. (2017). Earth's lost history of planet-altering eruptions revealed. Nature, 543, 295-296. https://doi.org/10.1038/543295a

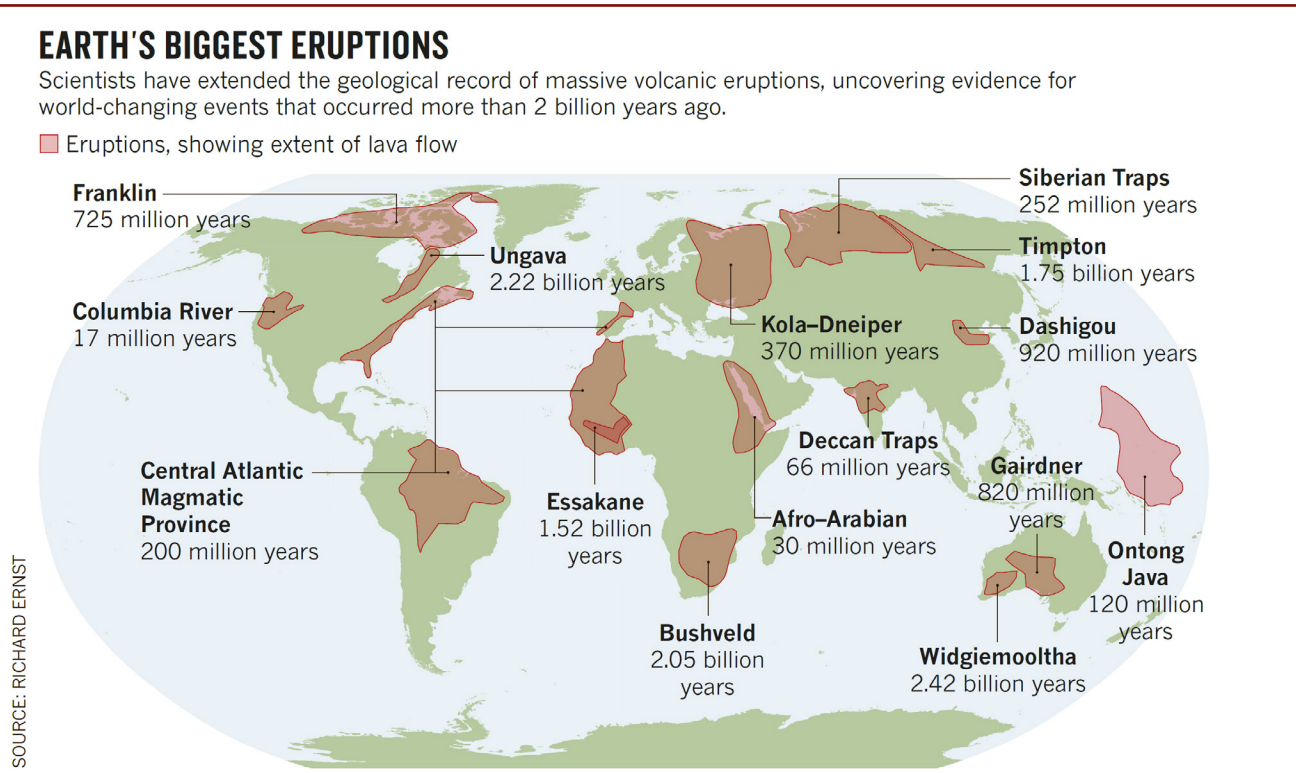

Fig. 84
The map displays the geographic locations and ages of the largest volcanic eruptions in Earth's history, along with the associated lava plateaus formed by these events.
Illustration: Richard Ernst.
Source: Witze, A. (2017). Earth's lost history of planet-altering eruptions revealed. Nature, 543, 295-296. https://doi.org/10.1038/543295a

As in previous geological epochs, magma will rise from the mantle, penetrating fractures in the Earth's crust, much like a soft substance seeping through a dense filter. This process will lead to surface overheating, the formation of numerous intracrustal magma intrusions, and the melting of the lithosphere.

Fig. 85 illustrates the distribution of effusive rocks in Siberia: lava flows are shown in purple, and magmatic bodies that solidified within the Earth's crust are marked in green. The green zones on the map highlight how magma eroded the Earth's crust, creating fractures and advancing along these weakened areas. Such increased magma pressure could once again initiate a similar process with potentially catastrophic outcomes.

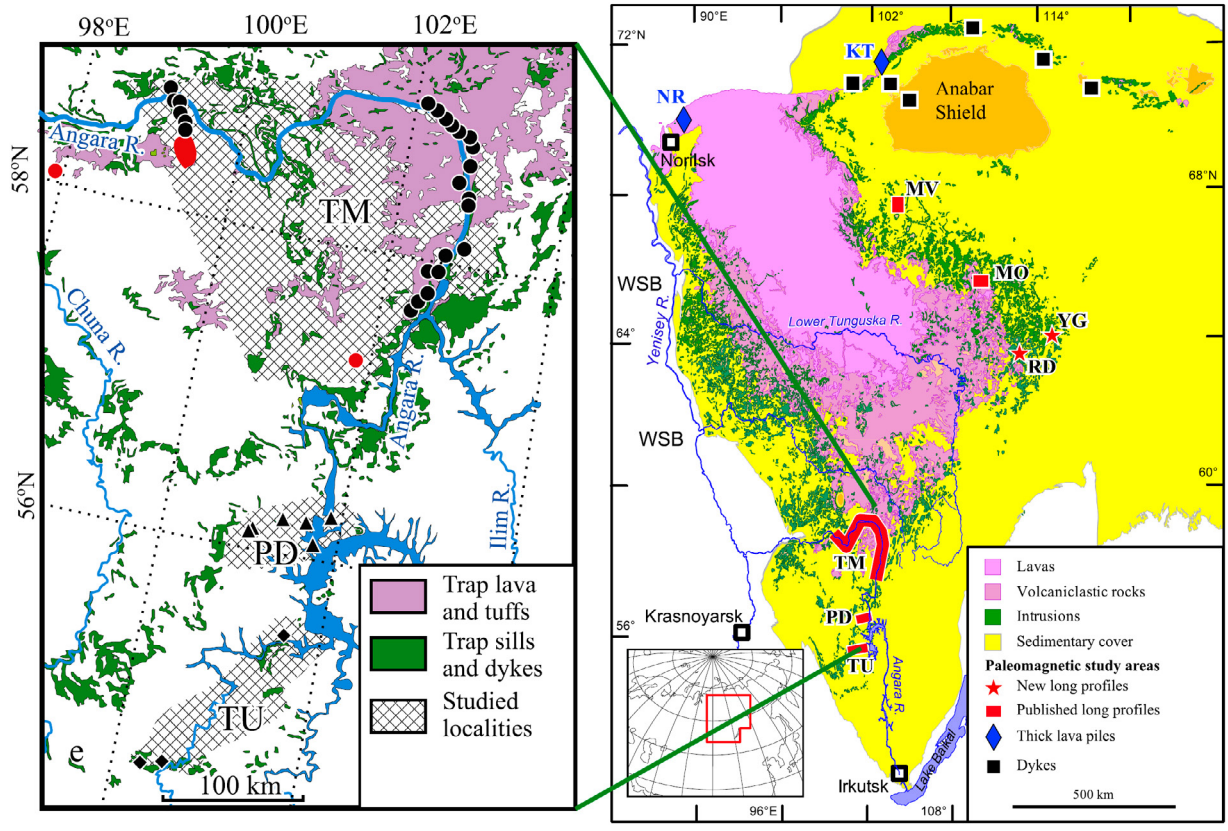

Fig. 85
The map on the right provides an overview of the Siberian Traps province (simplified and modified from Svensen et al., 2009), with key geological structures marked in different colors: pink for lava flows, green for intrusive bodies, and yellow for sedimentary cover. The detailed map on the left illustrates the distribution of trap magmatism: purple represents lavas and tuffs, and green denotes sills and dikes.

Source: Konstantinov, K. M., Bazhenov, M. L., Fetisova, A. M., & Khutorskoy, M. D. (2014). Paleomagnetism of trap intrusions, East Siberia: Implications to flood basalt emplacement and the Permo–Triassic crisis of biosphere. Earth and Planetary Science Letters, 394, 242–253.
https://doi.org/10.1016/j.epsl.2014.03.029

The gradual eruption scenario is comparable to the sudden explosion of the Siberian plume but stretched over time. It can be envisioned as a sequence of volcanoes erupting weekly alongside sudden fissures releasing basaltic lava flows across Western Siberia.

Fig. 86 illustrates these processes, with lava flow regions marked in purple. Lava spread across wide areas in the area of the denser, more stable crust of the East Siberian Platform. In contrast, in Western Siberia—characterized by thinner, younger, and heterogeneous crust—eruptions occurred along elongated depressions or rifts. The map highlights tuff zones, shown in red, composed of cemented pyroclastic fragments and ash.

Eruptions in Eastern and Western Siberia would differ significantly. Under Eastern Siberia, magma encounters the dense Archean craton, creating a substantial barrier. As it rises, the magma “digs” into the host rocks, cools, and becomes enriched with volatile components. This leads to explosive eruptions with high ash emissions and the potential formation of acidic, viscous magma.

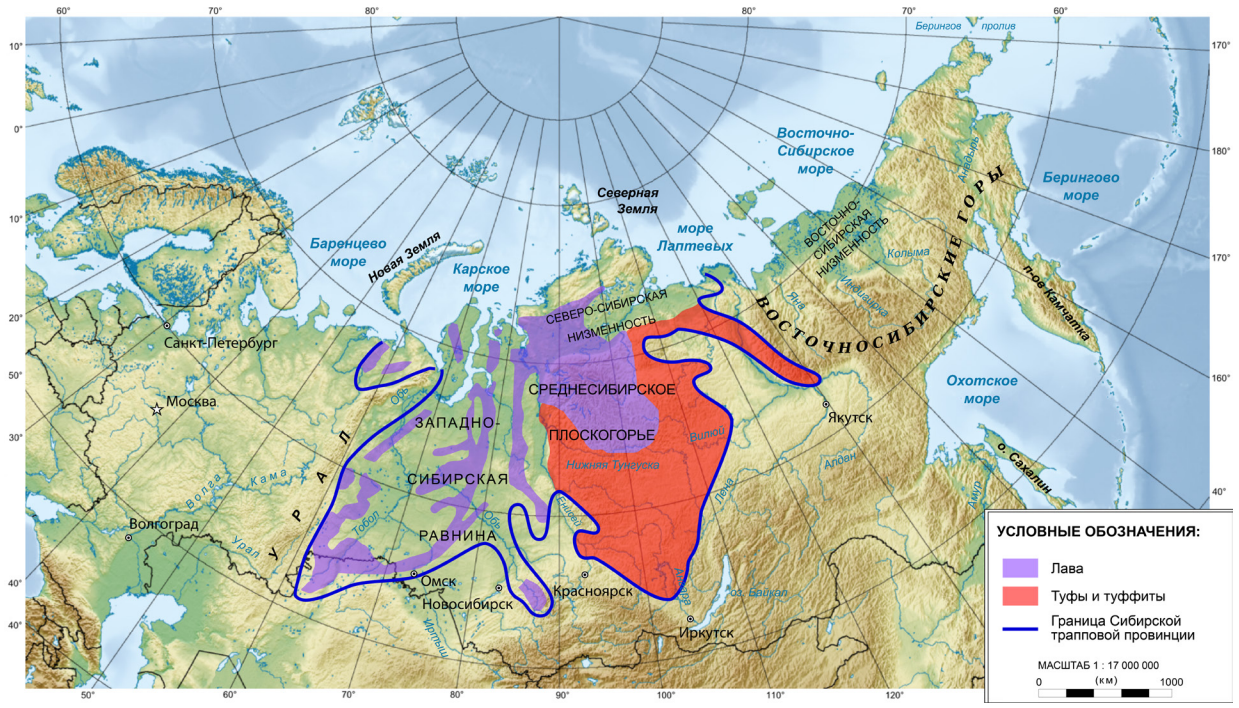

Fig. 86
Map of the Siberian Traps Province, showing major geological structures, including areas of lava flows (purple) and tuffs with tuffites (red). Blue lines indicate the boundaries of the Siberian Traps Province.
Source: wikipedia.org, based on data from Masaitis, 1983

In Western Siberia, with its thin, young crust, eruptions are expected to predominantly feature the outpouring of fluid basaltic lava.

The area expected to be covered by lava flows and tuffs is approximately 7 million km^2 (2.7 million mi^2) across Western and Eastern Siberia, comparable to the size of modern-day Australia. However, the regions subject to degradation are likely to exceed tens of millions of square kilometers. These territories would experience massive wildfires, erosion caused by acid rain, ashfall, landslides, and lahars carrying volcanic deposits. All of Siberia's permafrost will be at risk of destruction.

It is worth noting that the Taimyr Peninsula, west of the Putorana Plateau, hosts the world's largest deposits of nickel, copper, and platinum group metals, developed by the company Norilsk Nickel. These deposits are of magmatic origin and formed approximately 250 million years ago during the eruptions of the Siberian Traps magmatic province, which facilitated the creation of unique ore nodes. The high concentration of nickel in the magmas of that era is likely linked to the transport of materials from Earth's core to the surface.

The ascent of the Siberian magma plume is ongoing, with its acceleration traced to the 1998 core shift toward the Taimyr Peninsula, as determined by Dr. Yuri Barkin. In the near future, there is a significant risk of a breakthrough of the Siberian plume near the city of Norilsk—the very location where a similar event occurred 250 million years ago.

Next, we will examine the consequences this scenario would have for Russia and the world.

Consequences of the Gradual Breakthrough of the Siberian Plume for Russia

Studies have precisely mapped the locations of asthenospheric melt lenses within the lithosphere of southern Siberia, attributed to the region's thin crust. However, the northern part of Siberia remains largely unexplored on seismic maps, representing a "white spot" in research on the lower crust and mantle. This lack of data makes it impossible to predict the locations of the initial lava breakthroughs and eruptions of gas-rich magma, particularly given the absence of comprehensive subsurface monitoring in the Siberian plume zone.

The first warning signs of an impending catastrophe are known to include increased seismic activity and localized gas emissions. As magma advances toward the surface, rapid permafrost melting will begin, leading to the destabilization of infrastructure built on permafrost soils. Soil heating may also trigger gas hydrate explosions (methane trapped in ice structures), causing the formation of massive craters and the destruction of settlements.

Massive wildfires would become inevitable, driven by methane release, soil overheating, and the emission of volcanic gases. Hydrocarbon deposits in Siberia and coal basins like Kuzbass may ignite, as occurred during the Permian-Triassic period[54] when coal deposits were thermally heated to 600°C (1,112°F).

Eruptions would begin suddenly, affecting multiple points across a vast territory. Earthquakes with magnitudes of 7–8, combined with fissures and faults, would result in lava flows covering hundreds of thousands of square kilometers. Around the lava breakthroughs, toxic emissions would cause mass fatalities among plants, animals, and humans, forming a deadly "cocktail" in the atmosphere.

Within the first days, millions of people would perish. Volcanic ash would destroy transportation networks, accumulating on roads and railways, reducing visibility, and devastating infrastructure. Aviation would cease entirely due to the danger posed by ash to aircraft engines.

The melting of permafrost would exacerbate the crisis further: transportation routes, pipelines, buildings, and infrastructure would begin to collapse. Many cities would lose access to water, food, and electricity supplies, triggering a humanitarian crisis. Mass evacuation would be impossible in much of the eruption zone, as lava, gases, fires, and acid rain would render transportation routes unusable. Panic would engulf millions of people, and efforts to relocate the population of Siberia would lead to social instability and widespread unrest.

The country's economy would suffer catastrophic losses. Oil, gas, coal, diamonds, and metal production would cease due to the physical destruction of infrastructure, halting industrial operations and creating shortages of raw materials and energy. The volcanic activity would devastate the region's natural resources, including oil and coal reserves, eliminating critical economic assets for the nation.

[54] Elkins-Tanton, L. T., Grasby, S. E., Black, B. A., Veselovskiy, R. V., Ardakani, O. H., & Goodarzi, F. (2020). Field evidence for coal combustion links the 252 Ma Siberian Traps with global carbon disruption. Geology, 48(10), 986-991. https://doi.org/10.1130/G47365.1

Decades after the eruption, Siberia would remain an ecological disaster zone. The catastrophe would irreversibly alter Russia's geography, economy, and society. Only 25% of the country's territory would remain habitable, but it would face immense pressure from environmental and social crises. Economic strongholds, historical landmarks, and much of the nation's natural wealth would be lost, rendering Siberia uninhabitable for modern civilization.

Global Consequences of the Gradual Breakthrough of the Siberian Plume

The global consequences of the Siberian plume eruption will impact the entire world, unfolding in several stages.

In the first days, transportation between Europe and Asia through Siberia would cease, and air travel would halt due to volcanic ash in the atmosphere. These disruptions would cripple global logistics, triggering a large-scale food crisis, as Russia, a leading exporter of wheat and other products, would stop shipments. The cessation of oil, gas, and other resource exports from Russia would lead to surging prices, an energy crisis, and economic instability in numerous countries. A chain reaction of financial and social upheavals would ripple through the global economy.

Ash clouds and sulfur aerosols would create a global dimming effect, reducing solar radiation and causing a "volcanic winter" with a temperature drop of 2–3°C. Acid rain and soil contamination would devastate agriculture not only in Russia but worldwide. Widespread famine, water shortages, toxic air, and the breakdown of climate systems would result in the gradual demise of billions of humans and animals. Within a few years, social systems would collapse.

Over time, volcanic ash will begin to settle, but abrupt climatic changes will occur. The release of methane and carbon dioxide from thawing permafrost will amplify the greenhouse effect. Temperatures will gradually rise by 5–10 °C, leading to an unstable climate characterized by sharp temperature fluctuations. The destruction of the ozone layer will result in increased levels of ultraviolet radiation in the Northern Hemisphere, exacerbating the consequences of the eruptions.

Despite its distance from Siberia, Europe would face severe consequences from the Siberian plume eruption. Ash would blanket Northern and Eastern Europe, leading to widespread respiratory illnesses. Acid rain would destroy forests, urban infrastructure, and agricultural lands. After a phase of temporary cooling, a sharp warming trend would ensue, bringing droughts to the south and floods to Central and Northern Europe.

Mass migration from Russia, Asia, and the Middle East would trigger a demographic crisis and heightened competition for resources. European countries would struggle with persistent ecological, economic, and social challenges.

Asia would bear the brunt of the eruption's effects, being closest to its epicenter. Air pollution from dust and ash would cause widespread respiratory distress and acid rain, particularly in China, Mongolia, and Kazakhstan. Reduced sunlight and deteriorating soil quality would also devastate Northern China's agricultural heartland, a key food production region.

Temperature fluctuations would wreak havoc on infrastructure and agricultural systems across the continent. Gradual warming of the oceans would lead to deoxygenation, wiping out marine ecosystems and collapsing fisheries.

Over time, the ongoing eruptions would exacerbate global destruction. Climatic and ecological crises would intensify, erasing much of humanity's technological and intellectual progress and pushing civilization into a profound regression. Humanity would face the brink of total societal collapse.

Long-Term Consequences of the Gradual Breakthrough of the Siberian Plume for the Planet

A slow eruption of the Siberian plume would lead to profound and far-reaching impacts, transforming the planet for millions of years. The atmosphere would be inundated with toxic substances, resulting in planet-wide acid rain and the destruction of the ozone layer. This would amplify ultraviolet radiation and further destabilize global climate systems.

The oceans would experience critical acidification, causing the mass extinction of marine life. This would result in the collapse of marine ecosystems, disrupt global food chains, and lead to the loss of virtually all marine biodiversity.

On land, the fallout from toxic emissions, destruction of soil ecosystems, and the loss of most plant species would drive mass extinction. Without pollinators, terrestrial ecosystems would collapse, and it is estimated that 75 to 95% of existing species would vanish.

As a result of the eruption, a comprehensive climatic, biological, and geological crisis will unfold, completely transforming Earth's biosphere. This process will lead to the collapse of human civilization, the death of billions of people, and a regression of surviving, fragmented human groups to a Stone Age level of development. The scale of this catastrophe will be comparable to the largest mass extinctions in Earth's history, marking the beginning of a new evolutionary phase for the biosphere that will take at least millions of years to unfold.

Scenario 3:
Planned and Controlled Degassing

Existing Volcanic Geoengineering Methods

Given the increasing pressure beneath the West Siberian Plate and the East Siberian Craton caused by the rising Siberian Plume, immediate action is necessary to minimize potential consequences. One such solution is a controlled release of pressure, lava, and gasses approaching the surface from secondary chambers, i.e. **planned degassing**.

Contemporary scientific studies consider the degassing of magmatic chambers a viable method for preventing large-scale eruptions. This approach supports the application of volcanic geoengineering technologies not only to volcanoes or supervolcanoes but also to manage the activity of mantle plumes. Numerous scientific publications and patents developed by experts from various countries explore the concept of controlled degassing.

The theoretical foundations of volcanic geoengineering were established in the 20th century, with practical experiments conducted over the past century. Methods of volcanic intervention have included drilling into craters, draining volcanic lakes, creating channels to divert lava flows, cooling lava flows with seawater, bombarding lava streams, and extracting greenhouse gases such as carbon dioxide and methane (Fig. 87).

Since the 1960s, the U.S. Geological Survey (USGS) has carried out drilling operations in lava lake regions on Hawaii's Kilauea volcano to redirect lava flows. Similar initiatives have been implemented in Japan, Iceland, and Italy. For example, Japan has tested technologies for reducing pressure in magmatic chambers. Iceland has successfully redirected lava flows, such as on the island of Heimaey, where lava was cooled using water cannons. In Italy, early warning systems and methods to control lava flows have been developed, including the explosive destruction of lava barriers on Mount Etna in 1983.

International scientific conferences and symposia on deep drilling in zones of volcanic and geothermal activity are expanding the potential applications of volcanic geoengineering to prevent eruptions and mitigate their global consequences.

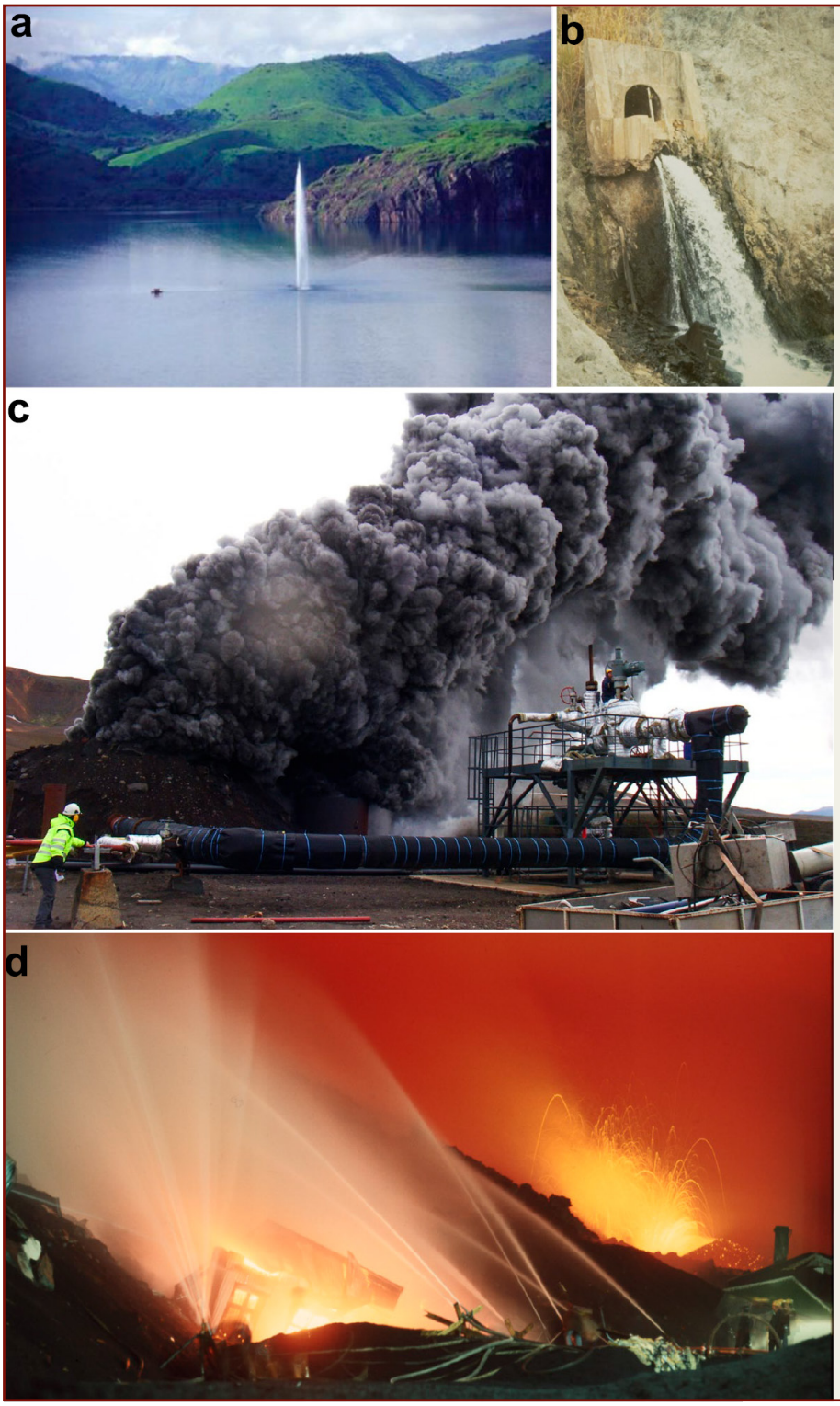

Fig. 87

(a) Degassing of carbon dioxide from Lake Nyos, Cameroon, as documented by Halbwachs et al. (2020).

(b) Drainage tunnel in the crater wall of Mount Kelud, Indonesia (Global Volcanism Program, image GVP-01120).

(c) Auxiliary drilling of a magmatic pocket at Krafla, Iceland, in 2009 (image courtesy of GO Friðleifsson/ IDDP).

(d) Cooling of lava flows with seawater injection at Heimaey, Iceland, in 1973, Tristan H. Benediktsson.

Source: Cassidy, M., Sandberg, A., & Mani, L. (2023). The Ethics of Volcano Geoengineering. Earth's Future, 11(10), e2023EF003714. https://doi.org/10.1029/2023EF003714

The Fig. 88 diagram presents the chronology of the most notable cases of volcanic geoengineering. Black circles represent deliberate interventions, while red circles denote unintentional effects on volcanic activity. There are also patented methods for planned degassing and reducing the risks of volcanic and supervolcanic eruptions.

For example, the technology, patented by two Russian experts, involves preventing uncontrolled, cascading volcanic eruptions by using angled drilling of boreholes to regulate pressure within magma chambers. (Fig. 89).

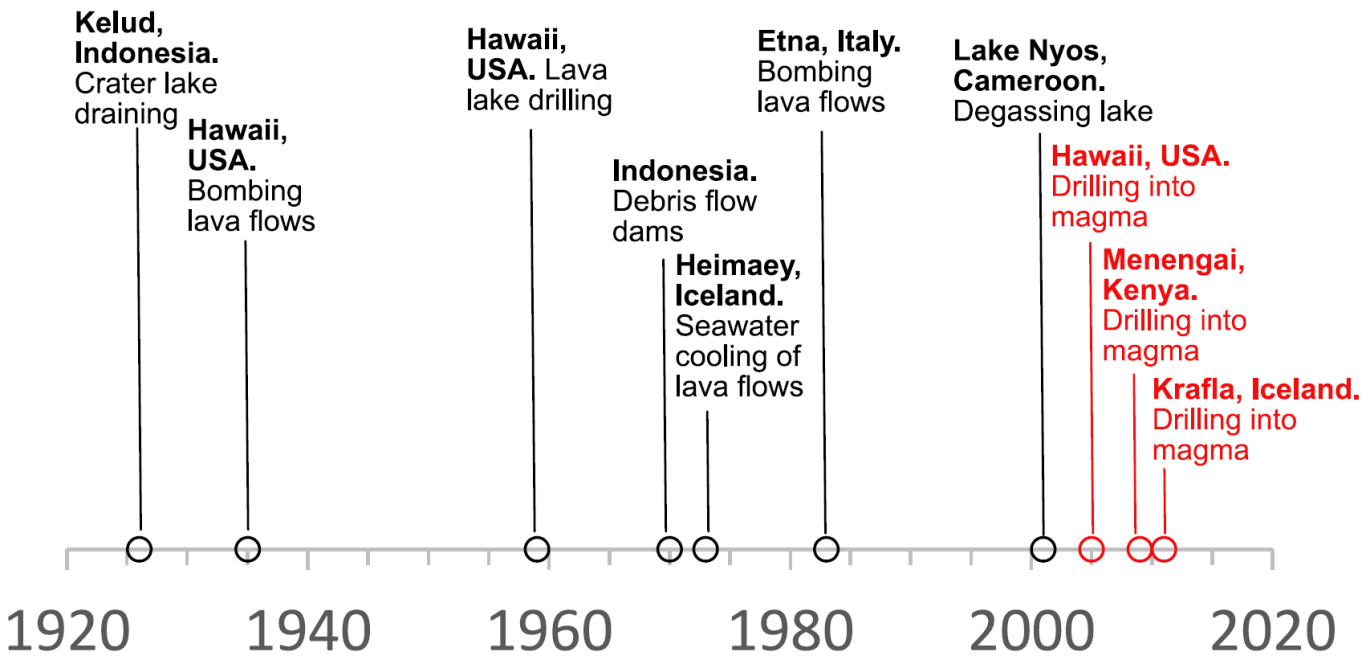

Fig. 88
A timeline of some notable instances of volcano geoengineering. Black circles indicate purposeful interventions, whereas the red circles indicate inadvertent volcano intervention.

Source: Cassidy, M., Sandberg, A., & Mani, L. (2023). The Ethics of Volcano Geoengineering. Earth's Future, 11(10), e2023EF003714. https://doi.org/10.1029/2023EF003714

РОССИЙСКАЯ ФЕДЕРАЦИЯ

(19) **RU** (11) **2 343 508** (13) **C1**

(51) МПК
G01V 9/00 (2006.01)
G01V 11/00 (2006.01)

ФЕДЕРАЛЬНАЯ СЛУЖБА
ПО ИНТЕЛЛЕКТУАЛЬНОЙ СОБСТВЕННОСТИ,
ПАТЕНТАМ И ТОВАРНЫМ ЗНАКАМ

(12) ОПИСАНИЕ ИЗОБРЕТЕНИЯ К ПАТЕНТУ

(21), (22) Заявка: 2007112443/03, 04.04.2007

(24) Дата начала отсчета срока действия патента:
04.04.2007

(45) Опубликовано: 10.01.2009 Бюл. № 1

(56) Список документов, цитированных в отчете о поиске: RU 2098850 C1, 10.12.1997. SU 1193223 A, 23.11.1985. RU 2073769 C1, 20.02.1997. RU 2057839 C1, 10.04.1996. RU 2231092 C2, 20.06.2004. SU 1699979 A1, 23.12.1991. US 4319648 A, 16.03.1982.

Адрес для переписки:
109145, Москва, Жулебинский б-р,1, кв.82,
Г.К.Мкртумяну

(72) Автор(ы):
Мкртычян Олег Альбертович (RU),
Мкртумян Георгий Каропетович (RU)

(73) Патентообладатель(и):
Мкртычян Олег Альбертович (RU),
Мкртумян Георгий Каропетович (RU)

RU 2343508 C1

(54) СПОСОБ ПРЕДОТВРАЩЕНИЯ ЛАВИНООБРАЗНОГО ИЗВЕРЖЕНИЯ ВУЛКАНОВ

(57) Реферат:

Изобретение относится к способам предотвращения неконтролируемого - лавинообразного извержения вулканов и организации контролируемого транспортирования магмы для ее использования при строительстве. Обеспечивает повышение эффективности способа. Сущность изобретения: по способу управляют давлением во вторичных магматических очагах под вулканами, проявляющими сольфатарную активность. Для этого производят наклонное бурение каналов в основание вторичного магматического очага. В этот очаг подают сжатый газ. Повышают давление во вторичном магматическом очаге и замедляют поступление в него магмы из первичного очага. При этом осуществляют добычу и транспортирование магмы для строительства, накопившейся во вторичном магматическом очаге, через пробуренные каналы. При этом не допускают достижения критической величины давления, при которой происходит лавинообразное извержение.

RU 2343508 C1

Fig. 89
Patent: Method for Preventing Avalanche-like Volcanic Eruptions.

This invention relates to methods for preventing uncontrolled, avalanche-like volcanic eruptions and for organizing the controlled transportation of magma for use in construction. It enhances the efficiency of the approach.

Summary of the Invention:

The method involves managing pressure in secondary magmatic chambers beneath sulfate-active volcanoes. This is achieved by inclined drilling of channels into the base of the secondary magmatic chamber. Compressed gas is injected into the chamber to increase pressure, thereby slowing the influx of magma from the primary chamber. Simultaneously, magma accumulated in the secondary chamber is extracted and transported for construction purposes through the drilled channels. The process ensures that the pressure does not reach critical levels, which could trigger an avalanche-like eruption.

Source: https://patentimages.storage.googleapis.com/0e/4a/51/11fd6e028d2813/RU2343508C1.pdf

Another technology was developed by an American inventor. (Fig. 90) This technology outlines methods for evacuating magma from volcanic magmatic chambers, such as the chamber of the Yellowstone supervolcano, to prevent potential catastrophic eruptions.

The core idea involves creating artificial channels (tubes) to direct magma to the surface, where it can be processed and potentially utilized, for example, in energy production.

(12) **United States Patent**
Stratford

(10) **Patent No.: US 7,284,931 B2**
(45) **Date of Patent: Oct. 23, 2007**

(54) **MAGMA EVACUATION SYSTEMS FOR THE PREVENTION OF EXPLOSIONS FROM SUPERVOLCANOES**

(76) Inventor: **Brian Stapleton Stratford**, 40 Field Ris , Little ver, Derby DE23 1DE (GB)

(*) Notice: Subject to any disclaimer, the term of this patent is extended or adjusted under 35 U.S.C. 154(b) by 0 days.

(21) Appl. No.: **10/230,549**

(22) Filed: **Aug. 29, 2002**

(65) **Prior Publication Data**

US 2003/0145592 A1 Aug. 7, 2003

(30) **Foreign Application Priority Data**

Feb. 4, 2002 (GB) 0202465.1

(51) **Int. Cl.**
E21B 36/00 (2006.01)
E21B 43/24 (2006.01)

(52) **U.S. Cl.** **405/131**; 405/258.1; 405/303; 166/302; 166/57

(58) **Field of Classification Search** 405/52, 405/258.1, 130, 131, 303; 165/45; 166/302, 166/304, 57–62
See application file for complete search history.

(56) **References Cited**

U.S. PATENT DOCUMENTS

3,115,194 A * 12/1963 Adams 376/273
3,357,505 A * 12/1967 Armstrong et al. 175/16
3,396,806 A * 8/1968 Benson 165/45
3,693,731 A * 9/1972 Armstrong et al. 175/16
3,957,108 A * 5/1976 Van Huisen 165/45
3,967,675 A * 7/1976 Georgii 166/302
3,991,817 A * 11/1976 Clay 165/45
4,134,462 A * 1/1979 Clay 175/16
4,776,169 A * 10/1988 Coles, Jr. 165/45

FOREIGN PATENT DOCUMENTS

GB 2362410 11/2001
JP 070071020 A 3/1995
JP 100076104 A 3/1998
JP 100077952 A 3/1998
JP 100078497 A 3/1998

* cited by examiner

Primary Examiner—Tara L Mayo
(74) *Attorney, Agent, or Firm*—Woodard, Emhardt, Moriarty, McNett & Henry LLP

(57) **ABSTRACT**

An apparatus controls the evacuation of volcanic magma to prevent explosions. Magma evacuation is through a single evacuation tube that heats the magma flow within the tube to prevent stickiness of the magma in the tube. The heating may use small combustion chambers to heat steam, which in turn heats and stabilizes the magma flow. Stability is aided by central cooling, where needed, using water jets from nozzles located at the wall of the tube.

25 Claims, 2 Drawing Sheets

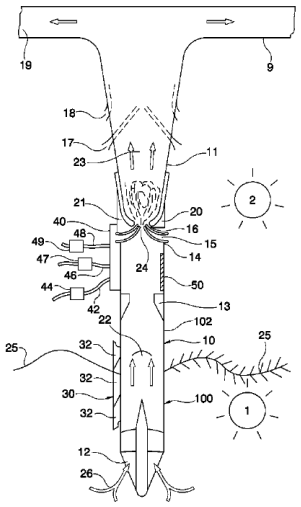

Fig. 90

Patent: Magma Evacuation Systems for the Prevention of Explosions from Supervolcanos.

An apparatus controls the evacuation of Volcanic magma to prevent explosions. Magma evacuation is through a single evacuation tube that heats the magma flow within the tube to prevent stickiness of the magma in the tube. The heating may use Small combustion chambers to heat steam, which in turn heats and stabilizes the magma flow. Stability is aided by central cooling, where needed, using water jets from nozzles located at the wall of the tube.

Source:
https://patentimages.storage.googleapis.com/5f/dc/0d/7b5b99d61d1a75/US7284931.pdf

An example of successful degassing is the Japanese project "Unzen Scientific Drilling Project" (USDP), a six-year initiative launched in April 1999. It aims to study the growth history, subsurface structure, and magma ascent processes of Mount Unzen (Fig. 91). The first phase involved drilling two boreholes on the volcano's slopes and creating a structural model. The second phase focused on drilling into the magma channel from the 1990–1995 eruptions to analyze the degassing mechanism. The drilling strategy included vertical drilling followed by gradually increasing the borehole's inclination (Fig. 92).

Fig 91
Drilling equipment used for the Unzen Volcano drilling project in 1995.
Source:
https://www.icdp-online.org/projects/by-continent/asia/usdp-japan/gallery/

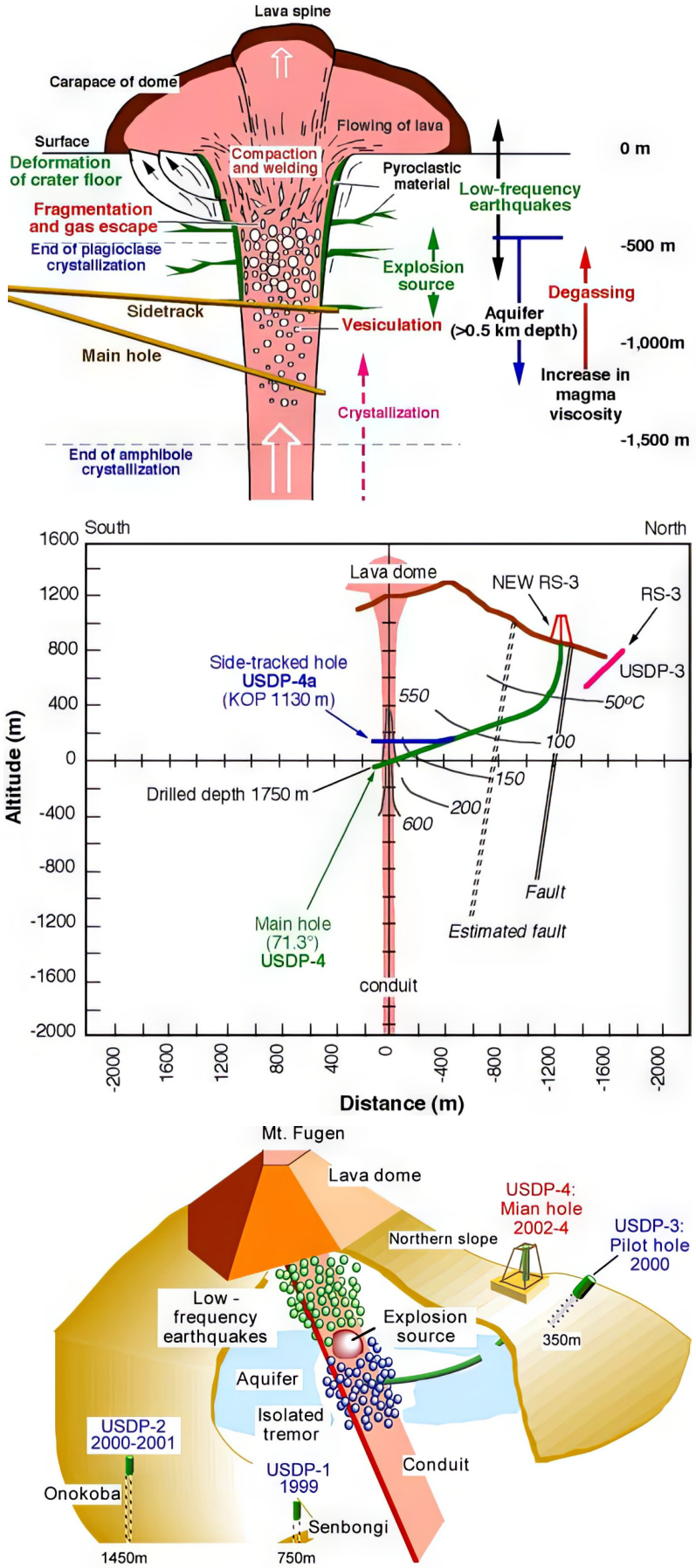

Fig. 92

(A)

Image of lava dome and upper part of the conduit at Unzen. Effective degassing from foamy magma occurred during its fragmentation and annealing in the upper part of conduit. The conduit condition will be investigated in drilling main hole (USDP-4) in 2003, and continuous coring will be performed by drilling sidetrack hole (USDP-4a) in 2004.

Source: USDP project. (n.d.). In Earthquake Research Institute, The University of Tokyo. Retrieved December 31, 2024, from https://www.eri.u-tokyo.ac.jp/KOHO/Yoran2003/sec4-5-eng.htm#:~:text=USDP%20consists%20of%20two%20phases%20

(B)

Trajectories of conduit drilling. New RS-3 and RS-3 are drilling sites of main-sidetrack holes and a pilot hole, respectively.

Source: USDP project. (n.d.). In Earthquake Research Institute, The University of Tokyo. Retrieved December 31, 2024, from https://www.eri.u-tokyo.ac.jp/KOHO/Yoran2003/sec4-5-eng.htm#:~:text=USDP%20consists%20of%20two%20phases%20

(C)

Three dimensional image of the conduit drilling

Source: Volcanic fluid research center. (n.d.). Understanding of the conduit system at Unzen Volcano. Earthquake Research Institute, The University of Tokyo. Retrieved December 31, 2024, from https://www.eri.u-tokyo.ac.jp/VRC/vrc/usdp/conduit.html

Today, humanity possesses sufficient technological and engineering potential to intervene in volcanic systems. However, each case of planned degassing requires the utmost preparation, including extensive data analysis and precise calculations. Even then, risks persist.

The methods outlined have primarily been tested on conventional volcanoes, which are fundamentally different in scale compared to the massive Siberian mantle plume. This plume represents a threat far exceeding the power of a single supervolcano. It is comparable to the energy of a thousand Yellowstone caldera eruptions. Nonetheless, addressing this issue has gained urgency precisely because potential approaches to mitigate it exist.

With proper commitment, humanity is capable of developing a program for the degassing of the Siberian mantle plume, drawing on the accumulated expertise of global specialists. The primary goal of such a program would be to minimize the consequences of the plume's ascent by reducing lava and gas pressure in secondary magmatic chambers, thereby preventing large-scale uncontrolled eruptions.

Implementing such a program will require close international cooperation and the collective efforts of scientists and engineers worldwide. Only a united approach can yield effective solutions to ensure the safety of humanity as a whole.

Example of a Program for the Planned Degassing of the Siberian Plume

The program may involve the parallel development of several key areas:

1. Establishing a Monitoring Network

1.1 Developing a network of high-sensitivity sensors and satellite surveillance systems to monitor seismic and thermal activity in the region. This will enable the timely detection of secondary magmatic chambers.

1.2 Conducting detailed mapping of secondary magmatic chambers using seismic exploration methods. Preliminary assessments of pressure and magma volume in each secondary chamber will be crucial.

1.3 Drilling scientific and monitoring boreholes in anomalous zones and installing pressure, temperature, and seismic activity sensors to gather critical data.

2. Developing Controlled Degassing and Magmatic Channel Blockage Technologies

2.1 It will be necessary to develop a plan for drilling inclined deep boreholes up to 5 miles (8 km) in depth in safe zones. Detailed trajectory calculations will be required to ensure the boreholes accurately reach secondary magmatic chambers. Drilling technologies resistant to high temperatures and pressure must be utilized. This includes using heat-resistant materials to reinforce borehole walls and establishing a monitoring system to track pressure and temperature within the boreholes for safety and effectiveness.

2.2 A process for diverting gases and lava must be carefully planned, involving step-by-step pressure management within secondary magmatic chambers through a system of boreholes. This requires controlling the degassing rate to prevent sudden pressure changes and utilizing compressor systems to regulate gas pressure. Filtration and cooling systems will be necessary to prevent the release of toxic substances into the atmosphere. The extraction of lava and gases will continue until the pressure in each chamber is stabilized.

2.3 A plan for a targeted nuclear explosion in specific boreholes must then be developed to seal the layers above secondary magmatic chambers. This approach aims to prevent excessive magma from reaching the surface and to minimize ash emissions.

Gradual pressure release will ensure stability of Siberia and protect key populated areas, although Norilsk and its surrounding settlements may remain at risk.

2.4 During the process of diverting lava from the chambers, efforts must be made to control its flow as much as possible. Lava should be directed through specially prepared channels toward the Arctic seas. Additionally, a program should be developed to utilize magma for construction purposes, such as creating artificial islands or reinforcing coastlines.

3. Evacuation of the Population:

A system of early warning must be implemented, along with the development of evacuation plans for unforeseen emergencies. Additionally, a structured plan for the safe evacuation of people from high-risk zones will be required. This plan should include measures for adapting and socially supporting evacuees, considering the possibility of long-term relocation.

4. Preservation of Infrastructure:

Plans must be developed for the protection and evacuation of strategic facilities from areas at risk of lava inundation. This includes establishing secure storage facilities in safe zones for the evacuation of the region's critical resources, such as oil, gas, non-ferrous and precious metals, ores, fertilizers, food supplies, water, and medical supplies.

Justification for Selecting Locations for Research Boreholes to Monitor the Dynamics of the Modern Siberian Mantle Plume

The primary step in understanding the speed and direction of the plume's ascent, its head's spread, and its penetration through cracks in the Earth's crust is to monitor geothermal and geophysical parameters at depth. This requires drilling new boreholes and conducting regular measurements of temperature, pressure, gas composition, markers of intensified magmatic processes, seismic noise, and other parameters within these boreholes.

Ten locations have been proposed for the drilling of research boreholes (Fig. 93, 94).

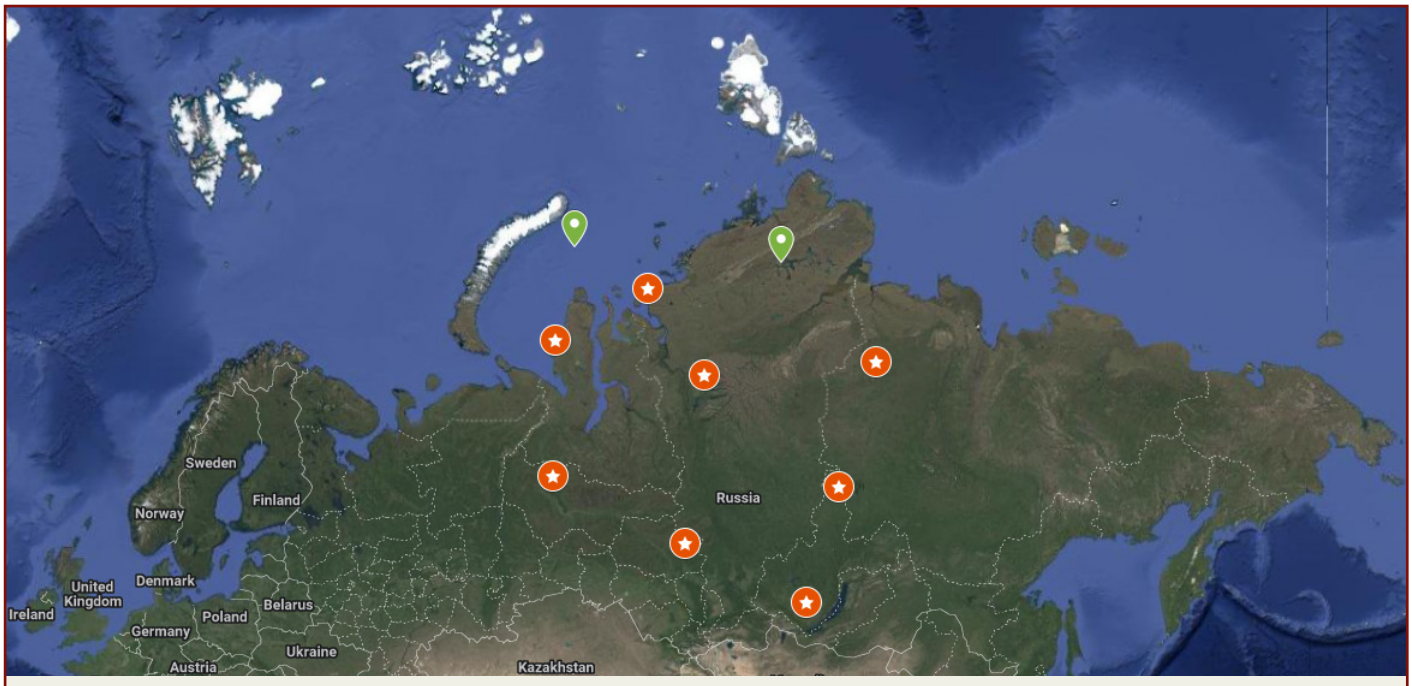

Fig. 93
Preliminary location of 10 recommended sites for drilling of research boreholes

Borehole name	Locality or nearby infrastructure	Coordinates X (Latitude)	Coordinates Y (Longitude)	Area
Ц 1	Talnakh District, Norilsk, Krasnoyarskiy Krai	69.4459423	88.7670478	Taymyr Peninsula
ЗСЗ 2	Kharasavey field, Yamal Peninsula	71.1849618	66.9830117	Western Siberia
ЗЮЗ 3	Kislorskoye field, Beloyarsky District, Khanty-Mansi Autonomous Okrug	63.6572613	66.5569363	Western Siberia
ЮЗ 4	Tsentralny settlement in Verkhneketsky District, Tomsk Region	58.9454	86.0127	Western Siberia
Ю 5	Chichkova village, Chichkovskoye municipal formation, Ust-Udinsky District, Irkutsk Region	54.19598	103.7021	Eastern Siberia
ЮВ 6	Nakanno village in Katangsky District, Irkutsk Region	62.89873	108.45027	Eastern Siberia
В 7	Zhilinda village in Olenyoksky District, Yakutia	70.1528916	113.9261131	Eastern Siberia
СЗ 8	Dikson settlement in Taymyrsky Dolgano-Nenetsky District, Krasnoyarskiy Krai	73.50246	80.5498	Taymyr Peninsula
СВ 9	Lead-zinc deposit to the northwest of Lake Taymyr, Taymyr Peninsula	74.52147	100.02184	Eastern Siberia
СЗ 10	Rogozinskaya-1 site, Kara Sea	75.16298	69.74128	Western Arctic Platform

Fig. 94
Table of 10 recommended research boreholes for monitoring the progression of the Siberian mantle plume. Including borehole name, coordinates, nearby settlement or infrastructure, and geological cross-section structure.

The selection criteria for these boreholes locations were based on the following principles:

1. Borehole locations were chosen relative to the maximum intersection of thermal and geodynamic anomalies associated with the plume head's ascent and spreading. Based on this principle, one borehole was placed in the central region of the proposed plume head uplift, seven boreholes were designated along the perimeter of the anticipated magma flow, another borehole was positioned near Lake Baikal, in the direction of the active magma advancement beneath the Eastern Siberian Craton, and one more was planned near the Kara Sea, to monitor the plume's progress beneath the Arctic shelf's oceanic crust.

2. Borehole placement was optimized for subsequent seismotomographic work, ensuring that seismic sensor data, once processed, would provide the clearest 3D imaging. In other words, the seismic sensor grid within the boreholes was designed to be optimally positioned for underground seismotomography.

3. Borehole locations considered the feasibility of equipment delivery for drilling and access routes (transport availability). Due to the difficult terrain, swampy landscapes, few roads, and extreme climatic conditions in northern Western and Eastern Siberia, drilling site selection relied on the proximity to existing infrastructure for scientific research—such as roads, settlements, and active drilling platforms. Two points were chosen on current oil fields operated by Gazprom and Rosneft, while the others were located near oil, gas, and other mineral fields. It should be noted that if drilling at the specified coordinates proves impossible, borehole locations may be adjusted by 10–20 km in any direction.

Recommended Research Methods for the Boreholes :

For comprehensive monitoring and study of the mantle plume, the following parameters must be collected from the research boreholes:

1. **Temperature monitoring:** This involves measuring temperatures at various depths to analyze thermal anomalies.
2. **Pressure:** Determining pressure levels within the strata to assess hydrodynamic conditions.
3. **Gas sampling:** Collecting samples of gasses from deep strata to study their composition and potential influence of magmatic activity on them.
4. **Seismic research:** Installation of both standard and wide-range seismic sensors to record seismic activity to create a detailed seismotomography of the Earth's crust and mantle for continuous monitoring of the state of the plume.
5. **Formation fluid composition:** Analyzing the composition of formation fluids to identify potential thermal or magmatic contributions.
6. **Geomechanical studies:** Taking measurements of stress in rocks to analyze the stressed condition of the lithosphere undergoing deformation due to the intrusion of the plume.
7. **Electromagnetic methods:** Carrying out electromagnetic research to record changes in the electrical properties of media associated with the intrusion of magma.

The data collected will form a basis for developing a comprehensive model of the mantle plume dynamics and evaluating its impact on geological processes in Siberia.

Characteristics of Drilling and Blocking Magmatic Channels During Planned Degassing

The primary goal of drilling boreholes during planned degassing is to reduce pressure in the plume's secondary magmatic reservoirs, prevent magma explosions, and establish a controlled release of gas and lava.

In the initial phase, drilling will be conducted with human operators, as at shallow depths, the process involves standard technological tasks with minimal risks to personnel. Traditional drilling rigs equipped with temperature and pressure monitoring systems will be used to control the process and promptly respond to deviations from the norm.

As the drilling approaches critical depths and nears active zones of the magmatic system, the risk to personnel increases significantly. At this stage, operations must transition entirely to automation. Specialized drilling rigs with automated control systems will be employed. The drilling process will be managed remotely using software that analyzes real-time data and adjusts equipment actions accordingly.

To enhance monitoring precision, operators will utilize virtual reality technologies, enabling detailed equipment control without physical presence in hazardous zones. This approach minimizes the likelihood of accidents caused by high-pressure gas discharges or equipment failure from shock waves.

Drones and robots will monitor the drilling complex and the surrounding environment. Drones equipped with cameras, thermal imaging, and sensors will detect gas leaks, thermal anomalies, and seismic activity. Robots operating directly in the drilling zone will collect data on temperature, pressure, and the chemical composition of the environment, transmitting this information to automated control centers. These technologies minimize human presence in high-risk areas and ensure a high level of precision and safety.

Following the completion of drilling, the next phase involves controlled degassing—gradually releasing pressure and expelling large volumes of lava. In the final stages, after a significant reduction in magma and gas volumes, a controlled explosion may be necessary to seal magma ascent pathways. One proposed method involves a directed nuclear explosion in the drilled borehole. The goal of this approach is to relieve tectonic stress and create stable structural barriers that block magmatic channels.

This approach involves breaking down rocks in high-stress zones, followed by their fusion and cooling under the influence of thermal energy. This process promotes the formation of a monolithic barrier capable of completely or partially obstructing magma access to the surface. The thermodynamic impact may also alleviate tectonic stress, reducing the likelihood of future eruptions.

Implementing nuclear explosions requires precise calculations, including assessments of lithostatic pressure, rock hardness and density, and the characteristics of magmatic melt. These factors must be carefully considered to maximize the method's effectiveness and minimize potential risks.

Selecting the Optimal Time for Drilling Boreholes During Planned Degassing

At present, our specialists are focused on studying the optimal timeframes for conducting drilling operations as part of planned degassing. While it is too early to draw definitive conclusions, preliminary calculations already indicate the potential for accurately selecting the most favorable time to commence degassing. The findings suggest that, with correctly determined timing, the risk of complications can be reduced severalfold.

The drilling process must account for not only the physical and mechanical properties of the rocks, such as their strength and fracturing but also temporal parameters linked to celestial mechanics. Calculations should be based on analyzing Earth's position along the ecliptic, the Moon's phase, the alignment of major planets like Jupiter, and the current level of solar activity. Additionally, monitoring deep-focus earthquakes in the drilling region is crucial, as such events can significantly increase local seismic activity.

Currently, we have formed a general understanding of the mechanism and key patterns governing the process, but these findings require extensive validation. The results must be rigorously reexamined by our scientific team and independently corroborated through research and models developed by other specialists.

Projected Outcomes of Planned Degassing of the Siberian Plume

Carrying out the planned degassing of the Siberian Plume can result in three primary scenarios, calculated across two project stages: the early and later phases. Below is a detailed consideration of each scenario.

1. Minimal Damage to Russian Territory.

If the process of degassing and releasing excess lava from secondary magma chambers is carefully modeled by an international team of experts, with calculations meticulously executed to account for all geological features, both stages of degassing can proceed without accidents or complications. Under this scenario, the damage to Russian territory would be minimized, with losses amounting to 5–7% of the country's area, or at most up to 10% (an affected radius of approximately 500–600 km). Major cities in the Krasnoyarsk Territory could be protected, and the loss of life could be avoided. Furthermore, favorable developments may allow lava diversion toward the Arctic seas, potentially expanding Russia's territory through the creation of new coastal land.

2. Moderate Damage to Russian Territory.

This scenario assumes the successful completion of the early degassing phase. Still, it anticipates unforeseen complications during later stages, such as a sudden gas explosion or lava discharge. By that time, some gasses and lava would already have been vented, reducing the overall impact. Possible outcomes could include flows of liquid basaltic lava, similar to those observed in Iceland or the Hawaiian Islands, or an eruption of moderate explosiveness. In this case, the potential loss of territory could increase to 25–30% (approximately 4–5 million square kilometers). This would affect cities within a 1,000 km radius of the active zone. However, this scenario would not result in a global catastrophe for civilization or irreversible destruction across Russian territory. Humanity would be capable of managing the ensuing climate and ecological challenges.

3. Maximum Damage to Russia and the World.

This scenario assumes that a late initiative or insufficient expertise among specialists could lead to significant complications. A lack of research, calculation errors, or drilling through soft or fractured rock could disrupt operations. If complications arise during the early degassing phase, when the pressure in the magma chambers is at its peak, one of two catastrophic outcomes could occur: an immediate explosion of the entire Siberian Plume system or slow but extensive lava flows akin to the formation of the Siberian Traps.

Despite the potential risks, the likelihood of such an outcome is extremely low, as it is hard to envision the implementation of such a complex project without proper international preparation.

An optimistic and most probable outcome involves the loss of only 5–7% of Russian territory with minimal damage. Even in the event of complications during later phases, losses might rise to 25–30%, which remains significantly more favorable than the consequences of inaction. The risk of more severe destruction during planned degassing, either for Russia or the world, is negligible.

The implementation of planned degassing will provide Russia with a unique opportunity to lead in managing global geodynamic risks, reinforcing its position as an international scientific and technological leader. Successfully executing the project will demonstrate the country's capacity to address planetary-scale challenges, fostering global collaboration to prevent natural disasters. This initiative will not only stabilize Russia's domestic political and social environment but also strengthen international cooperation in tackling global issues.

Controlled degassing of the Siberian plume could impact not only the local region but also other volcanic systems, such as Yellowstone and stratovolcanoes worldwide. Magmatic reservoirs and their dynamics form a single interconnected global network, functioning as a unified geomechanical system. Controlled pressure relief in one segment can reduce stress across the magmatic reservoirs, preventing chain reactions and eruptions. This can be likened to deflating a car tire: reducing pressure in one area redistributes the load and prevents rupture at critically stressed points. A similar approach to degassing could stabilize magmatic systems on a global scale.

Thus, undertaking a planned and controlled degassing operation remains humanity's only viable chance to avert disaster, both for Russia and the entire world. This scenario offers a pathway to avoid a global catastrophe while buying time for humanity to develop further solutions.

However, despite its immense promise, the successful realization of even the most optimistic scenario represents a monumental challenge. Immediate action is essential, as delays increase the likelihood of catastrophic events. Surprisingly, such a project might face opposition within Russia due to potential risks, such as infrastructure damage and reduced control over strategic resources.

Conclusions

The Siberian plume represents a global geodynamic threat comparable in scale to a thousand catastrophic eruptions of the largest supervolcanoes. An uncontrolled eruption could result in planetary-scale consequences, including the onset of an ice age, the destruction of ecosystems, the collapse of infrastructure, and the extinction of humanity. These risks necessitate the implementation of preventive measures, such as planned degassing of the Siberian plume's magmatic system.

Inaction poses the threat of spontaneous, uncontrolled eruptions, the consequences of which would be catastrophic not only for Russia but for the entire planet. Controlled pressure reduction in magma chambers can help avert the worst-case scenarios and provide humanity with critically needed time to develop long-term solutions.

Additionally, integrating atmospheric water generator technology into everyday use alongside the degassing of the Siberian plume could open new opportunities for restoring ecological balance. This would allow for ocean plastic cleanup, strengthen the water cycle, and reestablish the planet's thermal equilibrium. The comprehensive adoption of such measures could stabilize the climate and ensure a future for humanity, buying time to address the external cosmic influence responsible for catastrophic events during the 12,000-year cycle.

These objectives demand urgent international collaboration among scientists from diverse disciplines, including quantum physicists, to develop and implement comprehensive solutions. However, geopolitical and military conflicts hinder such cooperation. Therefore, a global moratorium on warfare and the redirection of military resources toward disaster mitigation and humanitarian efforts are imperative. Humanity has only 4–6 years of relatively stable conditions to take the necessary actions.

If conditions for open collaboration are established, scientists will not be starting from scratch, as existing research and an understanding of causal relationships in this area already provide a foundation. Humanity's inability to prioritize global unity and scientific collaboration will lead to irreversible consequences for life on Earth.

Appendix 1

The methodology for analyzing seismic activity involved downloading and processing data from the International Seismological Centre (ISC). Since the dataset includes contributions from various countries and research institutions, as well as different types of magnitude scales (Mw, Ms, Mb, ML, MD, etc.), a specific data processing algorithm was applied to select the most appropriate magnitude type from multiple sources. Two distinct approaches were used:

1. Referred to in the text as the **Special Median Magnitude Algorithm**, this method involves selecting a preferred magnitude estimate and including an event in the dataset only if the preferred estimate falls within the required magnitude range. The selection process follows a hierarchy of magnitude types in order of preference: Mw, ML, MS, Mb, MD, MV.

If multiple values of the preferred magnitude type exist for a given event, the median is calculated from all available estimates of that type for the event.

If no estimate of the preferred types are available for a given event (which is rare, accounting for only a few percent of events in the entire database), any magnitude estimate with a value matching the median calculated from all magnitude types for that event is selected.

2. Referred to in the text as the **Maximum Magnitude Algorithm**, this method selects the magnitude estimate with the highest value among all available magnitude estimates for the given event.

The first algorithm generally results in a slight reduction in magnitude values compared to the highest reported estimate. However, experience has shown that the Median Magnitude Algorithm provides a reliable representation of the Gutenberg-Richter law and other seismic patterns and aligns well with data from other seismological databases, such as the United States Geological Survey (USGS) and the Incorporated Research Institutions for Seismology (IRIS).

The second algorithm allows for an assessment of the number of earthquakes recorded by any research institution with a magnitude exceeding a selected threshold. This approach helps identify trends in the frequency of earthquakes within a given magnitude range.

All graphs presented in the section “Increase in Seismic Activity as an Indicator of Plate Destabilization Due to the Siberian Magmatic Plume Activity” were constructed using the first algorithm—the Special Median Magnitude Algorithm (Figs. 44–75).

After selecting the magnitude, the data were filtered by event type in the ISC database to exclude events caused by human activities related to mining operations, such as explosions, suspected explosions, and rockbursts. The following event types were excluded:

km = known mine explosion

sm = suspected mine explosion

kh = known chemical explosion (Not standard IMS)

sh = suspected chemical explosion (Not standard IMS)

kx = known experimental explosion

sx = suspected experimental explosion

kn = known nuclear explosion

sn = suspected nuclear explosion

Additionally, since Russia has a large number of mining operations, the ISC database was cross-referenced with data from the Unified Geophysical Service of the Russian Academy of Sciences as of January 2025. This dataset includes all known explosions and rockbursts within Russian territory. These events were also excluded to ensure that no explosion-related events remained in the final dataset.

References

Arushanov, M. L. (2023). Climate dynamics: Space factors. LAMBERT Academic Publishing.

Arushanov, M. L. (2023). Causes of Earth's climate change as a result of cosmic impact, dispelling the myth of anthropogenic global warming. Deutsche Internationale Zeitschrift Für Zeitgenössische Wissenschaft, 53, 4-14. https://doi.org/10.5281/zenodo.7795979

Barkin, Y.V. and Lyubushin, A.A. (2007) 'Movement of the Earth's geocenter and its geodynamic content', in Sagitov Readings 2007, Moscow State University, Moscow, 31 January-1 February [Online]. Available at: http://lnfm1.sai.msu.ru/grav/russian/life/chteniya/sagi2007/SAGITOV_BARKIN_2007.pdf

Barkin, Yu. V. (2009). Cyclic inversion changes of climate in the Northern and Southern hemispheres of the Earth. In Geology of Seas and Oceans: Proceedings of the XVIII International Scientific Conference on Marine Geology (Vol. 3, pp. 4-8). GEOS.

Barkin, Yu. V. (2011). Synchronous jumps in activity of natural planetary processes in 1997-1998 and their unified mechanism. In Geology of Seas and Oceans: Proceedings of the XIX International Scientific Conference on Marine Geology (Vol. 5, pp. 28-32). GEOS.

Barkin, Yu. V., & Smolkov, G. Ya. (2013). Abrupt changes in trends of geodynamic and geophysical phenomena in 1997-1998. In Proceedings of the All-Russian Conference on Solar-Terrestrial Physics (pp. 16-21). Irkutsk.

Barkin, Yu. V. (2014, September 16). Geofizicheskie sledstviya otnositel'nykh smeshcheniy i kolebaniy yadra i mantii Zemli [Geophysical consequences of relative displacements and oscillations of the Earth's core and mantle]. Institute of Physics of the Earth, Moscow.

Beerling, D.J., Harfoot, M., Lomax, B. & Pyle, J.A., 2007. The stability of the stratospheric ozone layer during the end-Permian eruption of the Siberian Traps. Philosophical Transactions of the Royal Society A, 365, pp.1843–1866. Available at: http://doi.org/10.1098/rsta.2007.2046

Black, B.A., Elkins-Tanton, L.T., Rowe, M.C., Ukstins Peate, I., 2012. Magnitude and consequences of volatile release from the Siberian Traps. Earth and Planetary Science Letters, 317–318, pp.363–373. Available at: https://doi.org/10.1016/j.epsl.2011.12.001

Black, B., Mittal, T., Lingo, F., Walowski, K., & Hernandez, A. (2021). Assessing the Environmental Consequences of the Generation and Alteration of Mafic Volcaniclastic Deposits During Large Igneous Province Emplacement. In R. E. Ernst, A. J. Dickson, & A. Bekker (Eds.), Geophysical Monograph Series (pp. 117-131). Wiley. https://doi.org/10.1002/9781119507444.ch5

Bogoyavlensky, V.I., Nikonov, R.A. & Bogoyavlensky, I.V., 2023. New data on intensive Earth degassing in the Arctic in the north of Western Siberia: thermokarst lakes with gas blowout craters and mud volcanoes. AEE, 13, pp.353–368. Available at: https://doi.org/10.25283/2223-4594-2023-3-353-368

Bogoyavlensky, V.I., 2023. New data on mud volcanism in the Arctic on the Yamal Peninsula. Doklady Rossiyskoy Akademii Nauk. Nauki o Zemle, 512, pp.92–99. Available at: https://doi.org/10.31857/S2686739723601084

Brown, S. K., Crosweller, H. S., Sparks, R. S. J., Cottrell, E., Deligne, N. I., Guerrero, N. O., ... & Takarada, S. (2014). Characterisation of the Quaternary eruption record: analysis of the Large Magnitude Explosive Volcanic Eruptions (LaMEVE) database. Journal of Applied Volcanology, 3(5). https://doi.org/10.1186/2191-5040-3-5

Bryson, R. A. (1989). Late quaternary volcanic modulation of Milankovitch climate forcing. Theoretical and Applied Climatology, 39, 115-125. https://doi.org/10.1007/bf00868307

Campbell I.H, Czamanske G.K, Fedorenko V.A, Hill R.I& Stepanov V. 1992 Synchronism of the Siberian Traps and the Permian–Triassic boundary. Science. 258, 1760–1763.doi:10.1126/science.258.5089.1760.

Cassidy, M., Sandberg, A., & Mani, L. (2023). The Ethics of Volcano Geoengineering. Earth's Future, 11(10), e2023EF003714. https://doi.org/10.1029/2023EF003714

Castro, J., & Dingwell, D. (2009). Rapid ascent of rhyolitic magma at Chaitén volcano, Chile. Nature, 461, 780-783. https://doi.org/10.1038/nature08458

Cheng, L., Abraham, J., Zhu, J., Trenberth, K. E., Fasullo, J., Boyer, T., Locarnini, R., Zhang, B., Yu, F., Wan, L., Chen, X., Song, X., Liu, Y., & Mann, M. E. (2020). Record-Setting Ocean Warmth Continued in 2019. Advances in Atmospheric Sciences, 37, 137–142. https://doi.org/10.1007/s00376-020-9283-7

Ciavarella, A., Cotterill, D., Stott, P., et al. (2021). Prolonged Siberian heat of 2020 almost impossible without human influence. Climatic Change, 166, 9. https://doi.org/10.1007/s10584-021-03052-w

Nikiforova, M. P., Vargin, P. N., Zvyagintsev, A. M., Ivanova, N. S., Kuznetsova, I. N., & Luk'yanov, A. N. (2016). Ozone mini-hole over the Northern Urals and Siberia. Proceedings of the Hydrometeorological Research Center of the Russian Federation, 360, 168–180. In Proc. of the Hydrometeorological Conf., February 9–10, Vol. 4, 91–96. Voronezh: Nauch-no-Issledovatelskie Publikatsii.

Cox, C., & Chao, B. F. (2002). Detection of a large-scale mass redistribution in the terrestrial system since 1998. Science, 297(5582), 831–833. https://doi.org/10.1126/science.1072188

Davydova, V.O., Shcherbakov, V.D., Plechov, P.Yu., Koulakov, I.Yu., 2022. Petrological evidence of rapid evolution of the magma plumbing system of Bezymianny volcano in Kamchatka before the December 20th, 2017 eruption. Journal of Volcanology and Geothermal Research, 421, 107422. Available at: https://doi.org/10.1016/j.jvolgeores.2021.107422

D'Auria, L., Koulakov, I., Prudencio, J., et al. (2022). Rapid magma ascent beneath La Palma revealed by seismic tomography. Scientific Reports, 12, 17654. https://doi.org/10.1038/s41598-022-21818-9

Dannberg, J., & Sobolev, S. (2015). Low-buoyancy thermochemical plumes resolve controversy of classical mantle plume concept. Nature Communications, 6, 6960. https://doi.org/10.1038/ncomms7960

Deng, S., Liu, S., Mo, X., Jiang, L., & Bauer Gottwein, P. (2021). Polar Drift in the 1990s Explained by Terrestrial Water Storage Changes. Geophysical Research Letters, 48(7). https://doi.org/10.1029/2020gl092114

Dobretsov, N.L., Kirdyashkin, A.G. & Kirdyashkin, A.A., 2001. Deep Geodynamics. Novosibirsk: Publishing House of the Siberian Branch of the Russian Academy of Sciences, GEO Branch, 408 p.

Dou, H., Xu, Y., Lebedev, S., Chagas de Melo, B., van der Hilst, R. D., Wang, B., & Wang, W. (2024). The upper mantle beneath Asia from seismic tomography, with inferences for the mechanisms of tectonics, seismicity, and magmatism. Earth-Science Reviews, 247, 104595. https://doi.org/10.1016/j.earscirev.2023.104595

Dyachenko, A. I. (2003). Earth's magnetic poles. MCCME.

Elkins-Tanton, L. T., Grasby, S. E., Black, B. A., Veselovskiy, R. V., Ardakani, O. H., & Goodarzi, F. (2020). Field evidence for coal combustion links the 252 Ma Siberian Traps with global carbon disruption. Geology, 48(10), 986-991. https://doi.org/10.1130/G47365.1

Ernst, R. E., & Buchan, K. L. (2002). Maximum size and distribution in time and space of mantle plumes: evidence from large igneous provinces. Journal of Geodynamics, 34, 309-342.

Federal Research Center, Unified Geophysical Service of the Russian Academy of Sciences, n.d. Available at: http://www.ceme.gsras.ru/zr/contents.html

Fedorenko, V. A., Lightfoot, P. C., Naldrett, A. J., Czamanske, G. K., Hawkesworth, C. J., Wooden, J. L., & Ebel, D. S. (1996). Petrogenesis of the Flood-Basalt Sequence at Noril'sk, North Central Siberia. International Geology Review, 38(2), 99-135. https://doi.org/10.1080/00206819709465327

Geyer, R., Jambeck, J. R., & Law, K. L. (2017). Production, use, and fate of all plastics ever made. Science Advances, 3(7). https://doi.org/10.1126/sciadv.1700782

Halldórsson, S. A., Marshall, E. W., Caracciolo, A., et al. (2022). Rapid shifting of a deep magmatic source at Fagradalsfjall volcano, Iceland. Nature, 609, 529-534. https://doi.org/10.1038/s41586-022-04981-x

Hantemirov, R. M., Corona, C., Guillet, S., et al. (2022). Current Siberian heating is unprecedented during the past seven millennia. Nature Communications, 13, 4968. https://doi.org/10.1038/s41467-022-32629-x

Holzworth, R.H., Brundell, J.B., McCarthy, M.P., Jacobson, A.R., Rodger, C.J. & Anderson, T.S., 2021. Lightning in the Arctic. Geophysical Research Letters, 48, e2020GL091366. Available at: https://doi.org/10.1029/2020GL091366

International Committee GCGE GEOCHANGE. (2010). Global environmental changes: Threat to civilization development (Vol. 1). London: GCGE. ISSN 2218-5798

Ivanov, A.V., He, H., Yan, L., Ryabov, V.V., Shevko, A.Y., Palesskii, S.V., Nikolaeva, I.V., 2013. Siberian Traps large igneous province: Evidence for two flood basalt pulses around the Permo-Triassic boundary and in the Middle Triassic, and contemporaneous granitic magmatism. Earth-Science Reviews, 122, pp.58–76. Available at: https://doi.org/10.1016/j.earscirev.2013.04.001

Khain V.E Geology of the USSR, Beiträge zur Regionalen Geologie der Erde. 1985 Berlin-Stuttgart, Germany:Gebrüder Bornträger.

Kirdyashkin, A.A. & Kirdyashkin, A.G., 2013. Interaction of a Thermochemical Plume with Mantle Free-Convective Flows and Its Influence on Mantle Melting and Recrystallization. Geology and Geophysics, 54(5), pp.707–721

Kiyosugi, K., Loughlin, S. C., Siebert, L., & Takarada, S. (2014). Characterisation of the Quaternary eruption record: analysis of the Large Magnitude Explosive Volcanic Eruptions (LaMEVE) database. Journal of Applied Volcanology, 3(5). https://doi.org/10.1186/2191-5040-3-5

Konstantinov, K. M., Bazhenov, M. L., Fetisova, A. M., & Khutorskoy, M. D. (2014). Paleomagnetism of trap intrusions, East Siberia: Implications to flood basalt emplacement and the Permo–Triassic crisis of biosphere. Earth and Planetary Science Letters, 394, 242-253. https://doi.org/10.1016/j.epsl.2014.03.029

Koptev, A., & Cloetingh, S. (2024). Role of Large Igneous Provinces in continental break-up varying from "Shirker" to "Producer." Communications Earth & Environment, 5, 27. https://doi.org/10.1038/s43247-023-01191-9

Koulakov, I. Y. (2008). Upper mantle structure beneath Southern Siberia and Mongolia from regional seismic tomography. Russian Geology and Geophysics, 49(3), 187-196. https://doi.org/10.1016/j.rgg.2007.06.012

Larson, R.L. & Olson, P., 1991. Mantle plumes control magnetic reversal frequency. Earth and Planetary Science Letters, 107(3–4), pp.437–447. Available at: https://doi.org/10.1016/0012-821X(91)90091-U

Li, S., Li, Y., Zhang, Y., Zhou, Z., Guo, J., & Weng, A. (2023). Remnant of the late Permian superplume that generated the Siberian Traps inferred from geomagnetic data. Nature Communications, 14, 1311. https://doi.org/10.1038/s41467-023-37053-3

Livermore, P. W., Hollerbach, R., & Finlay, C. C. (2017). An accelerating high-latitude jet in Earth's core. Nature Geoscience, 10, 62–68. https://doi.org/10.1038/ngeo2859

Lvova, E. V. (2010). Tectonics of mantle plumes: Evolution of basic concepts. Moscow University Geology Bulletin, 5, 21-29.

Mazaud, A. & Laj, C., 1991. The 15 m.y. geomagnetic reversal periodicity: a quantitative test. *Earth and Planetary Science Letters*, 107(3–4), pp.689–696. Available at: https://doi.org/10.1016/0012-821X(91)90111-T

Mikhailova, R. S. (2014). Strong earthquakes in the mantle and their influence in the near and far zone. Geophysical Survey RAS. http://www.emsd.ru/conf2013lib/pdf/seism/Mihaylova.pdf

Mikhailova, R. S., Ulubieva, T. R., & Petrova, N. V. (2021). The Hindu Kush earthquake of October 26, 2015 with Mw=7.5, I0~7: Previous seismicity and aftershock sequence. Earthquakes in Northern Eurasia, 24(2015), 324-339. https://doi.org/10.35540/1818-6254.2021.24.31

Nikiforova, M.P., 2017. Extremely low total ozone values over the northern Ural and Siberia in the end of January 2016. AOO. Available at: doi:10.15372/AOO20170102

Ostle, C., Thompson, R. C., Broughton, D., Gregory, L., Wootton, M., & Johns, D. G. (2019). The rise in ocean plastics evidenced from a 60-year time series. Nature Communications, 10(1622). https://doi.org/10.1038/s41467-019-09506-1

Popykina, A., Ilin, N., Shatalina, M., Price, C., Sarafanov, F., Terentev, A., & Kurkin, A. (2024). Thunderstorms near the North Pole. Atmosphere, 15(3), 310. https://doi.org/10.3390/atmos15030310

Rantanen, M., Karpechko, A. Y., Lipponen, A., Nordling, K., Hyvärinen, O., Ruosteenoja, K., Vihma, T., & Laaksonen, A. (2022). The Arctic has warmed nearly four times faster than the globe since 1979. Communications Earth & Environment, 3, 168. https://doi.org/10.1038/s43247-022-00498-3

Roger L. Larson, Peter Olson, Mantle plumes control magnetic reversal frequency, Earth and Planetary Science Letters, Volume 107, Issues 3–4, 1991, Pages 437-447, ISSN 0012-821X, https://doi.org/10.1016/0012-821X(91)90091-U

Romagnoli, C., Zerbini, S., Lago, L., Richter, B., Simon, D., Domenichini, F., Elmi, C., & Ghirotti, M. (2003). Influence of soil consolidation and thermal expansion effects on height and gravity variations. Journal of Geodynamics, 35(4-5), 521-539. https://doi.org/10.1016/S0264-3707(03)00012-7

Roshydromet. (2022). Report on climate features in the Russian Federation for 2021. Moscow: Federal Service for Hydrometeorology and Environmental Monitoring.

Roshydromet. (2024). Report on climate features in the Russian Federation for 2023. Moscow: Federal Service for Hydrometeorology and Environmental Monitoring.

Samenow, J. (2019, August 12). Lightning struck near the North Pole 48 times on Saturday, as rapid Arctic warming continues. The Washington Post. https://www.washingtonpost.com/weather/2019/08/12/lightning-struck-within-miles-north-pole-saturday-rapid-arctic-warming-continues/

Sawyer, D. E., Urgeles, R., & Lo Iacono, C. (2023). 50,000 yr of recurrent volcaniclastic megabed deposition in the Marsili Basin, Tyrrhenian Sea. Geology, 51(11), 1001-1006. https://doi.org/10.1130/G51198.1

Sherstyukov, B. G. (2023). Global warming and its possible causes. Journal of Hydrometeorology and Ecology, 70, 7-37. https://doi.org/10.33933/2713-3001-2023-70-7-37

Smirnov, S. Z., et al. (2021). High explosivity of the June 21, 2019 eruption of Raikoke volcano (Central Kuril Islands): Mineralogical and petrological constraints on the pyroclastic materials. Journal of Volcanology and Geothermal Research, 418, 107346. https://doi.org/10.1016/j.jvolgeores.2021.107346

Smolkov, G. Ya. (2018). Exposure of the solar system and the earth to external influences. Physics & Astronomy International Journal, 2(4), 310-321. https://doi.org/10.15406/paij.2018.02.00104

Smolkov, G. Y. (2020). Heliogeophysical research. Heliogeophysical Research, 25, 14-29. http://vestnik.geospace.ru/index.php?id=569

Sobolev, S. V., Sobolev, A. V., Kuzmin, D. V., Krivolutskaya, N. A., Petrunin, A. G., Arndt, N. T., Radko, V. A., & Vasiliev, Y. R. (2011). Linking mantle plumes, large igneous provinces and environmental catastrophes. Nature, 477, 312-316.

Sobolev, S.V., Sobolev, A.V., Kuzmin, D.V., Krivolutskaya, N.A., Petrunin, A.G., Arndt, N.T., Radko, V.A. & Vasiliev, Y.R., 2011. Linking mantle plumes, large igneous provinces and environmental catastrophes. Nature, 477, pp.312–316. Available at: DOI: 10.1038/nature10385

Swallow, E. J., Wilson, C. J. N., Charlier, B. L. A., & Gamble, J. A. (2019). The Huckleberry Ridge Tuff, Yellowstone: evacuation of multiple magmatic systems in a complex episodic eruption. Journal of Petrology, 60, 1371-1426. https://doi.org/10.1093/petrology/egz034

Syvorotkin, V.L., 2018. Deep degassing in polar regions of the planet and climate change. APOG. Available at: doi:10.29222/ipng.2078-5712.2018-23.art48

TASS. (2024, January). Russia's territory is warming 2.5 times faster than the rest of the planet. TASS News Agency. https://tass.ru/obschestvo/16009287

USDP project. (n.d.). In Earthquake Research Institute, The University of Tokyo. Retrieved December 31, 2024, from https://www.eri.u-tokyo.ac.jp/KOHO/Yoran2003/sec4-5-eng.htm#:~:text=USDP%20consists%20of%20two%20phases%20

Viterito, A. (2022). 1995: An important inflection point in recent geophysical history. International Journal of Environmental Sciences & Natural Resources, 29(5). https://doi.org/10.19080/ijesnr.2022.29.556271

Volcanic fluid research center. (n.d.). Understanding of the conduit system at Unzen Volcano. Earthquake Research Institute, The University of Tokyo. Retrieved December 31, 2024, from https://www.eri.u-tokyo.ac.jp/VRC/vrc/usdp/conduit.html

Watts, J.D., Potter, S., Rogers, B.M., Virkkala, A.-M., Fiske, G., Arndt, K.A., et al., 2025. Regional hotspots of change in northern high latitudes informed by observations from space. Geophysical Research Letters, 52, e2023GL108081. Available at: https://doi.org/10.1029/2023GL108081

Why the Tongan eruption will go down in the history of volcanology. (2022). Nature, 602, 376-378. https://doi.org/10.1038/d41586-022-00394-y

Witze, A. (2017). Earth's lost history of planet-altering eruptions revealed. Nature, 543, 295-296. https://doi.org/10.1038/543295a

Xia, Y. et al., 2021. Significant contribution of severe ozone loss to the Siberian- Arctic surface warming in spring 2020. Geophysical Research Letters, 48, e2021GL092509. Available at: https://doi.org/10.1029/2021GL092509

Zonenshain, L.P. & Kuzmin, M.I., 1993. Deep Geodynamics of the Earth. Geology and Geophysics, 34(4), pp.3–13.

Zonenshain, L.P., Kuzmin, M.I. *Deep Geodynamics of the Earth* // *Geology and Geophysics*, 1993, Vol. 34 (4), pp. 3–13.

Zotov, L. V., Barkin, Yu. V., & Lyubushin, A. A. (2009). Geocenter motion and its geodynamics. In Proceedings of the Conference "Space Geodynamics and Modeling of Global Geodynamic Processes" (pp. 98-101). Siberian Branch of RAS.